GRADUATE AERONAUTICAL LABORATORIES
CALIFORNIA INSTITUTE OF TECHNOLOGY

TURBULENT SHEAR LAYER MIXING WITH FAST CHEMICAL REACTIONS

Paul E. DIMOTAKIS

GALCIT REPORT FM87-1

10 June 1987

Firestone Flight Sciences Laboratory

Guggenheim Aeronautical Laboratory

Karman Laboratory of Fluid Mechanics and Jet Propulsion

Pasadena

GRADUATE AERONAUTICAL LABORATORIES
of the
CALIFORNIA INSTITUTE of TECHNOLOGY
Pasadena, California 91125

TURBULENT SHEAR LAYER MIXING WITH FAST CHEMICAL REACTIONS[†]

by,

Paul E. DIMOTAKIS

GALCIT Report FM87-1

10 June 1987

[†] Invited lecture at the United States — France Joint Workshop on Turbulent Reacting Flows, 6-10 July 1987, Rouen, FRANCE

ABSTRACT

A model is proposed for calculating mixing and chemical reactions in the limit of infinitely fast chemical kinetics and negligible heat release, in fully developed turbulent shear layers. The model is based on the assumption that the topology of the interface between the two entrained reactants in the layer, as well as the strain field associated with it, can be described by the similarity laws of the Kolmogorov cascade. The calculation yields the integrated volume fraction across the layer occupied by the chemical product, as a function of the stoichiometric mixture ratio of the reactants carried by the free streams, the velocity ratio of the shear layer, the local Reynolds number, and the Schmidt number of the flow. The results are in good agreement with measurements of the volume fraction occupied by the molecularly mixed fluid in a turbulent shear layer and the amount of chemical product, in both gas phase and liquid phase chemically reacting shear layers.

1. INTRODUCTION

Understanding chemically reacting, turbulent free shear flows is important not only for the obvious technical reasons associated with the engineering of a variety of reacting and combusting devices but also for reasons of fundamental importance to fluid mechanics and our perception of turbulence.

From a theoretical point of view, chemically reacting flows provide important tests of turbulence theories by adding to the dimensionality of the questions that can be asked of turbulence models. To compute chemical reactions in turbulent flow, the physics of reactant species turbulent transport and mixing need to be described correctly down to the diffusion scale level. A much more stringent specification than needs be imposed on momentum transport turbulence models.

From an experimental point of view, the chemical reaction provides a probe with an effective spatial and temporal resolution and sensitivity that is usually unattainable by conventional direct flow field measurement techniques in high Reynolds number turbulent flows. Chemically reacting turbulent flow experiments are therefore to be regarded as a complementary means of interrogation; a valuable adjunct to the more conventional probing of the behavior of turbulent flow.

A broad class of current efforts to understand chemically reacting turbulent flows is based on classical turbulence formulations founded on the Reynolds-averaged Navier-Stokes equations. In such formulations, species transport is conventionally modeled as proportional to the gradient of the corresponding mean species concentration, with an effective diffusivity that is prescribed to be some function of the flow. See Tennekes & Lumley (1972), for an introduction. Estimates of mixing at the molecular scale, in these formulations, must be modeled separately, in a manner that unfortunately cannot be addressed without additional assumptions that are essentially ad hoc. See Sreenivasan,

Tavoularis & Corrsin (1981), the introduction in Broadwell & Breidenthal (1982) and the discussion in Broadwell & Dimotakis (1986) for a recent examination of these issues.

A different approach is taken by modeling efforts based on attempts to write transport equations for the probability density functions (PDF) of the conserved scalars, or joint PDFs for scalars, and/or the (vector) velocity field and pressure. See, for example, Pope (1985) and also related work by Kollmann & Janicka (1982) and Kollmann (1984). These efforts, which are, at least in principle, capable of addressing the issues of transport and mixing in a unified manner, must nevertheless resort to equally ad hoc assumptions in closing the set of equations that need to be solved to extract the desired information. In other words, while having the correct fluctuation statistics through the relevant PDFs, and conditional statistics through one-time joint PDFs, would undoubtedly permit the mixing and resulting chemical product formation to be computed correctly, it would appear that those PDFs are no easier to obtain than the ab initio solution of the original problem.

Finally, a model was recently proposed by Broadwell & Breidenthal (1982), which is not based on gradient transport concepts. This model will be discussed below in the context of recent data on chemically reacting shear layers in both gas phase and liquid phase shear layers.

1.1 Recent experimental results

The aspirating probe (Brown & Rebollo 1972) measurements of Konrad (1976) of the probability density function of the high speed fluid fraction in a non-reacting, gas phase shear layer suggested that the mixed fluid composition does not vary appreciably across the width of the layer, even as the mean high speed fluid fraction varies smoothly from unity, on the high speed side, to zero on the low speed side. Additionally, as Konrad recognized, the most likely values of the mixed

fluid high speed fluid fraction seem to be centered around the shear layer entrainment ratio. The smooth variation of the mean is then to be understood as the variation of the local probability of finding:

a. pure high speed fluid,

b. mixed fluid,

and,

c. pure low speed fluid,

as we traverse the width of the layer.

The near uniformity in the mixed fluid composition, apparent in Konrad's passive scalar non-reacting shear layer experiments, can be seen to have an important counterpart in the gas-phase, chemically reacting shear layer experiments (e.g. Mungal & Dimotakis 1984). Measuring the temperature field in the reaction zone of a mixing layer bringing together H_2 and F_2 reactants carried in a N_2 diluent, it is found that within the discernible regions that can be associated with the interior of the large scale structures the temperature was nearly uniform. See figure 1. The resulting mean temperature (chemical product) profile that peaks in the interior of the reaction zone is more a consequence of the variation of the fraction of the time a given fixed point is visited by the hot large scale cores (duty cycle), rather than the variation of the temperature field within a core. See figure 2. These results and conclusions are in good agreement with the results of Fiedler (1975), who measured the instantaneous temperature at several points across a shear layer, one free stream of which was marked by a small temperature difference, serving as a passive conserved scalar label.

Measurements in both reacting and non-reacting liquid phase shear layers, using laser induced fluorescence techniques (Koochesfahani & Dimotakis 1986) of the PDF of the high speed fluid fraction, corroborate

these findings. See figure 3.

An important conclusion can be drawn from these results, which is also consistent with the results of the flow visualization studies and the earlier pilot, liquid phase, chemically reacting experiments in Dimotakis & Brown (1976), as well as the subsequent systematic study of liquid phase reacting layers by Breidenthal (1981): the large scale motion within the cores of the shear layer vortical structures is capable of transporting a small fluid element from one edge of the layer to the other, before any significant change in composition can occur. During this transport phase, initially unmixed fluid within the fluid element will mix to contribute to the amount of molecularly mixed fluid, but will do so at a range of compositions centered at the value corresponding to the relative amounts of unmixed fluid originally within the small fluid element. This is the reason why the mixed fluid composition cannot exhibit a substantial systematic variation across the layer and, in particular, is not centered about the value of the local mean. This observation represents an important simplification to the problem, as it suggests that it may be justified to treat the composition field in a uniform manner across the shear layer width.

In the gas phase, hydrogen-fluorine experiments of Mungal & Dimotakis (1984), the stoichiometric mixture ratio ϕ, defined by

$$\phi = \frac{c_{02}/c_{01}}{(c_{02}/c_{01})_s}, \qquad (1.1)$$

was varied, where c_{02} and c_{01} are the low and high speed free stream reactant concentrations respectively, and the subscript "s" in the denominator denotes the corresponding chemical reaction stoichiometric ratio (unity for the $H_2 + F_2$ reaction). The quantity ϕ can be viewed as representing the mass of high speed fluid required (to be mixed and react) to completely consume a unit mass of low speed fluid. For uniform density, chemically reacting shear layers (low heat release), ϕ can also be interpreted in terms of the requisite volumes of the free

stream fluids for complete reaction.

For a given value of ϕ, the total amount of chemical product in the mixing layer can be expressed in terms of the integral product thickness

$$\delta_{P1} = \frac{1}{c_{01}} \int_{-\infty}^{\infty} c_P(y,\phi)\, dy, \tag{1.2}$$

where the subscript 1 in δ_{P1} denotes that c_{01}, the high speed stream reactant concentration, was used to normalize $c_P(y,\phi)$, the mean chemical product concentration profile across the layer. Using the mean temperature rise $\Delta T(y,\phi)$ as the measure of product concentration and normalizing the transverse coordinate y by the total width of the layer δ, we can also write

$$\frac{\delta_{P1}}{\delta} = \frac{1}{\delta} \int_{-\infty}^{\infty} \frac{\Delta T(y,\phi)}{\Delta T_{flm}(\infty)}\, dy\ . \tag{1.3}$$

For a fixed c_{01} and matched heat capacities for the free stream fluids, we have that

$$\Delta T_{flm}(\phi) = \frac{2\phi}{\phi + 1}\, \Delta T_{flm}(1) \tag{1.4}$$

is the adiabatic flame temperature rise, as a function of ϕ, and $\Delta T_{flm}(1)$ is the adiabatic flame temperature rise corresponding to the stoichiometric reactant concentration ratio. Note that, for a fixed high speed stream reactant concentration c_{01}, the normalizing temperature in equation 1.3 is given by $\Delta T_{flm}(\infty) = 2\, \Delta T_{flm}(1)$. The experimental values are plotted in figure 4. In the data in figure 4, the width of the layer δ is estimated by δ_1, the width where the product concentration (mean temperature rise) has fallen to 1% of its peak mean value. To remove the small differences in the values of δ_1 computed from the temperature profiles (see Mungal & Dimotakis 1984, Table I), a fixed value for δ/x ($= 0.165$) was used in normalizing the data in figure

4, which was estimated from the data for each of the different ϕ's. It should be noted that δ_1, the 1% width, was found in both the gas phase reacting layers and the liquid phase measurements of Koochesfahani & Dimotakis (1986) to be very close to the visual width δ_{vis} of Brown & Roshko (1974).

As can be seen in the data in figure 4, as ϕ is increased from small values, the amount of chemical product at first increases rapidly. Beyond a certain value, however, a further increase in ϕ (increase of the low speed stream reactant concentration) is not accompanied by a commensurate increase in the chemical product, as the fluid in the shear layer is already low speed reactant rich and most of the entrained high speed stream reactant has already been consumed. The smooth curve in figure 4 was drawn to aid the eye.

A slightly different definition of product thickness, which avoids the asymmetric choice of using one stream or the other as a reference, is to use the adiabatic flame temperature $\Delta T_{flm}(\phi)$ to normalize the temperature profile, corresponding to each value of ϕ. This yields a new normalized product thickness δ_p/δ, given by

$$\frac{\delta_p}{\delta} = \frac{1}{\delta}\int_{-\infty}^{\infty} \frac{\Delta T(y,\phi)}{\Delta T_{flm}(\phi)}\, dy \ . \qquad (1.5)$$

Note that the integrand is in the units of the normalized mean temperature rise profile, as was plotted in figure 2, and that $\delta_p/\delta = (\delta_{p_1}/\delta)/\xi_\phi$, where

$$\xi_\phi = \frac{\phi}{\phi + 1} \ . \qquad (1.6)$$

It may be worth noting that, for equal density free streams, negligible heat release, and a given free stream reactant stoichiometric mixture ratio ϕ, the quantity ξ_ϕ represents the high speed fluid volume

fraction, in the mixed fluid, required for complete consumption of both reactants. A volume fraction $\xi < \xi_\phi$ in the mixed fluid, for example, corresponds to an excess of high speed fluid, relative to that required by the stoichiometry of the reaction, and would result in complete consumption of the low speed reactant in the mixture and a remainder of unreacted high speed fluid. A plot of the experimental values of δ_p/δ for the hydrogen-fluorine gas phase data, versus ξ_ϕ, appears in figure 5. The smooth curve through the gas phase data of Mungal & Dimotakis (1984) denoted by circles is the same curve that appears in figure 4, transformed to the coordinates of figure 5. The data point denoted by the triangle corresponds to the similarly defined chemical product volume fraction in a liquid phase two dimensional shear layer, as measured by Koochesfahani & Dimotakis (1986) at the same free stream speed ratio and comparable Reynolds number.

Since (for equal species and heat diffusivities) $\Delta T_{flm}(\phi)$ is the highest temperature that can be achieved in the reaction zone, we can think of the ratio δ_p/δ as a measure of the shear layer turbulent mixing and chemical reactor "efficiency". If the two reactants were entrained from the two free streams in such a way as to produce mixed fluid everywhere within the layer at a single-valued composition corresponding to a mixture fraction ξ_ϕ, then the resulting temperature profile would be a top-hat of height $\Delta T_{flm}(\phi)$ and width δ, resulting in a value of δ_p/δ of unity. This clearly represents the highest possible total chemical product that can be formed within the confines of the shear layer turbulent region. If, on the other hand, the mean temperature rise profile was a triangle whose base was equal to δ and which reached $\Delta T_{flm}(\phi)$ at the apex somewhere within the layer, then δ_p/δ would be equal to 1/2. It is interesting that, in these units, the gas phase data (circles) in figure 5, for all the values of the stoichiometric mixture ratio investigated, are in the relatively narrow range of a chemical product volume fraction of $\delta_p/\delta \approx 0.31 \pm 0.03$.

Shear layer mixing and chemical reactions

Comparison of the total amount of chemical product measured in gas phase reacting layers (Mungal & Dimotakis 1984), and liquid phase reacting layers (Breidenthal 1981, Koochesfahani & Dimotakis 1986), points out a second important feature of these data; at comparable flow conditions, the amount of chemical product formed at high Reynolds numbers is a function of the (molecular) Schmidt number $Sc = \nu/D$ of the fluid, where ν is the kinematic viscosity and D is the relevant species diffusivity. Roughly twice as much product is formed in the gas phase chemically reacting shear layer ($Sc \approx 0.8$) than in the liquid phase layer ($Sc \approx 600$). See figure 5.

Finally, in a further investigation in gas phase reacting shear layers (Mungal et al 1985), the Reynolds number was varied over a range of almost an order of magnitude, keeping all other conditions as constant as was feasible. The resulting data for δ_p/δ, for a fixed stoichiometric mixture ratio of $\phi = 1/8$, are plotted in figure 6. It can be seen that there is a modest but unmistakeable decrease in the total amount of product in the layer as the Reynolds number is increased. The authors estimate that, at the operating conditions for those experiments, a factor of 2 increase in the Reynolds number results in approximately a 6% reduction in chemical product volume fraction δ_p/δ. Also included in the same plot, for comparison purposes, are the reacting liquid layer data of Koochesfahani & Dimotakis (1986) at a stoichiometric mixture ratio of $\phi = 10$. As can be seen, the data indicate a much weaker Reynolds number dependence of the liquid phase product volume fraction δ_p/δ. We note, however, that the lower Reynolds number liquid data point may be at a value of the Reynolds number that is too close to the shear layer mixing transition (Konrad 1976, Bernal et al 1979, Breidenthal 1981) and the flow may not have attained fully turbulent behavior.

1.2 Entrainment ratio for a spatially growing shear layer

An important conclusion drawn by Konrad (1976) from his observations was that a spatially growing shear layer entrains fluid from each of the two free streams in an asymmetric way, even for equal free stream densities. For equal free stream densities ($\rho_2/\rho_1 = 1$) and a free stream speed ratio of $U_2/U_1 = 0.38$, Konrad measured a volume flux entrainment ratio E of 1.3. For a free stream density ratio of $\rho_2/\rho_1 = 7$ (helium high speed fluid and nitrogen low speed fluid), and the same velocity ratio, he measured an entrainment ratio of $E = 3.4$.

This behavior can be understood in terms of the upstream/downstream asymmetry that a given large scale vortical structure sees in a spatially growing shear layer. Simple arguments suggest that the volume flux entrainment ratio can be estimated and is given by

$$E \approx \sqrt{\rho_2/\rho_1}\,(1 + \ell/x) \,, \tag{1.7a}$$

where ℓ/x is the large structure spacing to position ratio. See Dimotakis (1986) for the arguments leading to this result. Konrad's data support the hypothesis that $\langle \ell/x \rangle$, the ensemble averaged value of ℓ/x, is independent of the free stream density ratio ρ_2/ρ_1. Fitting available data for ℓ/x one finds that the relation

$$\langle \ell/x \rangle \approx 0.68\,\frac{1-r}{1+r} \,, \tag{1.7b}$$

where $r = U_2/U_1$ is the free stream speed ratio, is a good representation for this quantity.

In the context of chemically reacting flows, it is important to recognize that fluid mixed at the entrainment ratio E produces a (high speed fluid) mixture fraction ξ_E given by,

$$\xi_E = \frac{E}{E+1} \tag{1.8}$$

which, for $E > 1$, corresponds to a value for ξ_E which is greater than 1/2. The mixture fraction ξ_E is a special value in the shear layer, as Konrad recognized, and helps explain the large differences in the composition fluctuations between his equal free stream density data and his helium/nitrogen free stream data. See sketch and discussion on page 27 in Konrad (1976).

This picture suggests a zeroth order model for mixing in a two-dimensional shear layer in which the reactants are entrained at the ratio E, as dictated by the large scale dynamics, and eventually mixed to a (nearly) homogeneous composition centered around ξ_E by the efficient action of the turbulence within the confines of the shear layer width. This idea was used by Konrad (1976) to account for the density ratio dependence of his concentration fluctuation measurements in the shear layer.

The asymmetric entrainment ratio helps explain the outcome of the "flip" experiments. In particular, it is known that if the concentration of the reactants carried by the two free streams corresponds to a stoichiometric mixture ratio $\phi \neq 1$, then one obtains more or less total chemical product, depending on whether or not the lean reactant is carried by the free stream fluid that is preferentially entrained. This can be seen in the gas phase reacting shear layer data pairs for $\phi = (1/4, 4)$ and $\phi = (1/8, 8)$, which correspond to "flipping" the side on which the lean reactant is carried. See figures 9 and 17 and related discussions in Mungal & Dimotakis (1984), and also the liquid phase "flip" experiments documented in Koochesfahani et al (1983), and the subsequent ones in Koochesfahani & Dimotakis (1986).

1.3 The Broadwell-Breidenthal model

In the Broadwell/Breidenthal (1982) mixing model for the two-dimensional shear layer, the entrained fluid is described as existing in one of three states:

1. recently entrained, as yet unmixed fluid, from each of the two free streams,

2. homogeneously mixed fluid at a composition ξ_E corresponding to the entrainment ratio E (equation 1.8),

and,

3. fluid mixed at strained laminar interfaces (flame sheets).

In the context of this picture, the total chemical product is computed as the sum of the contribution corresponding to the homogeneously mixed fluid, and the contribution from the flame sheets.

The volume fraction in the reaction zone, corresponding to the homogeneously mixed fluid at $\xi = \xi_E$, is at a temperature rise (product concentration) $\Delta T_H(\xi_E,\xi_\phi)$, corresponding to the complete consumption of the lean reactant, and is given by

$$\Delta T_H(\xi_E,\xi_\phi) = \Theta_H(\xi_E,\xi_\phi) \times \Delta T_{flm}(\phi) \ , \qquad (1.9a)$$

where, for a fixed low speed stream reactant concentration, $\Delta T_{flm}(\phi)$ is given by equation 1.4 . $\Theta_H(\xi_E,\xi_\phi)$ is the temperature, normalized by the adiabatic flame temperature, that results when the two fluids characterized by a stoichiometric mixture fraction of ξ_ϕ are homogenized at the entrainment mixture fraction ξ_E, i.e.

$$\Theta_H(\xi_E,\xi_\phi) = \begin{cases} \dfrac{\xi_E}{\xi_\phi}\,, & \text{for } \xi_E \le \xi_\phi \\ \dfrac{1-\xi_E}{1-\xi_\phi}\,, & \text{for } \xi_E > \xi_\phi\,. \end{cases} \qquad (1.9b)$$

See figure 7 .

The heat released (amount of product) in the strained laminar interfaces (flame sheets), for equal species and heat diffusivities, is found proportional to

$$(Sc\cdot Re)^{-1/2}\, F(\xi_\phi)\, \Delta T_{flm}(\phi)\,, \qquad (1.10)$$

where $F(\xi_\phi)$ is the Marble & Broadwell (1977) flame sheet function and given by

$$F(\xi_\phi) = \frac{e^{-z_\phi^2}}{\sqrt{\pi}\,\xi_\phi\,(1-\xi_\phi)}\,, \qquad (1.11a)$$

with z_ϕ implicitly defined by

$$\mathrm{erf}(z_\phi) = \frac{2}{\sqrt{\pi}} \int_0^{z_\phi} e^{-\zeta^2}\, d\zeta = \frac{\phi-1}{\phi+1}\,, \qquad (1.11b)$$

where erf(z) is the error function. The flame sheet function $F(\xi_\phi)$ is plotted in figure 8 . We note here that in the original discussion (Broadwell & Breidenthal 1982) the exponent for the Reynolds number dependence could be taken as $-1/2$ or $-3/4$, depending on whether the appropriate flame sheet strain rate was estimated from the large scales of the flow or the small (Kolmogorov) scales, respectively. The Reynolds number exponent is taken here (equation 1.10) as $-1/2$, corresponding to the large scale strain rate, following the recommendation in the revised discussion of this model in Broadwell &

Mungal (1986).

The contributions from the homogeneously mixed fluid and the mixed fluid on the flame sheets should be added. Normalizing the total amount of product with $\Delta T_{flm}(\phi)$, as in equation 1.5, we obtain the Broadwell-Breidenthal expression for the product volume fraction, i.e.

$$\frac{\delta_P}{\delta} = c_H \Theta_H(\xi_E, \xi_\phi) + c_F \left(Sc \cdot Re\right)^{-1/2} F(\xi_\phi) , \qquad (1.12)$$

where c_H and c_F are undetermined dimensionless constants.

In the more recent discussion of this model, Broadwell & Mungal (1986) recommend that the coefficients c_H and c_F in equation 1.12 should be determined by fitting the experimental value for δ_P/δ at $\phi = 1/8$, $Sc \approx 0.8$ and $Re \approx 6.6 \times 10^4$, derived from the gas phase data of Mungal & Dimotakis (1984), and the experimental value for δ_P/δ at $\phi = 1/10$, $Sc \approx 600$ and $Re \approx 2.2 \times 10^4$ derived from the liquid phase data of Koochesfahani & Dimotakis (1986). It should be mentioned, however, that in the latter discussion (which models finite chemical kinetic rate effects in two-dimensional shear layers using the Broadwell-Breidenthal model) Broadwell & Mungal concluded, on the basis of their model calculations, that the gas phase data of Mungal & Dimotakis (1984) and Mungal et al (1985) were not quite in the fast chemistry limit. This issue had been addressed in Mungal & Dimotakis (1984), who had concluded on the basis of a pilot experimental investigation of kinetic rate effects that (within the 3 - 5% experimental uncertainty in δ_P/δ) their results could be accepted as in the fast chemistry limit. The latter assertion will be adopted here (the differences in the resulting estimates for the model coefficients are not large) and in the notation of equation 1.12, we have

$$c_H = 0.27 , \quad c_F = 11.5 . \qquad (1.13)$$

The curve in figure 9 represents the resulting model predictions for the gas phase product thickness $\delta_{p1}(\phi)/\delta$ data that were plotted in figure 4. The δ_p/δ product volume fraction data and the corresponding Broadwell-Breidenthal model curves are plotted in figure 10 versus ξ_ϕ. The top solid curve in figure 10 is computed for the gas phase data (circles; $Sc \approx 0.8$, $Re \approx 6.6 \times 10^4$). The dashed curve is computed for the lower Reynolds number $\phi = 1/10$ and $\phi = 10$ (inverted triangles; $Re \approx 2.3 \times 10^4$), while the dot-dashed curve is computed for the higher Reynolds number experimental value at $\phi = 10$ (upright triangle; $Re \approx 7.8 \times 10^4$) of the liquid phase data ($Sc \approx 600$) of Koochesfahani & Dimotakis (1986).

It can be seen that several features of the reacting shear layer data can be accounted for by this model. For a given Reynolds number, the $1/\sqrt{Sc}$ Schmidt number dependence of the flame sheet part renders its contribution in a liquid ($Sc \sim 600$) negligible (~ 25 times smaller) as compared to that in a gas ($Sc \sim 1$). Secondly, we can see that even though the flame sheet contribution is symmetric with respect to a change from ϕ to $1/\phi$, i.e. $F(\xi_\phi) = F(1-\xi_\phi)$, the homogeneous mixture contribution is not, since $\Theta_H(\xi_E, 1-\xi_\phi) = \Theta_H(\xi_E, \xi_\phi) / E$ (compare the solid triangle function with the dashed triangle function in figure 7). This allows the outcome of the "flip" experiments to be accommodated. We note here that, for values of the stoichiometric mixture ratio ϕ close to the entrainment ratio E, the model predicts a relatively smaller difference for the product volume fraction between gases and liquids, than for small (or high) values of ϕ. Unfortunately, no relevant chemically reacting liquid phase data are available at present to provide a direct comparison in this regime.

Plots of the Broadwell-Breidenthal model predictions for the product volume fraction versus Reynolds number are depicted in figure 11 along with the corresponding gas phase data at $\phi = 1/8$ of Mungal et al (1985) and the liquid phase data at $\phi = 10$ of Koochesfahani & Dimotakis (1986). The predicted curves start at a Reynolds number of 2×10^4, based

on the velocity difference and the local visual width of the layer, estimated to be the minimum Reynolds number for the quasi-asymptotic behavior to have been attained, following the shear layer mixing transition (Konrad 1976, Bernal et al 1979, Breidenthal 1981). The solid line is the model prediction for the gas phase data. The dashed line corresponds to the model prediction for the liquid phase data. Note that the predicted curves for the gas and the liquid phase product thickness curves are computed for the values of the stoichiometric mixture ratio corresponding to the one used in the experiments (ϕ = 1/8 and ϕ = 10 respectively) and will cross at some Reynolds number as a consequence of the larger homogeneous fluid contribution for the (ϕ = 10) liquid data. There would, of course, be no crossing of the model predictions at the same ϕ, as the gas phase product volume fraction would always be larger than the corresponding liquid phase estimate for each value of the Reynolds number.

It can be seen that an additional important feature of the data is well represented by the model. The Reynolds number dependence of the product thickness for the gas phase data is predicted to be stronger than that for the liquid data. In fact, the model prediction is that at a Schmidt number of 600 the liquid product thickness will be almost independent of the Reynolds number. It would appear, however, that the Broadwell-Breidenthal model predicts a Reynolds number dependence for the gas phase product thickness that may be too strong (algebraic), when compared to the experimental dependence of the product thickness versus Reynolds number of Mungal et al (1985), which suggests a dependence on Reynolds number that may be closer to logarithmic (recall that those authors suggest a 6% drop in δ_p/δ, per factor of two in Reynolds number, for the range of Reynolds numbers investigated). It may be interesting to note that the model dependence on Schmidt number and Reynolds number is through the product Sc×Re (Peclet number) considered as a single variable. Lastly, in the limit of infinite Reynolds number, the model prediction is that gas phase shear layers should behave like liquids, with an asymptotic value of δ_p/δ, the chemical product volume fraction,

given by $c_H \Theta_H(\xi_E, \xi_\phi)$.

From a theoretical vantage point, the Broadwell/Breidenthal model considers the mixed fluid as residing in strained flame sheets, as would be appropriate for interfaces separated from each other by distances large enough such that the composition ξ (mixture fraction) swings from 0 to 1 across them, and as homogeneously mixed fluid, as would perhaps be appropriate at scales of the order of the (scalar) diffusion scale λ_D, after the diffusion process has homogenized adjacent layers of the entrained fluids. This partition of the mixed fluid states is an idealization, as the actual dynamics of this process would be expected to result in a smooth transition from one regime to the other. The authors argue that the Lagrangian time associated with that transition is short and, therefore, intermediate states can be neglected. It can also be argued, however, that the volume fraction associated with the molecularly mixed fluid in this intermediate state is not small, increasing rapidly as the diffusion scales are approached by the force of the same arguments, and is consequently not necessarily negligible.

Another related difficulty of the Broadwell/Breidenthal model, in my opinion, is the assignment of the volume fraction given to the homogeneously mixed fluid at $\xi \approx \xi_E$, i.e. the value of the coefficient c_H in equation 1.12. According to the model, c_H is a constant and, in particular, is independent of both Schmidt number and Reynolds number. It is reasonable to expect, however, that the fraction of the mixed fluid generated at the scalar diffusion scales of the flow will be a function of the ratio λ_D/δ, i.e. of the scalar diffusion scale λ_D to the overall transverse extent of the flow δ.

We shall return to these issues in the discussion of the model proposed in this paper and the comparison of its predictions with those of the Broadwell-Breidenthal model.

2. THE PROPOSED MODEL

The approach that is adopted in the proposed model is that of viewing an Eulerian slice of the spatially growing shear layer, at a downstream station at x, and imagining the instantaneous interface between the two interdiffusing and chemically reacting fluids as well as the associated strain field imposed on that interface. It is recognized that both the Eulerian state and the local behavior of that interface are the consequence of the Lagrangian shear layer dynamics from all relevant points upstream of the station of interest at x. It is assumed, however, that this upstream history acts in such a manner as to produce a self-similar state at x, whose statistics can be described in terms of the local parameters of the flow. In particular, it is assumed that a Kolmogorov cascade process has been the appropriate description of the upstream dynamics, leading to the local Eulerian spectrum of scales and associated strain rate field at x.

The justification for this approach is that while the large scale dynamics are all important in determining such things as the growth rate and entrainment ratio into the spatially growing shear layer, the predominant fraction of the interfacial area is associated with the smallest scales, which can perhaps be adequately dealt with in terms of universal similarity laws. The large scales, therefore, are viewed as feeding the reactants that are entrained at some upstream station into the smaller scale turbulence at the appropriate rate. These reactants subsequently get processed by the evolution of the cascade processes upstream to produce the local spectrum of scales at x (see discussion in Broadwell & Dimotakis 1986). This conceptual basis is also aided by the notion of a conserved scalar, according to which the state of diffusion and the progress of an associated chemical reaction, in the limit of fast (diffusion-limited) chemical kinetics, is completely determinable by the local (Eulerian) state of the conserved scalar. See, for example, Bilger (1980).

Shear layer mixing and chemical reactions

An important part of the proposed procedure is the normalization that will be imposed on the statistical weight (contribution) of each scale λ to the total amount of molecularly mixed fluid and associated chemical product. This is done via the expected interfacial surface per unit volume ratio that must be assigned to each scale λ. When totalled over all scales, these statistical weights must add up to unity.

The results are first obtained conditional on a uniform value of the dissipation rate ε. An attempt to incorporate and assess the effects of the fluctuations in the local dissipation rate, i.e. $\varepsilon(\underline{x},t)$, will be made by folding the conditional results over a probability density function for ε.

In a similar vein, a refinement of the entrainment ratio idea is proposed, in which it is recognized that the large scale spacing ℓ/x is a random variable and that therefore, by the force of equation 1.7a, the entrainment ratio is itself a random variable of the flow. Accordingly, the results will be obtained conditional on a given value of the entrainment ratio E, and will subsequently be folded over the expected distribution of values of E about its average value $\overline{E}$.

In the calculations that follow, it is assumed that the molecular diffusivities for all relevant species are equal to each other, but not necessarily equal to the kinematic viscosity. Heat release effects and temperature dependence effects of the molecular transport coefficients are also ignored. This is appropriate for the liquid phase measurements of Koochesfahani & Dimotakis (1986), and may be adequate for the description of the gas phase measurements of Mungal & Dimotakis (1984) and the Reynolds number study of Mungal et al (1985). The issue of heat release effects on the flow was specifically addressed elsewhere (see Hermanson et al 1987). In computing the temperature corresponding to the heat released in the reaction, equal heat capacities are also assumed for the two fluids brought together within the mixing zone. While some of these assumptions are not necessary for the proposed formulation outlined below, they allow calculations to be performed in

closed form permitting, in turn, the examination of the dependence of the results on the various dimensionless parameters of the problem.

The proposed procedure assumes that the relevant statistics of the velocity field are known (or can be estimated) and computes the behavior of the passive scalar process in response to that velocity field. Finally, the procedure is "closed" in that it yields the (absolute) chemical product volume fraction δ_p/δ in the shear layer at x, with no adjustable parameters.

2.1 Turbulent diffusion of a conserved scalar

Consider the shear layer as it entrains fluid from each of the two free streams and is interlaced with the resulting interfaces formed between the interdiffusing free stream fluids into a "vanilla-chocolate cake jelly roll" like structure. In describing the ensuing interdiffusion process it is useful to consider the scalar concentration field of, say, the high speed fluid mixture fraction $\xi(\underline{x},t)$, where $\xi = 0$ represents pure low speed fluid and $\xi = 1$ represents pure high speed fluid. A space curve intersecting the interface of the two interdiffusing fluids everywhere normal to this interface, i.e. in the direction of the local gradient of $\xi(\underline{x},t)$, would see at an instant in time a concentration field $\xi(s,t)$, where s is the arc length along the space curve. See figure 12. Note that, for an entrainment ratio E of high speed fluid relative to low speed fluid which is greater than unity, we would expect that the intervals along the space curve for which $\xi \sim 1$, labeled "a" in figure 12, would be longer, on average, than the intervals labeled "b", for which $\xi \sim 0$. In fact, the ratio of expected values for a and b for adjacent layers would be given by

$$\frac{\langle a \rangle}{\langle b \rangle} = E \, . \qquad (2.1)$$

Correspondingly, for portions of the segment that may have captured "jelly-roll" layers, which have been diffusing into each other for some time, we would expect that the high speed fluid fraction, in the resulting molecularly mixed fluid, would tend to homogenize to a local composition value ξ_E determined by the entrainment ratio E, i.e.

$$\xi \rightarrow \xi_E \approx \frac{\langle a \rangle}{\langle a + b \rangle} \approx \frac{E}{E+1} . \qquad (2.2)$$

In this context, ξ_E is equal to the long term (local) value of the scalar ξ, resulting from the interdiffusion of several successive $\xi \sim 1$ and $\xi \sim 0$ layers into each other, in a manner that preserves the (conserved) scalar ξ. This special role of the value of the scalar $\xi = \xi_E$ allows us to be more precise with the definition of the interfacial surface between the two entrained fluids, which we will define below as the three dimensional surface on which $\xi(\underset{\sim}{x},t) = \xi_E$.

The evolution of the composition $\xi(s,t)$ from the initial stages, which bring together adjacent layers of newly entrained high speed fluid ($\xi \sim 1$) and low speed fluid ($\xi \sim 0$), to the (local) completion of the molecular mixing ($\xi \rightarrow \xi_E$), is an unsteady diffusion problem that proceeds under the important influence of the straining field, imposed on the diffusion process by the turbulent velocity field. For the purposes of the present discussion, we will idealize this unsteady diffusion process as taking place in cells of length

$$\lambda \approx \frac{a+b}{2} , \qquad (2.3)$$

extending from the zero $\nabla\xi$ point in the $\xi \approx 1$ ("a") interval on one side of the interface to the zero $\nabla\xi$ point in the $\xi \approx 0$ ("b") interval on the other. See figure 12 .

Using the scale λ, it is convenient to define a dimensionless space variable $\eta = s/\lambda$, for each cell of extent λ, where

$$0 \leq \eta \leq 1 , \tag{2.4}$$

and a dimensionless time $\tau(\lambda)$, corresponding to the cell scale λ, given by

$$\tau(\lambda) = \frac{D\,t}{\lambda^2} , \tag{2.5}$$

where D is the scalar species molecular diffusivity. The initial conditions for this problem are given by

$$\xi(\eta,0) = \begin{cases} 1 , & \text{for } 0 \leq \eta < \dfrac{E}{E+1} \\ 0 , & \text{for } \dfrac{E}{E+1} < \eta \leq 1 , \end{cases} \tag{2.6a}$$

with adiabatic boundary conditions at the edges, i.e.

$$\frac{\partial}{\partial \eta}\xi(\eta,t) = 0 , \quad \text{at } \eta = 0 \text{ and } 1 . \tag{2.6b}$$

2.2 Strain-limited diffusion

It is important to appreciate the role of strain in this unsteady diffusion process.

Imagine a point on the $\xi(\underline{x},t) = \xi_E$ surface associated with an arc interval λ between the zero gradient points on either side of the interface. Imagine also a Taylor expansion of the velocity field component in the direction of the local $\nabla\xi$, in a frame convecting with that point. If we denote by s the arc length measured from the $\xi(\underline{x},t) = \xi_E$ surface and along the space curve in the direction of $\nabla\xi$,

we expect the local expression

$$\underline{u} \cdot \frac{\partial \xi}{\partial \underline{x}} = u_s \frac{\partial \xi}{\partial s} \approx -\sigma(\lambda)\, s \frac{\partial \xi}{\partial s} ,$$

to be an adequate approximation for this scalar product, over the transverse extent of the diffusing layer on either side of the interface. The quantity $\sigma(\lambda)$ represents the expected value of the local strain rate and which we should be able to approximate as

$$\sigma(\lambda) \approx -\frac{1}{\lambda} \frac{d\lambda}{dt} . \qquad (2.7)$$

We note that if $\sigma_1 \geq \sigma_2 \geq \sigma_3$ are the local strain rate tensor eigenvalues, where $\sigma_1 + \sigma_2 + \sigma_3 = \nabla \cdot \underline{u} = 0$, $\sigma(\lambda)$ is not necessarily identified here with $-\sigma_3$. We do expect that identification to represent an improving approximation as the viscous scales are approached, however, in as much as we expect the scalar interfaces to orient themselves normal to the direction of the local maximum contraction strain rate eigenvector in the limit of small scales, and the approximate relation of equation 2.7 to become exact in that limit. This was assumed by Batchelor (1959) in his discussion of the scalar spectrum at high wavenumbers and recently corroborated by the analysis by Ashurst et al (1987) of the Rogers et al (1986) shear flow direct turbulence simulation data.

Returning to the unsteady diffusion problem, if the initial/boundary value problem has been proceeding in the cell of extent λ for a time $t(\lambda)$ that is large compared to the reciprocal of the imposed (contraction) strain rate $\sigma(\lambda)$ then the solution to the diffusion problem becomes independent of the time $t(\lambda)$ and a function of the strain rate $\sigma(\lambda)$ only. See figure 13. Specifically, for $\sigma(\lambda) \gg 1/t(\lambda)$, the appropriate dimensionless "time" for the problem is given by substituting $1/\sigma(\lambda)$ for t, in equation 2.5, or

$$\tau(\lambda) \rightarrow \frac{D}{\lambda^2 \sigma(\lambda)} , \quad \text{as } t \rightarrow \infty . \tag{2.8}$$

This can be seen directly from the form of the diffusion equation, i.e.

$$\frac{\partial \xi}{\partial t} + \underset{\sim}{u} \cdot \frac{\partial \xi}{\partial \underset{\sim}{x}} = D \nabla^2 \xi ,$$

which can approximately be expressed locally as

$$\frac{\partial \xi}{\partial t} - \sigma s \frac{\partial \xi}{\partial s} = D \frac{\partial^2 \xi}{\partial s^2} . \tag{2.9}$$

Physically, as the aspect ratio of the volume containing the strained interface changes, we can see that for long times the dominant species transport mechanism towards the interface becomes the convection due to the strain field velocity normal to the interface. At equilibrium, the diffusive thickening of the mixed fluid layer is balanced by the steepening caused by the strain field in a manner that results in a time-independent concentration gradient and associated diffusive flux per unit area of interface. It can be ascertained, by solving the diffusion equation 2.9 for $\partial/\partial t \rightarrow 0$, that the resulting equilibrium flux corresponds to its value for the unsteady, time-dependent, zero strain problem, at the time $t = 1/\sigma(\lambda)$, hence, equation 2.8 . It can be argued that, for $\lambda \ll \delta$, which will prove to be the important regime for the problem, the Lagrangian cascade time $t(\lambda)$ required to reach the scale λ is long compared to $1/\sigma(\lambda)$, the reciprocal of the strain rate we will associate with the scale λ. Consequently, we are encouraged to consider the additional simplification of the diffusion process as it proceeds down the turbulent cascade of scales, as evolving in quasi-equilibrium with the associated strain rate $\sigma(\lambda)$, corresponding to the scale λ.

The unsteady diffusion problem in the normalized unit cell can be handled numerically in a straightforward manner. Nevertheless, it is worth noting that, for small $\tau(\lambda)$, the thickness of the diffusion layer

will be small compared to its distance from either of the two cell edges. Consequently, the composition field can be approximated by the infinite domain solution to the problem, i.e.

$$\xi(z) = \frac{1}{2}\left[1 - \mathrm{erf}(z)\right] , \tag{2.10a}$$

where, corresponding to the boundary conditions of the problem (equation 2.6a),

$$z = \frac{1}{2\sqrt{\tau}}\left(\eta - \frac{E}{E+1}\right) , \tag{2.10b}$$

and erf(z) is the error function (equation 1.11b). This result should be valid for times τ that are short such that ξ is not appreciably different from 1 and 0, at $\eta = 0, 1$ respectively, in which case the imposition of the boundary conditions at a finite distance from the interface has not been felt as yet in the interior of the cell.

All this can, of course, be verified by the exact numerical solution to the problem. In particular, a numerical solution sequence, for a value of $E = 1.3$, is depicted in figure 14, for a sequence of values of the dimensionless time τ given by

$$\tau_{n+1} = \tau_n + n^2 \tau_0, \quad n = 1, 2, \ldots$$

where $\tau_0 = 1.6 \times 10^{-4}$. Note that, consistent with the area-preserving diffusion process, guaranteed in this case by the adiabatic boundary conditions, the composition field in the cell tends, for long times, to the value $\xi_E = E/(E+1)$ corresponding to the conserved value of

$$\langle \xi(\eta,\tau) \rangle = \int_0^1 \xi(\eta,\tau)\, d\eta = \xi_E \tag{2.11}$$

(recall also equation 1.8 and the related discussion).

2.3 Diffusion of chemically reacting species

Consider now a fast chemical reaction, with negligible heat release, between the two interdiffusing species. By fast here we mean that the thickness of the overlap region required to sustain a reaction rate, per unit area of interface that can consume the diffusive flux of reactant towards the interface, is small compared to the diffusion layer thickness. In this fast reaction regime, commonly referred to as a "diffusion-limited" chemical reaction regime, the rate of production is dictated by the diffusive flux per unit area towards the interface and not by the reaction kinetics. More importantly, however, wherever ξ would be different from 0 or 1, as a result of the inter-diffusion process, in the absence of a chemical reaction, the amount of chemical product will be equal to that corresponding to the complete local consumption of the lean reactant in the mixed fluid.

We can use temperature rise (heat release) as a means of monitoring the formation of chemical product, corresponding to the reaction between the species carried by the free streams at a stoichiometric mixture ratio ϕ, as described in section 1. In that case, the fast chemistry assumption allows us to compute the amount of product (temperature rise) as a function of ξ, by assuming complete consumption of the lean reactant. Specifically,

$$\theta(\xi,\xi_\phi) = \frac{\Delta T(\xi,\phi)}{\Delta T_{flm}(\phi)} = \begin{cases} \dfrac{\xi}{\xi_\phi}, & \text{for } 0 \le \xi \le \xi_\phi \\ \dfrac{1-\xi}{1-\xi_\phi}, & \text{for } \xi_\phi \le \xi \le 1, \end{cases} \tag{2.12a}$$

where ξ_ϕ is given by equation 1.6, i.e. $\xi_\phi = \phi/(\phi+1)$, and where

$$\Delta T_{flm}(\phi) = \frac{2\phi}{\phi+1}\,\Delta T_{flm}(1) = 2\,\xi_\phi\,\Delta T_{flm}(1) \tag{2.12b}$$

is the adiabatic flame temperature rise corresponding to the stoichiometric mixture ratio ϕ. See figure 15 and discussion following equation 1.4 .

Using equation 2.12 and the solution sequence depicted in figure 14 we can compute the amount of chemical product, or temperature (heat release) along η as a function of τ. Again, it is useful to consider the result for small "times" τ. In particular, we have for the total normalized temperature rise (chemical product) in the cell,

$$\theta(\xi_\phi,\tau) = \langle \theta[\xi(\eta,\tau),\xi_\phi] \rangle = \frac{1}{z_2 - z_1} \int_{z_1}^{z_2} \theta[\xi(z),\xi_\phi]\, dz \ , \qquad (2.13a)$$

where z_1 and z_2 are the values of the similarity coordinate (equation 2.10b) at the cell edges (at "time" τ), i.e.

$$z_1 = -\frac{1}{2\sqrt{\tau}} \left(\frac{E}{E+1}\right) , \qquad z_2 = \frac{1}{2\sqrt{\tau}} \left(\frac{1}{E+1}\right) . \qquad (2.13b)$$

Note that

$$z_2 - z_1 = \frac{1}{2\sqrt{\tau}} \qquad (2.14)$$

(independently of E), and therefore, for small τ,

$$\theta(\xi_\phi,\tau) \approx \sqrt{\tau} \left\{ \frac{1}{\xi_\phi} \int_{-\infty}^{z_\phi} [1 - \mathrm{erf}(z)]\, dz + \frac{1}{1-\xi_\phi} \int_{z_\phi}^{\infty} [1 + \mathrm{erf}(z)]\, dz \right\} \qquad (2.15a)$$

where z_ϕ is the value of the similarity coordinate z at which the stoichiometric composition is attained, i.e.

$$\mathrm{erf}(z_\phi) = 2\xi_\phi - 1 = \frac{\phi - 1}{\phi + 1} \ . \qquad (2.15b)$$

Note also that, consistently with the small τ (boundary layer)

approximation, the limits of integration have been taken to infinity. The indefinite integrals in equation 2.15 can be computed in closed form and we have, after a little algebra,

$$\theta(\xi_\phi,\tau) \approx \sqrt{\tau}\, F(\xi_\phi) , \qquad (2.16)$$

where $F(\xi_\phi)$ is the flame sheet function of equation 1.11, plotted in figure 8.

We have, of course, recovered the strained flame sheet result of Marble & Broadwell (1977) by different arguments. The (weak) divergence of $F(\xi_\phi)$, as $\xi_\phi \to 0$ and $\xi_\phi \to 1$, can be seen to be an artifact of the "boundary layer" approximation and the additional approximation of taking z_1 and z_2 in the integral limits of equation 2.13a to infinity and can be lifted by folding the numerical solution sequence in equation 2.13 instead of the approximate closed form solution of equation 2.10 .

Recall now that the $\sqrt{\tau}$ increase in the average temperature in the cell with "time", as indicated in equation 2.16, is expected to be valid for small τ only. For large τ, we know that the average temperature in the cell cannot exceed the temperature (total chemical product) resulting from the complete consumption of the lean reactant. Equivalently, if we <u>first</u> homogenize the reactants in the cell, to produce a composition ξ_E, and <u>then</u> allow them to react, we will reach an average temperature $\theta_H(\xi_\phi)$ that cannot be exceeded by the transient diffusion problem. In other words,

$$\theta(\xi_\phi,\tau) \to \theta_H(\xi_\phi) = \theta(\xi_E,\xi_\phi) , \quad \text{as } \tau \to \infty , \qquad (2.17)$$

where $\theta(\xi,\xi_\phi)$ is given by equation 2.12. See also equation 1.9b and related discussion.

Sample exact numerical calculations of the solution to the original problem (without the "boundary layer" approximation) are plotted in figure 16, for E = 1.3 and for two values of ξ_ϕ, using the diffusion equation solutions depicted in figure 14. They suggest that the "boundary layer" approximation, as given by equation 2.16 — expected to be valid for small τ — can in fact be used almost until the homogeneous composition temperature is attained. In other words,

$$\Theta(\xi_\phi,\tau) \approx \begin{cases} \sqrt{\tau}\, F(\xi_\phi) , & \text{for } \tau < \tau_H \\ \Theta_H(\xi_\phi) , & \text{for } \tau \geq \tau_H , \end{cases} \tag{2.18a}$$

where τ_H, in this approximation, is the dimensionless "time" when the homogeneous mixture temperature (completion of the reaction) is attained by the boundary layer solution. Matching at $\tau = \tau_H$ we then have

$$\sqrt{\tau_H} = \frac{\Theta_H(\xi_\phi)}{F(\xi_\phi)} . \tag{2.18b}$$

See figure 17.

2.4 The scale diffusion "time" $\tau(\lambda)$

To proceed further, we need an estimate for $\sigma(\lambda)$. In particular, if $u(\lambda)$ is the expected velocity difference across a scale λ, we have the Kolmogorov (1941) relation for the self-similar inviscid inertial range,

$$u^2(\lambda) \sim \varepsilon^{-2/3} \lambda^{2/3} , \tag{2.19}$$

where ε is the local dissipation rate. Consequently, for diffusion

interfaces spaced by distances λ in the inertial range, the associated strain rate $\sigma(\lambda)$ imposed on these interfaces should be scaled by

$$\sigma(\lambda) \sim \frac{u(\lambda)}{\lambda} \sim \varepsilon^{-1/3} \lambda^{-2/3} , \tag{2.20}$$

i.e. the highest strain rates are associated with the smallest scales.

These power laws should hold for scales λ smaller than δ, where δ is identified here with the transverse extent of the vorticity-bearing region (δ_{vis} of Brown & Roshko 1974), but larger than the viscous dissipation (Kolmogorov 1941) scale λ_K, given by

$$\lambda_K = (\nu^3/\varepsilon)^{1/4} , \tag{2.21}$$

where ε is the kinetic energy dissipation rate (per unit mass) in the shear layer turbulent region. Accepting ε as an integral quantity averaged over the extent δ of the turbulent region, and scaling with the outer flow variables, we can write

$$\varepsilon = \alpha \frac{(\Delta U)^3}{\delta} , \tag{2.22}$$

where α is a dimensionless factor. This yields a relationship between λ_K and the outer variables given by

$$\frac{\lambda_K}{\delta} = (\alpha^{1/3} \mathrm{Re})^{-3/4} = \alpha^{-1/4} \mathrm{Re}^{-3/4} . \tag{2.23}$$

where,

$$\mathrm{Re} = \frac{\Delta U \, \delta}{\nu} \tag{2.24}$$

is the local Reynolds number for the shear layer. We note here that the dependence of λ_K/δ on the scaled dissipation rate α is weak.

In the opposite limit of small scales, corresponding to the viscous flow $\lambda \lesssim \lambda_K$ regime, the associated velocity gradients are imposed onto the small scales λ by the aggregate effect of the larger scales in the flow. In this case,

$$u(\lambda) \sim \lambda , \qquad \text{for } \lambda \lesssim \lambda_K ,$$

and therefore,

$$\sigma(\lambda) \approx \text{constant} = \sigma_c , \qquad \text{for } \lambda \lesssim \lambda_K ,$$

where σ_c is the expected contraction strain rate in the viscous regime. Consequently, we see that, in the inertial range, the strain rate increases as λ decreases, in accord with equation 2.20 , until a maximum value is reached, corresponding to a scale λ_c . Below this scale, the associated expected strain rate can be taken to be a constant.

The assumption of a scale-independent expected strain in the viscous range was first proposed by Townsend (1951), who suggested (to quote Batchelor 1959), that "the action of the whole flow field on small-scale variations of any quantity ... is primarily to impose a uniform persistent straining motion". This idea was used by Batchelor (1959) to derive the k^{-1} conserved temperature fluctuation spectrum in a high Prandlt number ($Pr = \nu/\kappa$) fluid.

Gibson (1968) has argued that the estimate for σ_c can be bracketed by the inequality

$$\sqrt{3} < \frac{1}{\sigma_c t_K} \lesssim 2\sqrt{3} , \qquad (2.25a)$$

where $t_K = \sqrt{\nu/\varepsilon}$ is the Kolmogorov dissipation time scale, but notes that if fluctuations in the local dissipation rate ε are taken into account these bounds must be increased (see also Novikov 1961 and discussion in Monin & Yaglom II 1975, end of section 22.3). Defining

$$\beta = \frac{1}{\sigma_c t_K} \tag{2.25b}$$

and in view of Gibson's caveat with respect to the effect of fluctuations in ε, we shall accept the upper limit of the inequality as an estimate, corresponding to a value for β of $2\sqrt{3}$.

Matching to the $\lambda^{-2/3}$ behavior of $\sigma(\lambda)$ in the inertial range (equation 2.20), we now have for the expected value of $\sigma(\lambda)$, over the complete range of scales,

$$\sigma(\lambda) \approx \begin{cases} \sigma_c \left(\frac{\lambda_c}{\lambda}\right)^{2/3}, & \text{for } \lambda > \lambda_c \\ \sigma_c, & \text{for } \lambda < \lambda_c, \end{cases} \tag{2.26a}$$

where λ_c is a cut-off scale where the two regimes match. In other words,

$$\lambda_c = \beta^{3/2} \lambda_K \quad \rightarrow \quad \lambda_c \approx 6.4 \lambda_K, \quad \text{for } \beta \sim 2\sqrt{3}, \tag{2.26b}$$

which yields for the maximum expected contraction strain rate,

$$\sigma_c \approx \frac{\nu}{\beta \lambda_K^2} = \frac{\beta^2 \nu}{\lambda_c^2} \sim \frac{12 \nu}{\lambda_c^2}, \tag{2.26c}$$

and where the numerical estimate is again for $\beta \sim 2\sqrt{3}$. A sketch of $\sigma(\lambda)$, versus λ, is depicted in figure 18. Using these relations for the strain rate $\sigma(\lambda)$ associated with the scale λ, we can now associate the "time" $\tau(\lambda)$ to the scale λ, as required by the proposed approximate solution to the transient diffusion problem. In particular, combining equations 2.8 for $\tau(\lambda)$ and 2.23 for $\sigma(\lambda)$, we have

$$\tau(\lambda) \approx \begin{cases} \dfrac{1}{\beta^2\, Sc} \left(\dfrac{\lambda}{\lambda_c}\right)^{-4/3}, & \text{for } \lambda > \lambda_c \\ \dfrac{1}{\beta^2\, Sc} \left(\dfrac{\lambda}{\lambda_c}\right)^{-2}, & \text{for } \lambda < \lambda_c \,, \end{cases} \tag{2.27}$$

where $Sc = \nu/D$ is the Schmidt number. See figure 19.

The picture to be borne in mind is one in which the energy dissipation is concentrated in intermediate sized regions in the flow of extent smaller that the outer scale δ of the flow but larger than the molecular diffusion scales. In the spirit of the earlier similarity hypotheses of Kolmogorov and Obukhov, we would expect that the dynamics within these regions would be described in terms of their dissipation rate, which must be allowed to vary from one region to another, however, as formulated in the refined similarity hypotheses put forth by Kolmogorov (1962) and Obukhov (1962). The conceptual frame here is one in which the progress of the unsteady diffusion process is computed separately for each of these regions, conditional on their local value of the dissipation rate, and the total mixing is subsequently estimated as an ensemble average over regions whose dissipation rate can be treated as a random variable.

2.5 The reaction completion scale

The idealizations permitting the association of the unsteady diffusion "time" τ with a definite scale λ, through equation 2.27, and the "time" τ_H at which the homogeneous mixture temperature $\Theta_H(\xi_\phi)$ is attained (equation 2.18b), allow us to define, in turn, a reaction completion scale λ_H, at which the lean reactant in the cell has been consumed and the homogeneous temperature has been reached. Substituting in the referenced equations, we find that the ratio λ_H/λ_c is determined, in turn, by the function

$$G(\xi_\phi) = \frac{F(\xi_\phi)}{\beta \sqrt{Sc}\, \Theta_H(\xi_\phi)} , \tag{2.28}$$

where $F(\xi_\phi)$ is the flame sheet function of equation 2.16b. In particular, we have

$$\frac{\lambda_H}{\lambda_C} = \begin{cases} [G(\xi_\phi)]^{3/2} , & \text{for } G(\xi_\phi) > 1 \\ \\ G(\xi_\phi) , & \text{for } G(\xi_\phi) < 1 . \end{cases} \tag{2.29}$$

We note here that the controlling function $G(\xi_\phi)$ can be made large or small, other things held constant, by manipulating the value of the Schmidt number. Accordingly, corresponding to the two cases of equation 2.29 dictated by the magnitude of $G(\xi_\phi)$, we will recognize two reacting flow regimes:

1. gas-like, for which the reaction is completed before λ_C is reached, i.e. $\lambda_H > \lambda_C$, [$G(\xi_\phi) > 1$, low Sc]

and

2. liquid-like, for which the reaction is completed at scales smaller than λ_C, i.e. $\lambda_H < \lambda_C$. [$G(\xi_\phi) < 1$, large Sc]

Combining these results with the expressions for the chemical product associated with a particular diffusion "time" $\tau(\lambda)$, see equations 2.18 and 2.27, we then have for these two diffusion-reaction regimes,

Gas-like: $[\ x_H = \lambda_H/\lambda_c = G^{3/2}(\xi_\phi) > 1\ ]$

$$\frac{\theta(x)}{\theta_H} = \begin{cases} 1 \ , & x < 1 < x_H \\ 1 \ , & 1 < x < x_H \\ \dfrac{G}{x^{2/3}} \ , & 1 < x_H < x \ , \end{cases} \tag{2.30a}$$

and

Liquid-like: $[\ x_H = \lambda_H/\lambda_c = G(\xi_\phi) < 1\ ]$

$$\frac{\theta(x)}{\theta_H} = \begin{cases} 1 \ , & x < x_H < 1 \\ \dfrac{G}{x} \ , & x_H < x < 1 \\ \dfrac{G}{x^{2/3}} \ , & x_H < 1 < x \ , \end{cases} \tag{2.30b}$$

where

$$x = \frac{\lambda}{\lambda_c} \tag{2.30c}$$

is the dimensionless interface scale λ, normalized by the strain rate cross-over scale λ_c.

2.6 Normalization

The preceding approximations yield an estimate for the contribution to the total chemical product in the shear layer from each scale λ of the reactant interface, per unit surface area associated with λ. To compute the total product per unit volume of shear layer fluid, however, we need to estimate the statistical weight $W(\lambda)$ for the scale λ in the

range $d\lambda$ as the expected surface per unit volume of interface associated with the scale λ, where, evidently

$$\int_V W(\lambda)\, d\lambda \;=\; \int_0^{\delta} W(\lambda)\, d\lambda \;=\; 1 \;. \tag{2.31}$$

It will be convenient to first consider the interface that would be formed between the two entrained fluids in the absence of any scalar diffusion, i.e. in the limit of $Sc \to \infty$. It will also be convenient for the discussion below to factor $W(\lambda)$ into the surface to volume ratio of a scale λ and the probability $p(\lambda)$ of finding that scale λ in our Eulerian slice. This yields the relation

$$W(\lambda)\, d\lambda \;=\; \frac{1}{\lambda}\, p(\lambda)\, d\lambda \tag{2.32}$$

or, equivalently,

$$W(\lambda)\, d\lambda \;=\; \tilde{p}\,[\ln(\lambda)]\; d\ln(\lambda), \tag{2.32'}$$

within a normalization constant.

If we may regard the self-similar inertial range ($\lambda_c \ll \lambda \ll \delta$) as not possessing an intrinsic characteristic scale, we must accept that the (dimensionless) product $W(\lambda)\, d\lambda$ can only depend on the scale λ itself. Accordingly, within a normalization constant, we must have

$$W(\lambda)\, d\lambda \;\sim\; \frac{d\lambda}{\lambda}\;, \tag{2.33}$$

as the only dimensionless group that can be formed between $d\lambda$ and λ. It can be seen that, in this range of scales, $\tilde{p}\,[\ln(\lambda)]$, and therefore also $p(\lambda)$, must be uniform (independent of λ), as perhaps one could have argued a priori.

It is reasonable to assume that interface scales below the strain rate cross-over scale λ_c are primarily generated within regions of extent λ_c or smaller. We can imagine a Taylor expansion of the velocity field about the center of one such sub-λ_c region and a (non-inertial) frame of reference that convects with the velocity field at the point of expansion and rotates about the local vorticity axis at a rate that cancels the local value of the (nearly uniform) vorticity in that region. It has been a common assumption to regard the direction of the principal strain rate axes as also fixed in that frame (Townsend 1951, Batchelor 1959, Novikov 1961), at least for a time interval of the order of $t_K = (\nu/\varepsilon)^{1/2}$. We shall accept this same approximation here, and also assume that within each of these sub-λ_c regions the local normal to the scalar interface has already been aligned with the principal contraction axis. As mentioned earlier, this latter was also assumed by Batchelor (1959) and recently corroborated for shear flows by the analysis of Ashurst et al (1987). We should note, however, that the time that the axes need to stay fixed in the rotating frame is scaled by the time t_{DK} to diffuse across λ_K, which at high Schmidt numbers can be longer than t_K[†]. Consider now any two points P_1 and P_2 that remain on the principal contraction axis in this frame and, in view of our assumptions, can be regarded as moving with the fluid. It can be seen that the number of intersections of the interface and the principal contraction axis between the points P_1 and P_2 will be constant, as the

---

[†] Considering the diffusion geometry in figure 13 for $\lambda = \lambda_K$ and $Sc > 1$, this time can be estimated to be of the order of $t_{DK} \approx t_K \ln(\sqrt{Sc})$. Batchelor (1959) was aware of this time scaling, but the issue is ignored in the implicit assumption made about the contraction axis alignment during the diffusion process. We should also note, however, that if the diffusion geometry is one of sheets rolled up around vortex filaments, as assumed by Lundgren (1982,1985), then the vorticity axis is <u>normal</u> to the maximum contraction axis and the scalar gradient, and the assumption (and the k^{-1} spectrum) remains valid. In that case, however, the scalar gradient would be at 45° to the maximum contraction axis (corroborated for the Kerr 1985 isotropic flow data analysis by Ashurst et al 1987) and not aligned with it, as appears to be the case in the Rogers et al (1986) shear flow data (Ashurst et al 1987) and as assumed here.

interface geometry is strained continuously reducing the normal spacings λ of the intersections of the interface with the principal contraction axis. This conclusion is the same regardless of whether the interface crosses the principal contraction axis with a zig-zag sheet topology, or as a rolled-up sheet, or a combination of these two possibilities. See figure 20. Moreover, the subsequent reduction of the normal spacings λ of these crossings along the contraction axis will proceed in accord with equation 2.7, which we may accept as exact for this flow regime and which we shall rewrite as

$$\frac{d}{dt}\ln(\lambda) = -\sigma_c \ . \tag{2.34}$$

Imagine now that we are tracking a group of crossing spacings on the $\ln(\lambda)$ axis, as they evolve, transformed in time by the strain field within the sub-λ_c region, initially between the limits, say, $\lambda_1 < \lambda < \lambda_2 \leq \lambda_c$, and described by a probability density function $\tilde{p}[\ln(\lambda) - \ln(\lambda_1)] = \tilde{p}[\ln(\lambda/\lambda_1)]$. Since they all "move" in Lagrangian time as a packet with a common (and constant) group velocity along the $\ln(\lambda)$ axis, we would find that their probability density function $\tilde{p}[\ln(\lambda/\lambda_1)]$ will be preserved, even as the spacings $\lambda(t)$ and $\lambda_1(t)$ themselves decrease (exponentially) with time, as dictated by equation 2.34. See figure 21. We conclude that, in this sense, the straining field in the sub-λ_c regions does not alter the probability density function $\tilde{p}[\ln(\lambda)]$ of the larger scales that are supplied to these regions by the inertial range.

These arguments suggest that $\tilde{p}[\ln(\lambda)]$, and therefore also $p(\lambda)$, must be constant not only within the inertial range but also in the viscous range and therefore throughout the spectrum of the interface scales. Consequently, equation 2.33 may be accepted as a uniformly valid description of the expected surface to volume ratio of the interface as a function of λ, in the limit of $Sc \to \infty$.

Shear layer mixing and chemical reactions

To investigate the effect of a finite Schmidt number on the associated expected surface to volume ratio of a scale λ, we first consider the following model problem. Imagine that we are sliding a ball of diameter d_b whose center rides on the $Sc \to \infty$ interface and we wish to estimate the volume swept by this ball, per unit volume of flow, as its center scans the whole surface. It can be seen that for portions of the curve for which the local scale λ is large compared with the ball radius, the volume swept will be well approximated by the product of the ball diameter and the associated interface surface to volume ratio. Consequently, the volume swept by the ball as the interface scale decreases, per unit volume of fluid, will continue to increase in accord with equation 2.33, until we reach the scale $\lambda \sim d_b$, below which the contributions per unit interface surface area can be no larger that those at the scale $\lambda \sim d_b$. This picture suggests an estimate for the statistical weight of a scale λ, at finite values of the Schmidt number, given by

$$W(\lambda)\, d\lambda = \frac{1}{N(Sc,Re)} \begin{cases} \dfrac{d\lambda}{\lambda_D}, & \text{for } \lambda < \lambda_D \\ \dfrac{d\lambda}{\lambda}, & \text{for } \lambda > \lambda_D , \end{cases} \tag{2.35}$$

where λ_D is an appropriate diffusion scale and N(Sc,Re) is the normalization function, as required by equation 2.31 . In particular, integrating over the range of scales, we have

$$N = \left\{ \int_0^{\lambda_D} + \int_{\lambda_D}^{\delta} \right\} W(\lambda)\, d\lambda ,$$

or

$$N = 1 + \ln\left(\frac{\delta}{\lambda_D}\right) = 1 + \ln\left(\frac{\lambda_c}{\lambda_D}\right) + \ln\left(\frac{\delta}{\lambda_c}\right) . \tag{2.36}$$

To proceed further, we need an estimate for λ_D/λ_c, the ratio of the appropriate diffusion scale to the strain rate cut-off scale λ_c.

For high Schmidt number fluids (Sc > 1), we will base our estimate on the Batchelor (1959) scale. In particular,

$$\lambda_D = C_B \lambda_K \left(\frac{\beta}{Sc}\right)^{1/2}$$

where λ_K is the Kolmogorov scale, $\beta \sim 2\sqrt{3}$ (recall equation 2.25 and related discussion), and C_B is a dimensionless constant of order unity. To assign a numerical value to C_B, we use the Batchelor (1959) estimates for the scalar space correlation function

$$D_{\xi\xi}(r) = \langle \xi(\underline{x})\, \xi(\underline{x}+\underline{r}) \rangle_{\underline{x}} ,$$

which he expresses in terms of a double integral over $r' < r$. He finds that, for distances r small compared with the diffusion scale, asymptotically $D(r) \sim \zeta/6$, whereas for distances large compared to the diffusion scale, but small compared with the Kolmogorov scale $D(r) \sim \ln(\zeta)$, where

$$\zeta = \frac{\beta}{Sc}\left(\frac{r}{\lambda_K}\right)^2 .$$

Monin & Yaglom II (1975, section 22.4) express these results in terms of a differential equation for $D_{\xi\xi}(r)$, given by

$$4\zeta h'' + (6+\zeta) h' = 1 , \quad h(0) = 0 ,$$

where $h = h(\zeta)$ is the scaled (dimensionless) $D_{\xi\xi}(r)$ and which can be obtained by numerical integration of the differential equation. The resulting solution transitions from the linear behavior to the

logarithmic behavior rather smoothly over the interval $1 \leq \zeta \leq 4$. Accepting the mid-point $\zeta_c = 2.5$ of this interval as the cross over between the linear (diffusive) behavior and the logarithmic (convective) behavior, we obtain the estimate $C_B = \sqrt{\zeta_c} = 1.6$. Finally, expressing the diffusion scale λ_D in terms of the strain rate cross-over scale λ_c, as required by the normalization function, we have

$$\frac{\lambda_D}{\lambda_c} \sim \frac{C_B}{\beta\, Sc^{1/2}} , \quad \text{for} \quad Sc > 1 .$$

For $Sc < 1$, Batchelor, Howells & Townsend (1959) find that $\lambda_D/\lambda_K \sim Sc^{-3/4}$. As we are not interested in Schmidt numbers that are much smaller than unity, and requiring continuity at $Sc = 1$, we will accept the estimate

$$x_D = \frac{\lambda_D}{\lambda_c} = \begin{cases} \dfrac{C_B}{\beta\, Sc^{1/2}} , & \text{for} \quad Sc > 1 , \\ \dfrac{C_B}{\beta\, Sc^{3/4}} , & \text{for} \quad Sc < 1 , \end{cases} \tag{2.37}$$

with $C_B \sim 1.6$. Substituting for δ and λ_D in equation 2.36, we then obtain the expression for the normalization function,

$$N(Sc,Re) = 1 + \ln\left(\frac{\beta\, Sc^q}{C_B}\right) + \frac{3}{4}\ln\left(\frac{\alpha^{1/3}\, Re}{\beta^2}\right) , \tag{2.38}$$

where $q = 1/2$ for $Sc > 1$, $3/4$ for $Sc \leq 1$, $C_B \sim 1.6$, $\beta \sim 2\sqrt{3}$ (recall equation 2.25 and related discussion) and α is the dimensionless ratio of the dissipation rate ε and $(\Delta U)^3/\delta$ (recall equation 2.22 and related discussion).

These considerations suggest that the problem is characterized by four length scales:

$\delta \approx (\alpha^{1/3} Re / \beta^2)^{3/4} \lambda_c$: large scale of the flow,

λ_H : reaction completion scale (equation 2.29)

λ_c : strain cross-over scale,

and,

λ_D : the species diffusion scale (equation 2.37)

All four scales have been referenced to λ_c, the strain cross-over scale, related, in turn, to the Kolmogorov scale through the constant β (see equation 2.26b). These scales define the arena in which the species diffusion and chemical reaction proceeds, bounded by δ as the large scale limit, on the one hand, and λ_D as the smallest scale at which it makes sense to attempt to track the species diffusion and chemical reaction interface, on the other, in a manner dictated by the ratio $x_H = \lambda_H/\lambda_c$.

The preceding arguments also lend credence to the conjecture that the preponderant fraction of molecularly mixed fluid, and hence chemical product, resides on interfaces associated with the smallest scales. This, in turn, supports the following picture. The main role of the more complex large scales ($\lambda \sim \delta$) of the flow can be regarded as dictating the growth rate of the shear layer δ/x and the entrainment ratio E. With this important understanding, however, we may consider the large scale structures as less important in the overall tally of the total amount of mixed fluid and chemical product (product volume or mass fraction) than the small scales, the latter of which can perhaps be adequately described by the simple arguments proposed. This is further strengthened by the observation that the amount of product associated with a scale λ increases monotonically as the scale size decreases (equations 2.30). The combination of these two effects renders the overall description of the mixed fluid and chemical product fortuitously forgiving to the treatment of the large scales in the flow.

2.7 The effect of dissipation rate fluctuations

Thus far we have treated the local dissipation rate ε as an integral constant (of the station x). In particular, scaling with the outer variables of the flow we wrote for the dissipation rate per unit mass (equation 2.33),

$$\varepsilon = \alpha \frac{(\Delta U)^3}{\delta} ,$$

where α is a dimensionless factor. As Landau noted soon after Kolmogorov and Obukhov formulated their initial similarity hypotheses, however, the local dissipation rate ε (and therefore α) cannot be treated as a constant in the turbulent region, but must be regarded as a strongly intermittent field. This objection was addressed in the revised similarity hypotheses of Kolmogorov (1962), Obukhov (1962) and Gurvich & Yaglom (1967), which will be adopted here as yielding an adequate description of the dissipation rate fluctuations.

We can cast the revised similarity hypothesis in our notation by normalizing the fluctuating dimensionless factor α with its mean value $\overline{\alpha}$, i.e. $\alpha' = \alpha / \overline{\alpha}$, such that $\overline{\alpha'} = 1$. This yields a log-normal distribution for the values of the (scaled) dissipation rate α', averaged over a region of extent r_ε. In particular,

$$p(\alpha')\, d\alpha' = \frac{1}{\sqrt{2\pi}\,\Sigma\,\alpha'} \exp\left\{ -\frac{1}{2}\left(\frac{\ln(\alpha')}{\Sigma} + \frac{\Sigma}{2} \right)^2 \right\} d\alpha' , \qquad (2.39a)$$

where $\Sigma^2 = \Sigma^2(r_\varepsilon)$, is the variance of the distribution, given by

$$\Sigma^2(r_\varepsilon) = A + \mu \ln\left(\frac{\delta}{r_\varepsilon} \right) . \qquad (2.39b)$$

The term A in this expression may depend on the large scales of the flow and μ is a constant.

Monin & Yaglom II (1975, section 25) reviewed this hypothesis, and found that it represents a good approximation to measurements of the local dissipation rate. Additionally, they concluded on the basis of comparisons with data that the constant μ should be taken in the range of $0.2 \leq \mu \leq 0.5$. More recently, Van Atta & Antonia (1980) considered the consequences of this proposal on the dependence of velocity derivative moments on Reynolds number and concluded, if r_ε is taken all the way to the Kolmogorov scale λ_K, that μ should be taken as $\mu \sim 0.25$. Ashurst et al (1987) have also estimated the value of μ on the basis of direct turbulence simulation computation data (Kerr 1985, Rogers et al 1986) and concluded that $\mu \approx 0.3$. We shall accept this value as representative and as our estimate for μ.

Estimates for $\bar{\alpha}$, corresponding to the mean value of the dissipation $\bar{\varepsilon}$, are difficult to obtain for turbulent shear layers. There is enough information, however, in the data of Wygnaski & Fiedler (1970) to permit an estimate of $\bar{\alpha} \geq 0.02$. An estimate can also be made from the data of Spencer & Jones (1971), which leads to the same value. It is difficult to assess the probable error of these estimates, not to speak of the possibility intimated by Saffman (1968) that $\bar{\alpha}$ may not necessarily be a constant, i.e. independent of the Reynolds number. Nevertheless, considering the nature of the experimental difficulties, the assumptions made about isotropy, and in view of the realizable spatial and temporal resolution relative to λ_K and λ_K / U_c, where U_c is the local flow convection velocity, we can say that this estimate is probably low, even though perhaps not by more than a factor of 2 to 3. This leads to a plausible range of values for $\bar{\alpha}$ of

$$0.02 \leq \bar{\alpha} \leq 0.06. \qquad (2.40)$$

In applying these results to the present discussion we will take r_ε down to a (fixed) viscous scale λ_0 that is a function of the (local) Reynolds number and equal to the strain rate field cut-off scale λ_c

corresponding to the mean value of the dissipation, i.e.

$$\frac{\delta}{\lambda_0} \sim \left(\frac{\bar{\alpha}^{1/3}\,\mathrm{Re}}{\beta^2}\right)^{3/4} . \tag{2.41}$$

(see equation 2.31). This yields an expression for the variance of α given by

$$\Sigma_\alpha^2(\mathrm{Re}) \approx A + \frac{3\mu}{4} \ln\left(\frac{\bar{\alpha}^{1/3}\,\mathrm{Re}}{\beta^2}\right) . \tag{2.42}$$

Finally, an estimate can be made for the constant A with the aid of the following argument. As the local Reynolds number is increased from very small values, the flow is initially essentially steady with no fluctuations in the dissipation rate field. At some minimum value of the Reynolds number, however, the flow will evolve into a fluctuating field with a spatial scale of the order of δ and an associated variance in the local dissipation rate fluctuations. At that critical value of the Reynolds number we must have $\Sigma_\alpha^2(\mathrm{Re}_{cr}) \sim 0$. This fixes the flow-specific constant A (and also removes the unpleasant dependence of the variance on the particular choice of the reference scale λ_0) and we have

$$\Sigma_\alpha^2(\mathrm{Re}) \approx \frac{3\mu}{4} \ln\left(\frac{\mathrm{Re}}{\mathrm{Re}_{cr}}\right) . \tag{2.43}$$

While, strictly speaking, a free shear layer does not possess a critical Reynolds number, one can conclude from the linear stability analysis for viscous (but parallel) flow of a hyperbolic tangent profile (Betchov & Szewczyk 1963) that an unstable mode with a spatial extent of order δ requires a minimum Reynolds number of the order of $15 \lesssim \mathrm{Re} \lesssim 50$, which we will accept as bounds for Re_{cr}. Note that Re here is based on δ, the total width of the sheared region, and not on the (smaller) hyperbolic tangent maximum slope thickness. See also discussion by

Betchov (1977). It is interesting that this estimate for a critical Reynolds number is not too different from the one made by Saffman (1968), who explored the idea that the structure of the flow in the dissipation range was essentially that resulting from the Taylor-Görtler instability of curved vortex sheets.

To compute the probability density function of the ratio λ_c/λ_0, we note that since

$$\lambda_c = \lambda_0 (\alpha')^{-1/4} , \tag{2.44a}$$

we must have

$$p(y)\,dy = \frac{1}{\sqrt{2\pi}} \exp\left\{ -\frac{1}{2}\left(y - \Sigma_a/2\right)^2 \right\} dy , \tag{2.44b}$$

where

$$y = \frac{4}{\Sigma_a} \ln\left(\frac{\lambda_c}{\lambda_0}\right) . \tag{2.44c}$$

This is correct to within a (near unity) normalization constant, as we wish to restrict λ_c to the range $0 \leq \lambda_c \leq \delta$.

To compute the effect of the dissipation fluctuations on the expected value of the scales normalization function N(Sc,Re) discussed in the preceding section, we also note that if we assume that the ratio λ_c / λ_D is independent of the dissipation rate ε (a function of Sc only), we have

$$\langle N(Sc,Re) \rangle_\varepsilon = 1 + \ln\left(\frac{\lambda_c}{\lambda_D}\right) + \ln\left(\frac{\delta}{\lambda_0}\right) - \langle \ln\left(\frac{\lambda_c}{\lambda_0}\right) \rangle_\varepsilon .$$

Then since

$$\langle \ln\left(\frac{\lambda_c}{\lambda_0}\right) \rangle_\varepsilon = \frac{\Sigma_\alpha}{4} \langle y \rangle ,$$

where

$$\langle f(y) \rangle = \frac{\int_{-\infty}^{y_\delta} f(y)\, p(y)\, dy}{\int_{-\infty}^{y_\delta} p(y)\, dy} \quad ; \qquad y_\delta = \frac{4}{\Sigma_a} \ln\left(\frac{\delta}{\lambda_0}\right) , \tag{2.46}$$

and since, in particular (at high Reynolds numbers)

$$\langle y \rangle = \frac{\Sigma_\alpha}{2} - \frac{\exp\left\{ -\frac{1}{2}\left(y_\delta - \Sigma_\alpha/2\right)^2 \right\}}{\sqrt{2\pi}\left[1 - \frac{1}{2}\operatorname{erfc}\left(\frac{y_\delta - \Sigma_\alpha/2}{\sqrt{2}}\right)\right]} \approx \frac{\Sigma_\alpha}{2} , \tag{2.47}$$

we have (see equations 2.38 and 2.43)

$$\langle N(Sc,Re) \rangle_\varepsilon = 1 + \ln\left(\frac{\beta\, Sc^q}{C_B}\right) + \frac{3}{4}\left[\ln\left(\frac{\bar{\alpha}^{1/3}\, Re}{\beta^2}\right) - \frac{\mu}{8} \ln\left(\frac{Re}{Re_{cr}}\right)\right] . \tag{2.48}$$

It is useful to rewrite this expression by defining a constant γ through the relation

$$\gamma = \frac{\bar{\alpha}^{1/3}}{\beta^2}\, Re_{cr} , \tag{2.49a}$$

and where we note, at least on the basis of our numerical estimates for these quantities, that $\gamma \sim 1$. In terms of γ, we then have

$$\langle N(Sc,Re) \rangle_\varepsilon \approx 1 + \ln\left(\frac{\beta\, Sc^q}{C_B}\right) + \frac{3}{4}\left[\left(1 - \frac{\mu}{8}\right) \ln\left(\frac{Re}{Re_{cr}}\right) + \ln(\gamma)\right] . \tag{2.49b}$$

Returning to the derivation of the quantity in the brackets, however, we can argue that it should vanish as $Re \to Re_{cr}$ and that therefore we must

in fact have $\Upsilon \approx 1$. This provides us with a consistency estimate for Re_{cr}, through equation 2.49a, and associated plausible bounds (see inequality 2.40) given by

$$31 \lesssim Re_{cr} = \frac{\beta^2}{\bar{\alpha}^{1/3}} \lesssim 44 \qquad (2.49c)$$

(recall $\beta^2 \sim 12$), which we can also use to rewrite the expression for the ratio δ/λ_0 (equation 2.41), i.e.

$$\frac{\delta}{\lambda_0} = \left(\frac{Re}{Re_{cr}}\right)^{3/4} . \qquad (2.49d)$$

Finally, for high Reynolds numbers, we may certainly ignore the $\ln(\Upsilon)$ term in favor of $\ln(Re / Re_{cr})$ and we have,

$$\langle N(Sc,Re) \rangle_\varepsilon \approx 1 + \ln\left(\frac{\beta\, Sc^q}{C_B}\right) + \frac{3}{4}\left(1 - \frac{\mu}{8}\right) \ln\left(\frac{Re}{Re_{cr}}\right) , \qquad (2.50)$$

where $\beta \sim 2\sqrt{3}$, $q = 1/2$ for $Sc > 1$, and $3/4$ for $Sc \lesssim 1$, $C_B \sim 1.6$, $\mu \sim 0.3$ and Re_{cr} is bounded by the limits in equation 2.49c. It may be worth noting that the resulting estimate for the normalization function is quite robust, as the various uncertainties in the constants appear as arguments of logarithms.

We conclude that the effects of the dissipation fluctuations on the expected value of the normalization function, which are confined to the contribution to the final result owing to a non-zero value for μ, are small.

2.8 The total product in the mixing layer

The total chemical product can now be computed as the weighted average of the contribution of each scale, i.e.

$$\Theta_T = \int_0^{\delta} \theta(\lambda/\lambda_c)\, W(\lambda)\, d\lambda = \int_0^{x_\delta} \theta(x)\, w(x)\, dx \,, \tag{2.51}$$

where $x = \lambda/\lambda_c$, $x_\delta = \delta/\lambda_c$, $\theta(x)$ is given by equations 2.30, and

$$w(x)\, dx = \frac{1}{\langle N \rangle_\varepsilon} \begin{cases} \dfrac{dx}{x_D} \,, & \text{for } x < x_D \\ \dfrac{dx}{x} \,, & \text{for } x_D < x \end{cases} \tag{2.52}$$

(see equation 2.36), with $x_D = \lambda_D/\lambda_c$ (see equation 2.37). We will first perform the computations conditional on a fixed value of the dissipation rate, and therefore λ_c, and then compute the total as the expectation value over the distribution of values of λ_c.

For gas-like flow-diffusion regimes (see equation 2.30), we have the relation

$$x_H = \frac{\lambda_H}{\lambda_c} = G^{3/2} > 1 \,,$$

where $G = G(\xi_\phi, \xi_E, Sc)$ is given by equation 2.28, and we need to distinguish between two cases depending on the relative values of x_D and x_H. The first case corresponds to $x_D < x_H$, for which

$$\langle N \rangle_\varepsilon \frac{\Theta_T}{\Theta_H} = \frac{1}{x_D} \int_0^{x_D} dx + \int_{x_D}^{x_H} x^{-1}\, dx + G \int_{x_H}^{x_\delta} x^{-5/3}\, dx$$

or,

$$\langle N \rangle_\varepsilon \frac{\Theta_T}{\Theta_H} = \frac{5}{2} - \ln(X_D) + \frac{3}{2}\ln(G) - \frac{3}{2} G x_\delta^{-3/2} . \qquad (2.53a)$$

In the second case, we have $x_H < x_D$ and therefore

$$\langle N \rangle_\varepsilon \frac{\Theta_T}{\Theta_H} = \frac{1}{x_D}\int_0^{x_H} dx + \frac{G}{x_D}\int_{x_H}^{x_D} x^{-2/3}\,dx + G\int_{x_D}^{x_\delta} x^{-5/3}\,dx$$

or

$$\langle N \rangle_\varepsilon \frac{\Theta_T}{\Theta_H} = \frac{1}{x_D}\left(\frac{9}{2} G x_D^{1/3} - 2G^{2/3}\right) - \frac{3}{2} G x_\delta^{-3/2} . \qquad (2.53b)$$

Of these two cases, the first [$x_D < x_H$] would typically be applicable for $Sc \lesssim 1$, if $\beta \sim 2\sqrt{3}$ and we have reasonable values for the stoichiometric mixture ratio ϕ and entrainment ratio E.

For <u>liquid-like</u> flow-diffusion regimes we have the relation

$$x_H = \frac{\lambda_H}{\lambda_c} = G < 1 ,$$

and, in principle, we need to distinguish between three cases. The first liquid-like case corresponds to the inequalities $x_D < x_H < 1$ and the integrals

$$\langle N \rangle_\varepsilon \frac{\Theta_T}{\Theta_H} = \frac{1}{x_D}\int_0^{x_D} dx + \int_{x_D}^{x_H} x^{-1}\,dx + G\int_{x_H}^{1} x^{-2}\,dx + G\int_1^{x_\delta} x^{-5/3}\,dx ,$$

which yields

$$\langle N \rangle_\varepsilon \frac{\Theta_T}{\Theta_H} = 2 - \ln(x_D) + \frac{G}{2} + \ln(G) - \frac{3}{2} G x_\delta^{-3/2} . \qquad (2.54a)$$

For the second liquid-like case, we have $x_H < x_D < 1$, and

$$\langle N \rangle_\varepsilon \frac{\Theta_T}{\Theta_H} = \frac{1}{x_D} \int_0^{x_H} dx + \frac{G}{x_D} \int_{x_H}^{x_D} x^{-1} dx + G \int_{x_D}^{1} x^{-2} dx + G \int_1^{x_\delta} x^{-5/3} dx ,$$

or

$$\langle N \rangle_\varepsilon \frac{\Theta_T}{\Theta_H} = G \left[\frac{1}{2} + \frac{1}{x_D} \left(2 + \ln(x_D) - \ln(G) \right) \right] - \frac{3}{2} G x_\delta^{-3/2} . \qquad (2.54b)$$

Finally, we may also have $x_H < 1 < x_D$, in which case

$$\langle N \rangle_\varepsilon \frac{\Theta_T}{\Theta_H} = \frac{1}{x_D} \int_0^{x_H} dx + \frac{G}{x_D} \left[\int_{x_H}^{1} x^{-1} dx + \int_1^{x_D} x^{-2/3} dx \right]$$

$$+ G \int_1^{x_\delta} x^{-5/3} dx ,$$

which yields

$$\langle N \rangle_\varepsilon \frac{\Theta_T}{\Theta_H} = \frac{G}{x_D} \left(\frac{9}{2} x_D^{1/3} - 2 - \ln(G) \right) - \frac{3}{2} G x_\delta^{-3/2} . \qquad (2.54c)$$

Of the three cases for the liquid-like regime, the first one [$x_D < x_H < 1$] would typically be applicable for $Sc \gg 1$.

If treating the variable β of equation 2.25 as a constant represents an adequate approximation, it can be seen that only the last

term in each of these expressions will be modified by the fluctuations in the dissipation rate. With that proviso, since $x_\delta^{-2/3} = (\lambda_c/\delta)^{2/3}$, the contribution of the last term is small for Reynolds numbers that are large (but not too large). In any event, expressing λ_c/δ in terms of the corresponding distribution variable y (equation 2.44), we find for $Re \gg Re_{cr}$

$$< x_\delta^{-2/3} >_\varepsilon \approx \left(\frac{Re}{Re_{cr}} \right)^{-(1 - 7\mu/48)/2} . \tag{2.55}$$

Substituting in the results for the two typical cases (equations 2.53a and 2.54a), for example, we obtain for the expected value of the gas-like (G > 1), product volume fraction in the layer,

$$< \Theta_T >_\varepsilon \approx \left\{ \frac{\frac{5}{2} - \ln(x_D) + \frac{3}{2}\ln(G) - \frac{3}{2} G < x_\delta^{-2/3} >_\varepsilon}{1 - \ln(x_D) + \frac{3}{4}(1 - \frac{\mu}{8}) \ln\left(\frac{Re}{Re_{cr}} \right)} \right\} \Theta_H , \tag{2.56}$$

and for the typical (Sc $\gg$ 1) liquid-like (G < 1) product fraction

$$< \Theta_T >_\varepsilon \approx \left\{ \frac{2 - \ln(x_D) + \frac{G}{2} + \ln(G) - \frac{3}{2} G < x_\delta^{-2/3} >_\varepsilon}{1 - \ln(x_D) + \frac{3}{4}(1 - \frac{\mu}{8}) \ln\left(\frac{Re}{Re_{cr}} \right)} \right\} \Theta_H , \tag{2.57}$$

where x_D is given by equation 2.37 and $< x_\delta^{-2/3} >_\varepsilon$ by equation 2.55 .

2.9 The effect of entrainment ratio fluctuations

We should note, at this point, that in the discussions thus far we have treated the entrainment ratio E, and the resulting homogeneous mixture fraction ξ_E (equation 1.8), as single-valued. We should recognize, however, that ξ_E is a variable that we would expect to be distributed according to some probability density function $p(\xi_E)$. This can then be used to obtain the estimate for the expected product thickness, as would be measured in the laboratory, by weighting $\theta_T(\xi_\phi,\xi_E)$, for each value of ξ_E, with $p(\xi_E)$. An estimate for $p(\xi_E)$ can be obtained with the aid of a refined model for the entrainment ratio E of the layer, which is outlined below.

If equation 1.7 can be used to estimate the entrainment ratio, then, even though the mean entrainment ratio would be given by

$$\bar{E} = \sqrt{\rho_2/\rho_1}\,(1 + \bar{\ell}/x) \,, \tag{2.58}$$

we must allow for a distribution of possible values of E about $\bar{E}$, since, experimentally, one finds that the large structure spacing to position ratio ℓ/x is rather broadly distributed about its mean value $\bar{\ell}/x$. In particular, Bernal (1981) has presented data and theoretical arguments in support of a log-normal distribution, which we can write, following the notation in section 2.7, as

$$p_\ell(\ell')\,d\ell' = \frac{1}{\sqrt{2\pi}\,\Sigma_\ell} \exp\Big[-\frac{1}{2}\Big(\frac{\ell n(\ell')}{\Sigma_\ell} + \frac{\Sigma_\ell}{2}\Big)^2\Big]\,\frac{d\ell'}{\ell'} \,, \tag{2.59a}$$

where

$$\ell' = \ell / \bar{\ell} \,. \tag{2.59b}$$

This is plotted in figure 22, where the dashed line is computed from equation 2.59, using the value recommended by Bernal of $\Sigma_\ell = 0.28$. See

Roshko (1976, figure 5 and related discussion) as well as Bernal (1981, figure I.8) for a comparison with experimental data.

Equations 1.7 and 2.58 can be combined to yield an estimate for the expected distribution of the values of the entrainment ratio E. The picture to be borne in mind is one in which the entrainment ratio E corresponding to a particular large structure can be treated as more or less fixed, but that the value of E varies from structure to structure in accordance with the range of values of ℓ/x (as well as the history of ℓ/x of the structures that have amalgamated to form the ones passing through the station x). In particular, since

$$E = \sqrt{\rho_2/\rho_1}\,\left[\,1 + (\overline{\ell}/x)\,\ell'\,\right] , \tag{2.60}$$

we have, for equal free stream densities,

$$p_E(E)\,dE = p_\ell\,[\ell'(E)]\,\frac{dE}{\overline{\ell}/x} ,$$

where

$$\ell'(E) = \frac{E-1}{\overline{\ell}/x} ,$$

and therefore

$$p_E(E)\,dE = \frac{1}{\sqrt{2\pi}\,\Sigma_\ell}\,\exp\left\{-\frac{1}{2}\left[\frac{1}{\Sigma_\ell}\,\ln\left(\frac{E-1}{\overline{\ell}/x}\right) + \frac{\Sigma_\ell}{2}\right]^2\right\}\frac{dE}{E-1} . \tag{2.61}$$

Using similar arguments, one also obtains the distribution $p(\xi_E)$ of the corresponding values of the mixture fraction ξ_E in terms of $p_E(E)$, in particular

$$p(\xi_E)\,d\xi_E = p_E\,[E(\xi_E)]\,\frac{d\xi_E}{(1-\xi_E)^2} , \tag{2.62a}$$

where, inverting equation 1.8 , we have

$$E(\xi_E) = \frac{\xi_E}{1 - \xi_E} \quad . \tag{2.62b}$$

The dashed line in figure 23 is the resulting probability density function $p(\xi_E)$, corresponding to equal free stream densities, a velocity ratio of $U_2/U_1 = 0.38$ and the Bernal value of $\Sigma_\ell = 0.28$. Note that, in spite of the width in the $\ell / \bar{\ell}$ distribution, the values of ξ_E are relatively narrowly distributed about the value of $\xi_{\bar{E}} = 0.567$, corresponding to a mean entrainment ratio of $\bar{E} = 1.305$, given by equation 2.36 for $\rho_2/\rho_1 = 1$ and $U_2/U_1 = 0.38$.

It should be noted that the experimental determination by Bernal (1981) of the histogram of values of $\ell / \bar{\ell}$ involved the identification of the intersection of the "braids" of each structure with the line corresponding to the trajectory of their centers. Consequently, structures in the process of tearing or coalescence, or at any other phase or configuration during which they could not be easily identified, were not included in his sample population. In other words, the distribution of spacings contributing to Bernal's experimental histogram and the resulting fit of the log-normal distribution width Σ_ℓ was based on structures that were more or less clear of their neighbors and of interactions with them. Evidently, a full accounting of the possible large structure spacings will contribute values of ℓ/x, which if included in the population, would tend to broaden its width. Moreover, the expression for the entrainment ratio as given by equation 2.60 and as discussed elsewhere (Dimotakis 1986) refers to the entrainment flux ratio into a single large scale structure. The composition ratio of a given large scale structure, however, is the one resulting from the amalgamation of several structures, each of which was characterized by an entrainment ratio as dictated by its local ℓ/x and its fluctuations. While this consideration does not shift the mean value of E, it can be seen that it increases the variance of E, relative to its value

referenced to the fluctuations of the local ℓ/x. Accordingly, in estimating the distribution of values of the entrainment ratio E, and the resulting homogeneous composition values ξ_E, one should accept a broader distribution of values of E, which we will approximate by accepting a larger value of Σ_ℓ.

The curves depicted with the solid lines in figures 22 and 23 were computed by doubling the Bernal value of the log-normal distribution width, i.e. $\Sigma_\ell = 0.56$, as representing a reasonable estimate for that quantity and are plotted for comparison. It can be seen that even this factor of two increase in the width Σ_ℓ does not significantly alter the resulting probability density function width for the distribution of values of ξ_E.

Using the probability density of the values of ξ_E, the problem is finally closed and we can now estimate the expected product thickness δ_p/δ in the mixing layer, i.e.

$$\frac{\delta_p}{\delta} = \langle \theta_T \rangle_{\varepsilon,E} = \int_0^1 \langle \theta_T(\xi_E) \rangle_\varepsilon \, p(\xi_E) \, d\xi_E \,, \qquad (2.63)$$

where $\langle \theta_T(\xi_E) \rangle_\varepsilon$ is the expected value over the dissipation rate fluctuations, conditional on the fixed value of ξ_E, as discussed in the preceding section.

The dependence of the resulting estimates for δ_p/δ on the possible range of values of the variance Σ_ℓ of $\ell / \bar{\ell}$ is small and confined to values of the stoichiometric mixture fraction ξ_ϕ in the vicinity of $\bar{\xi_E}$. It will be discussed below in the context of the comparison of the theoretical values with the data.

3. RESULTS & DISCUSSION

Using the preceding formalism, one can estimate the expected volume (or mass) fraction of chemical product within the two-dimensional turbulent shear layer wedge boundaries.

We recall here that the proposed model applies to incompressible flow, i.e. in the limit of zero Mach number. In the case of gas phase reactions, the heat release is assumed small and, in the case where the (small) temperature rise is used to label the chemical product, that the heat capacities of the two free stream fluids are assumed matched. Differential diffusion effects have been ignored, i.e. all scalar species are assumed to diffuse with the same diffusivity. Finally, we will assume that the Reynolds number is high enough for the shear layer to be in a fully developed three-dimensional turbulent state, i.e. $Re > 1.6\times10^4 - 2\times10^4$.

In evaluating the theoretical estimates, the following values will be used for the dimensionless parameters:

1. The expected value of the entrainment ratio $\overline{E}$ will be computed using equation 2.58 .

2. The fluctuations of $E / \overline{E}$ will be estimated using equation 2.61 with a variance twice the Bernal value, i.e. $\Sigma_\ell = 0.56$, as discussed in section 2.9 .

3. The value of the expected maximum contraction rate σ_c , at or below the Kolmogorov scale, will be estimated using the expression $\sigma_c t_K = 1/\beta$ with $\beta \sim 2\sqrt{3} \approx 3.46$ (see equation 2.25 and related discussion).

4. Re_{cr} , the critical Reynolds number, will be estimated via equation 2.49c , using the mid-point of the expected dimensionless dissipation $\overline{\alpha}$ bounds, i.e. $\overline{\alpha} = 0.04$ (and

$\beta \sim 2\sqrt{3}$). This leads to the value of $Re_{cr} \approx 35$.

5. The Kolmogorov/Obukhov coefficient in the variance of $\ln(\varepsilon)$ will be taken as $\mu \sim 0.3$ (equation 2.43).

6. The ratio x_D of the diffusion scale λ_D to the strain rate cut-off scale λ_c will be computed using equation 2.37, with a value of $C_B \sim 1.6$, as discussed in section 2.6.

and, finally,

7. The product volume fraction δ_P/δ will be computed using equation 2.63, with $\langle \theta_T(\xi_E) \rangle_\varepsilon$ given by equations 2.56 or 2.57 (or 2.53, 2.54), as appropriate.

We note that the results are rather weakly sensitive to these choices, appearing in the final expressions, by and large, as arguments of logarithms.

3.1 Comparison with chemically reacting flow data

The proposed model predictions for the chemical product volume fraction $\delta_{P1}/\delta = \xi_\phi \delta_P/\delta$, versus the stoichiometric mixture ratio ϕ, for the hydrogen-fluorine gas phase data (Mungal & Dimotakis 1984), for which

1. $Sc \approx 0.8$,

2. $U_2/U_1 \approx 0.40$,

3. $Re \approx 6.6\times10^4$,

are plotted in figure 24. The predicted values are in good agreement with the gas phase chemical product volume fraction data. The correct

prediction of the absolute amount of product is perhaps fortuitous but nevertheless noteworthy.

A plot of the δ_p/δ predicted product thickness, versus ξ_ϕ, appears in figure 25. The top solid curve and data points (circles) are transformed from figure 24. The corresponding predictions are also plotted for the liquid data (Sc ≈ 600) of Koochesfahani & Dimotakis, i.e.

1. dashed curve (inverted triangles), Re ≈ 2.3×10^4,

2. dot-dashed curve (upright triangle), Re ≈ 7.8×10^4.

As can be seen, the Schmidt number dependence of the chemical product volume fraction, at comparable Reynolds numbers, appears also to be predicted correctly. The prediction for the lower Reynolds number data is a little high. As mentioned earlier, however, it may be that the Reynolds number for those data may not be high enough.

Figure 26 depicts the model predictions (solid line, Sc ≈ 0.8) for the dependence of the product thickness δ_p/δ on Reynolds number, as compared to the gas phase data of Mungal et al (1985) and the liquid phase (dashed line, Sc ≈ 600) data of Koochesfahani & Dimotakis (1986). As can be seen, the experimentally observed drop in the chemical product volume fraction of approximately 6% per factor of two in Reynolds number in the gas phase data, appears correctly accounted for by the proposed model. We note again that the lower Reynolds number liquid phase data point of Koochesfahani & Dimotakis may be too close to the mixing transition Reynolds number regime to be considered representative of the asymptotic behavior at large Reynolds numbers.

In figure 27, we investigate the sensitivity of the predictions on the value of the log-normal distribution width Σ_ℓ. The top cusped curve is computed for a single-valued entrainment ratio of $E = \overline{E}$, where $\overline{E}$ is given by equation 2.58, i.e. a Dirac delta function probability density function $p(\xi_E) = \delta[\xi_E - \overline{E}/(\overline{E}+1)]$, corresponding to a value for

the variance of $\Sigma_\ell = 0$. The curve below the cusped curve corresponds to the Bernal value of $\Sigma_\ell = 0.28$. Finally, the bottom line corresponds to the value accepted here as representative of the entrainment ratio fluctuations as reflected in the composition within a single structure, i.e. double the Bernal value, or $\Sigma_\ell = 0.56$, and the probability density functions plotted as dashed lines in figures 22 and 23. As could have been anticipated, the effect of incorporating the expected distribution of values of the entrainment ratio is very slight and confined to the neighborhood of $\xi_\phi - \xi_{\overline{E}} = \overline{E}/(\overline{E}+1)$, corresponding to the mean entrainment ratio $\overline{E}$, and resulting in the removal of the cusp in the product thickness at $\xi_\phi = \xi_{\overline{E}}$.

As discussed earlier, the sensitivity of the computed values of the product volume fraction to the various choices of the flow constants is weak. By way of example, the smooth curves in figures 4 and 5, which do not differ substantially from those in figures 24 and 25, were computed using a value of $\beta = 5$, leaving other constants at their nominal values.

3.2 The mixed fluid fraction

An important quantity in turbulent mixing is the mixed fluid fraction within the turbulent zone. It is to the mixing scalar (or scalar dissipation) field what intermittency is to the turbulent velocity (or energy dissipation) field. Operationally, it can be defined through the probability density function (PDF) of the conserved scalar, i.e. $p(\xi)$, integrated across the shear layer width. In particular the quantity

$$\frac{\delta_m(Sc,Re)}{\delta} = \int_{\xi_1}^{1-\xi_1} p(\xi,Sc,Re)\, d\xi \,, \qquad (3.1)$$

for some small value of ξ_1 which excludes the unmixed fluid

contributions from the neighborhood of $\xi \sim 0$ and $\xi \sim 1$, represents the volume fraction occupied by molecularly mixed fluid within the transverse extent of the turbulent shear layer. This quantity can be expected to be a function of the fluid Schmidt number and the flow Reynolds number (and potentially also of the free stream density ratio and velocity ratio). In particular, we would expect that an increase in the Schmidt number, at fixed Reynolds number, should result in a decrease of δ_m/δ, which should vanish in the limit of infinite Schmidt numbers. An a priori assessment of the behavior of the mixed fluid fraction at fixed Schmidt number in the limit of very large Reynolds numbers cannot be made as readily and will be discussed separately below.

While the integral indicated in equation 3.1 can, in principle, be estimated by direct measurement of the scalar field $\xi(\underline{x},t)$, and therefore also its PDF $p(\xi)$, it was pointed out by Breidenthal (1981) and Koochesfahani & Dimotakis (1986) that, as a consequence of the inevitable experimental finite resolution difficulties at high Reynolds numbers, such measurements will generally overestimate this quantity. It was also pointed out in Koochesfahani & Dimotakis, however, that reliable estimates are possible using the results of chemically reacting experiments, namely the chemical product fractions $\delta_P(\xi_o)/\delta$ and $\delta_P(1-\xi_o)/\delta$ from a "flip" experiment conducted at ϕ_o and $1/\phi_o$, for small values of ϕ_o, corresponding to a $\xi_o = \phi_o/(1+\phi_o) \ll 1$. In particular, the mixed fluid fraction can be estimated in terms of the chemically reacting flow results by means of the relation

$$\frac{\delta_m}{\delta} \approx \frac{1-\xi_o}{\delta}\left[\,\delta_P(\xi_o) + \delta_P(1-\xi_o)\,\right]. \qquad (3.2)$$

This is very close to the expression in equation 3.1 and is equivalent to computing the integral of the product of the probability density function with a "mixed fluid" function $\theta_m(\xi)$ given by,

$$\theta_m(\xi) = \begin{cases} \dfrac{\xi}{\xi_o} & , \quad \text{for } 0 \le \xi < \xi_o \ , \\ 1 & , \quad \text{for } \xi_o < \xi < 1 - \xi_o \ , \\ \dfrac{1-\xi}{\xi_o} & , \quad \text{for } 1 - \xi_o < \xi < 1 \ , \end{cases} \tag{3.3a}$$

i.e.

$$\frac{\delta_m}{\delta} \approx \int_0^1 \theta_m(\xi)\, p(\xi)\, d\xi \ . \tag{3.3b}$$

See figure 28. We should note that if the curvature in $p(\xi)$ in the regions $0 < \xi < \xi_o$ and $1 - \xi_o < \xi < 1$ can be ignored, this expression reproduces the result of equation 3.1 for $\xi_1 \approx \xi_o/2$.

Gas phase (Sc ~ 0.8) "flip" experiments ($\phi_o = 1/8$) are available from Mungal & Dimotakis (1984) at a Reynolds number of 6.6×10^4 (see figure 25). The liquid phase (Sc ~ 600) "flip" experiments ($\phi_o = 1/10$) of Koochesfahani & Dimotakis (1986) were at a lower Reynolds number (Re ~ 2.3×10^4). The value of δ_p/δ for their higher Reynolds number data at $\phi = 10$, however, is so close to their corresponding lower Reynolds number value (see figure 26) that the Reynolds number dependence of the liquid data can probably be ignored as a first approximation in comparing the gas phase and liquid phase results to assess the Schmidt number dependence of δ_m/δ .

A plot of the model estimate for the mixed fluid volume fraction $\delta_m(Sc,Re)/\delta$, using a value for ϕ_o of 1/8 corresponding to the gas phase data, is depicted in figure 29 as a function of Schmidt number. The plot ranges from a value of the Schmidt number of 0.01 , as would be appropriate in estimating the fluid at an intermediate temperature in a two-temperature free stream shear layer in mercury, for example, to a Schmidt number of 10^6 , as would be appropriate for mixing of a particulate cloud that diffuses via Brownian motion. The solid line in that figure is for Re $\approx 6.6 \times 10^4$ corresponding to the gas phase data.

The circle represents the gas phase experimental value while the triangle represents the liquid phase data. The other dashed lines are for $Re \approx 10^4$, 10^5 and 10^6, respectively, in order of decreasing values of δ_m/δ. The corresponding estimates using the Broadwell-Breidenthal model, with the values of the coefficients c_H and c_F in that model derived by fitting the gas/liquid difference (at low ϕ) of these data (equation 1.13), are plotted in figure 30 for comparison.

3.3 Discussion & conclusions

Several features of the predictions of the proposed theory for the expected mixed fluid or chemical product volume fraction, within the transverse extent of the shear layer, may merit discussion.

The absolute amount of molecular mixing appears to be estimated correctly, as a function of the Schmidt number and Reynolds number of the flow, with no adjustable parameters. The various experimental values for the parameters used in the theory pertain to the statistics of the turbulent velocity (and dissipation) fields, which are assumed given. In particular, they are not derived from the results of mixing or chemically reacting experiments, which the theory attempts to describe. Moreover, the theory is relatively robust in that variations within the admissible range of these parameters do not have a significant effect on the predictions. The usually difficult question of an a priori estimate of intermittency, or, in the present context, of the volume fraction in the flow occupied by unmixed (unreacted) fluid, is addressed through an attempt to normalize the volume-filling spectrum of scales. Finally, except for switching (matched) analytical expressions, depending on the relative magnitudes of the various (inner) scales of the problem (λ_D, λ_H, λ_C), liquids and gases are treated in a unified way through the explicit dependence of the results on Schmidt number.

The theory also predicts that, at sufficiently high Reynolds numbers, the amount of mixed fluid or chemical product in a gas phase shear layer would be less than what would be observed in a liquid layer at sufficiently low Reynolds numbers (recall figure 3.6). In fact, the interesting prediction is that the volume fraction of the mixed fluid tends to zero with increasing Reynolds number, albeit slowly, possessing no Reynolds number independent asymptotic (non-zero) value. This is perhaps a controversial result, as one might intuitively argue that as the Reynolds number increases, the interfacial surface area available for mixing must increase (under the action of the higher sustainable strain rates in the flow) and therefore also the mixing rate. This argument, however, is incomplete in that it fails to recognize that the thickness of the mixed fluid layer straddling the interface must be decreasing, in fact, approximately inversely as the interface area is increasing, by the force of the same arguments. Consequently, these two effects must approximately cancel each other. In particular, the model predicts that as the Reynolds number increases, the associated diffused layer thickness must be decreasing at a slightly faster rate, since the flow volume fraction occupied by the mixed fluid is decreasing (slowly) with increasing Reynolds number. This behavior is corroborated by the limited data available, which indicate a monotonically decreasing volume fraction of chemical product with increasing Reynolds number, in good quantitative agreement with the predicted Reynolds number dependence.

It should be emphasized that the prediction is not that mixing ceases in the limit of infinite Reynolds numbers. If one were to increase the Reynolds number by increasing the downstream coordinate x, for example, the integrated mixed fluid thickness $\delta_m(x)$ would increase almost proportionally to the shear layer thickness $\delta(x)$, specifically

$$\delta_m(x) \sim \frac{b_1(Sc)}{b_0(Sc) + \ln(x/x_t)} \delta(x) . \qquad (3.4a)$$

Consequently, however, the mixed fluid volume fraction would decrease logarithmically, or in terms of the Reynolds number,

$$\frac{\delta_m}{\delta} \sim \frac{B_1(Sc)}{B_0(Sc) + \frac{3}{4}\left(1 - \frac{\mu}{8}\right) \ln\left(\frac{Re}{Re_{cr}}\right)} \,. \tag{3.4b}$$

This result is a direct consequence of the assumed statistical weight and normalization over the range of scales of the problem. In particular, accepting the $W(\lambda)\, d\lambda \sim d\lambda/\lambda$ statistical weight for the moment, the dependence on the local Reynolds number enters through the ratio of the outer large scale δ to the inner scale $\lambda_c = \beta^{3/2} \lambda_K$, where $\beta = 2\sqrt{3}$ and λ_K is the Kolmogorov scale, i.e.

$$\frac{\delta_m}{\delta} \sim \frac{B_1(Sc)}{B_0(Sc) + \left\langle \ln\left(\frac{\delta}{\lambda_c}\right) \right\rangle_\varepsilon} \,. \tag{3.5}$$

The subscripted angle brackets denote the ensemble average over the fluctuations in the local dissipation rate. We note here that a non-zero asymptotic value for δ_m/δ at high Reynolds numbers would be the prediction only if $\langle \ln(\delta/\lambda_K) \rangle_\varepsilon \to$ constant, as $Re \to \infty$.

We have examples of such behavior in high Reynolds number turbulent flows. In particular, the skin friction coefficient for a turbulent boundary layer over a (smooth) flat plate at high Reynolds number appears to decrease logarithmically with Reynolds number. For similar reasons, the pressure gradient coefficient for turbulent (smooth wall) pipe flow also decreases logarithmically with Reynolds number. It is interesting to note, however, that in these examples, the behavior will asymptote to a Reynolds number independent regime, if the wall cannot be considered smooth compared to the smallest scales the turbulence can sustain and interferes with their participation in the dynamics; if a Reynolds number independent minimum scale is imposed on the dynamics of

the flow. Analogously, in my opinion, the assignment of an Eulerian, Reynolds number independent volume fraction occupied by the homogeneously mixed fluid in the Broadwell-Breidenthal model leads perforce to a Reynolds number independent mixed fluid (and chemical product) volume fraction in the limit of large Reynolds numbers. In a free shear layer, however, in which the turbulence does not have to contend with any intruding rough walls or externally imposed minimum scales, the flow will generate its minimum (dissipation/diffusion) scales, of ever decreasing size as the Reynolds number increases, and which will participate in the mixing and dissipation dynamics unimpeded.

We should recognize, however, that the Broadwell-Breidenthal argument is not Eulerian. These authors integrated the cascade time scale associated with each scale λ and concluded that the Lagrangian time to cascade to the Kolmogorov scale becomes independent of the Reynolds number at high Reynolds numbers. This is a central idea in the Broadwell-Breidenthal model. If one accepts it, one must also accept that fluid entrained at an upstream station x_1 cascades to the diffusion (Kolmogorov) scale by a station x_K, such that x_K/x_1 is independent of the Reynolds number. The argument is important and, if correct, difficult to reconcile with the proposed predicted shear layer mixing behavior at high Reynolds numbers.

We shall examine the Broadwell-Breidenthal argument by inverting equation 2.7 to yield the scaling for the differential time required to cascade from λ to $\lambda + d\lambda$. In particular, we have

$$-dt \sim \frac{1}{\sigma(\lambda)} \frac{d\lambda}{\lambda} \sim \frac{1}{\varepsilon^{1/3}} \frac{d\lambda}{\lambda^{1/3}} ,$$

where $\varepsilon = \alpha (\Delta U)^3/\delta$ is the dissipation rate. We note here that in their analysis, the dissipation rate was treated as a constant during the cascade. This is not a valid approximation for two reasons. First, because the distance to cascade is not small, corresponding to a non-negligible change in $\delta = \delta(x)$ in the process, and second, because α

must be considered as a random variable with a Reynolds number dependent variance. We can respond to these objections, however, by a proper separation of the problem variables, i.e.

$$- \varepsilon^{1/3}(t)\, dt \sim \lambda^{-1/3}\, d\lambda \ .$$

Substituting for the dissipation rate and transforming to δ as the independent variable, we then obtain

$$- \alpha^{1/3}(\delta)\, \frac{d\delta}{\delta^{1/3}} \sim \lambda^{-1/3}\, d\lambda \ .$$

This can be integrated from a thickness $\delta_1 = \delta(x_1)$ to a thickness $\delta_K = \delta(x_K)$ to yield

$$\int_{\delta_1}^{\delta_K} \alpha^{1/3}(\delta)\, \frac{d\delta}{\delta^{1/3}} \sim \delta_1^{2/3} \ ,$$

where we have used that $\lambda_K \ll \delta_1$. To estimate the effect of the fluctuations in α we compute the expectation value of the left hand side, which for the purposes of the scaling estimate we will commute with the integration to write

$$\int_{\delta_1}^{\delta_K} \langle \alpha^{1/3} \rangle_\varepsilon\, \frac{d\delta}{\delta^{1/3}} \sim \delta_1^{2/3} \ .$$

As before, the subscripted angle brackets denote the expectation value over the distribution of values of the dissipation rate. This can be estimated using the methods outlined in section 2.7 and we obtain

$$\langle \alpha^{1/3} \rangle_\varepsilon \sim \left(\bar{\alpha} \right)^{1/3} \left(\frac{Re}{Re_{cr}} \right)^{-\mu/12}$$

(recall $\mu \approx 0.3$). Substituting in our previous expression yields the

desired result, i.e.

$$\frac{x_K}{x_1} \sim \frac{1}{\bar{\alpha}^{1/2}} \left(\frac{Re_1}{Re_{cr}} \right)^{\mu/8} , \tag{3.6}$$

where Re_1 is the Reynolds number at $x = x_1$. While the preceding argument is not without its own shortcomings, we nevertheless note that, if we accept $\bar{\alpha}$ as a non-increasing function of the Reynolds number, we must admit the possibility that the distance to cascade is not Reynolds number independent.

This is an interesting observation, bearing also on Saffman's (1968) concern that the available arguments in support of the assumption that $\bar{\alpha}$ itself is Reynolds number independent may not be sufficiently compelling. We should mention, however, that the conclusions of the present model would survive in the event (which has not been really disallowed). In particular, a weak dependence of $\bar{\alpha}$ on Reynolds number, say,

$$\bar{\alpha} \sim \bar{\alpha}_0 \left(\frac{Re}{Re_0} \right)^{-p} ,$$

where presumably $p \ll 1$, would produce only minor changes in the results (see equations 2.48 and 2.49). A weaker possible dependence, e.g. logarithmic, need not even be incorporated as a correction.

Finally, we note that the predicted asymptotic behavior in the limit of infinite Reynolds numbers is traceable to the assumed statistical weight distribution of scales in the inertial range, i.e. $W(\lambda)\, d\lambda \sim d\lambda/\lambda$, as discussed in section 2.6. A very small deviation from this expression, for example

$$W(\lambda)\, d\lambda \sim \left(\frac{\delta}{\lambda} \right)^r \frac{d\lambda}{\lambda} ,$$

where $|r| \ll 1$†, would produce only minor differences in the range of Reynolds numbers of practical interest, but would alter the conclusions in the limit. In particular, the mixed fluid fraction would tend to a (small) non-zero asymptotic value in the limit of large Reynolds numbers, or to zero (with a weak power dependence on Re), depending on the sign of the exponent r and the (possible) dependence of the scaled mean dissipation rate $\bar{\alpha}$ on the Reynolds number.

We conclude by observing that, from an engineering vantage point, the amount of mixed fluid within the shear layer, i.e. δ_m/δ, is expected to possess a (broad) maximum at a Reynolds number in the range of 2×10^4 to 3×10^4 (based on the local thickness δ and velocity difference ΔU). This corresponds to the region shortly after the flow has emerged from its "mixing" transition (Bernal et al 1979) to a fully three dimensional, turbulent state.

---

† This is admissible under the revised similarity hypotheses of Kolmogorov (1962) and Obukhov (1962), or the fractal ideas put forth by Mandelbrot (e.g. 1976). On the other hand, if a power law is appropriate, the exponent r is likely to be small because the argument of no characteristic length scale in the inertial range, leading to the $d\lambda/\lambda$ distribution, must very nearly be right.

ACKNOWLEDGMENTS

I would like to acknowledge the many discussions within the GALCIT community, which directly or indirectly have contributed to this paper. Without wishing to imply endorsement, I would specifically like to acknowledge discussions with Dr. J. Broadwell, Prof. R. Narasimha and Prof. P. Saffman. Additionally, the critical comments by Prof. A. Leonard and Mr. P. Miller contributed to important improvements and clarifications in the final form of the text. Finally, I would like to thank Mr. C. Frieler for performing the numerical integration of the differential equation for the velocity correlation function $h(\zeta)$ in section 2.6 .

This work is part of a larger effort to investigate mixing and combustion in turbulent shear flows, sponsored by the Air Force Office of Scientific Research Contract No. F49620-79-C-0159 and Grant No. AFOSR-83-0213, whose support is gratefully acknowledged.

REFERENCES

ASHURST, W. T., KERSTEIN, A. R., KERR, R. M. and GIBSON, C. H. [1987] "Alignment of Vorticity and Scalar Gradient with Strain Rate in Simulated Navier-Stokes Turbulence", SAND86-8809 Report (submitted to the Phys. Fluids).

BATCHELOR, G. K. [1959] "Small-scale variation of convected quantities like temperature in turbulent fluid. Part 1. General discussion and the case of small conductivity", J. Fluid Mech. 5, 113-133

BATCHELOR, G. K., HOWELLS, I. D. and TOWNSEND, A. A. [1959] "Small-scale variation of convected quantities like temperature in turbulent fluid. Part 2. The case of large conductivity", J.

Fluid Mech. 5, 134-139.

BERNAL, L. P. [1981] The Coherent Structure of Turbulent Mixing Layers. I. Similarity of the Primary Vortex Structure, II. Secondary Streamwise Vortex Structure, Ph.D. Thesis, California Institute of Technology.

BERNAL, L. P., BREIDENTHAL, R. E., BROWN, G. L., KONRAD, J. H. and ROSHKO, A. [1979] "On the Development of Three Dimensional Small Scales in Turbulent Mixing Layers.", 2nd Symposium on Turbulent Shear Flows, 2-4 July 1979, Imperial College, England.

BETCHOV, R. [1977] "Transition", Handbook of Turbulence I (Ed. W. Frost and T. H. Moulden, Plenum Press), 147-164.

BETCHOV, R. and SZEWCZYK, A. [1963] "Stability of a shear layer between parallel streams", Phys. Fluids 6, 1391-96.

BILGER, R. W. [1980] "Turbulent Flows with Nonpremixed Reactants", Turbulent Reacting Flows (Springer-Verlag, Topics in Applied Physics 44, 1980, Ed. P. A. Libby, F. A. Williams), 65-113.

BREIDENTHAL, R. E. [1981] "Structure in Turbulent Mixing Layers and Wakes Using a Chemical Reaction", J. Fluid Mech. 109, 1-24.

BROADWELL, J. E. and BREIDENTHAL, R. E. [1982] "A Simple Model of Mixing and Chemical Reaction in a Turbulent Shear Layer", J. Fluid Mech. 125, 397-410.

BROADWELL, J. E. and DIMOTAKIS, P. E. [1986] "Implications of Recent Experimental Results for Modeling Reactions in Turbulent Flows", AIAA J. 24(6), 885-889.

BROADWELL, J. E. and MUNGAL, M. G. [1986] "The effects of Damköhler number in a turbulent shear layer", GALCIT Report FM86-01.

BROWN, G. L. and REBOLLO, M. R. [1972] "A Small, Fast-Response Probe to Measure Composition of a Binary Gas Mixture", AIAA J. 10(5), 649-652.

BROWN, G. L. and ROSHKO, A. [1974] "On Density Effects and Large Structure in Turbulent Mixing Layers", J. Fluid Mech. 64(4), 775-816.

DIMOTAKIS, P. E. [1986] "Two-Dimensional Shear-Layer Entrainment", AIAA J. 24(11), 1791-1796.

DIMOTAKIS, P. E. and BROWN, G. L. [1976] "The Mixing Layer at High Reynolds Number: Large-Structure Dynamics and Entrainment", J. Fluid Mech. 78(3), 535-560 + 2 plates.

FIEDLER, H. E. [1975] "On Turbulence Structure and Mixing Mechanism in Free Turbulent Shear Flows", from: (S. N. B. Murthy, Ed.) Turbulent Mixing in Non-Reactive and Reactive Flows (Plenum Press), 381-409.

GIBSON, C. H. [1968] "Fine Structure of Scalar Fields Mixed by Turbulence. II. Spectral Theory", Phys. Fluids 11(11), 2316-2327.

GURVICH, A. S. and YAGLOM, A. M. [1967] "Breakdown of Eddies and Probability Distributions for Small Scale Turbulence", Phys. Fluids (1967 Sup.), 59-65.

HERMANSON, J. C., MUNGAL, M. G. and DIMOTAKIS, P. E. [1987] "Heat Release Effects on Shear Layer Growth and Entrainment", AIAA 23rd Aerospace Sciences Meeting 14-17 January 1985 (Reno, Nevada), AIAA J. 25(4), 578-583 (AIAA Paper 85-0142).

KERR, R. M. [1985] "Higher-order derivative correlations and the alignement of small-scale structures in isotropic numerical turbulence", J. Fluid Mech. 153, 31-58.

KOLLMAN, W. [1984] "Prediction of intermittency factor for turbulent shear flows", AIAA J. 22(4), 486-492.

KOLLMANN, W. and JANICKA, J. [1982] "The Probability Density Function of a Passive Scalar in Turbulent Shear Flows", Phys. Fluids 25, 1755-1769.

KOLMOGOROV, A. N. [1941] "Local structure of turbulence in an incompressible viscous fluid at very high Reynolds numbers", Dokl. Akad. Nauk SSSR 30, 299, reprinted in Usp. Fiz. Nauk 93, 476-481 (1967), translated into English in Sov. Phys. Usp. 10(6), 734-736 (1968).

KOLMOGOROV, A. N. [1962] "A refinement of previous hypotheses concerning the local structure of turbulence in a viscous incompressible fluid at high Reynolds number", J. Fluid Mech 13, 82-85 (translation of the Russian text of the lecture by the author at the Colloque International du C.N.R.S de Mèchanique de la Turbulence, Marseilles 28-Aug to 2-Sep 1961).

KONRAD, J. H. [1976] An Experimental Investigation of Mixing in Two-Dimensional Turbulent Shear Flows with Applications to Diffusion-Limited Chemical Reactions, Ph.D. Thesis, California Institute of Technology, and Project SQUID Technical Report CIT-8-PU (December 1976).

KOOCHESFAHANI, M. M. and DIMOTAKIS, P. E. [1986] "Mixing and chemical reactions in a turbulent liquid mixing layer", J. Fluid Mech. 170, 83-112.

LUNDGREN, T. S. [1982] "Strained Spiral Vortex Model for Turbulent Fine Structure", Phys. Fluids 25(12), 2193-2203.

LUNDGREN, T. S. [1985] "The concentration spectrum of the product of a fast bimolecular reaction", Chem. Eng. Sc. 40(9), 1641-1652.

MANDELBROT, B. [1976] "Intermittent turbulence and fractal dimension: kurtosis and the spectral exponent 5/3 + B", Turbulence and the Navier Stokes Equations (Conf. Proc., U. Paris-Sud, Orsay, 12-13 June 1975, Publ: Lecture Notes in Mathematics 565, Ed. A. Dold, B. Eckmann, Springer-Verlag), 121-145.

MAARBLE, F. E. and BROADWELL, J. E. [1977] "The coherent flame model for turbulent chemical reactions", Project SQUID Technical Report TRW-9-PU.

MONIN, A. S. and YAGLOM, A. M. [1975] Statistical Fluid Mechanics: Mechanics of Turbulence 2 (English translation of the 1965 Russian text. Ed. J. L. Lumley, MIT Press).

MUNGAL, M. G. and DIMOTAKIS, P. E. [1984] "Mixing and combustion with low heat release in a turbulent mixing layer", J. Fluid Mech. 148, 349-382.

MUNGAL, M. G, HERMANSON, J. C. and DIMOTAKIS, P. E. [1985] "Reynolds Number Effects on Mixing and Combustion in a Reacting Shear Layer", AIAA J. 23(9), 1418-1423.

NOVIKOV, E. A. [1961] "Energy Spectrum of an Incompressible Fluid in Turbulent Flow", Reports Ac. Sc. USSR 139(2), 331-334, translated in Sov. Phys. Doklady 6(7), 571-573 (1962).

OBUKHOV, A. M. [1962] "Some specific features of atmospheric turbulence", J. Fluid Mech. 13, 77-81.

POPE, S. B. [1985] "PDF Methods for Turbulent Reactive Flows", Prog. Energy Comb. Sc. 11, 119-192.

ROGERS, M. M., MOIN, P. and REYNOLDS, W. C. [1986] "The Structure and Modeling of the Hydrodynamic and Passive Scalar Fields in Homogeneous Turbulent Shear Flow", Stanford University Report TF-25.

ROSHKO, A. [1976] "Structure of Turbulent Shear Flows: A New Look", AIAA J. 14, 1349-1357, and 15, 768.

SAFFMAN, P. G. [1968] Topics in Non-Linear Physics (Ed. N. Zabusky, Springer-Verlag, Berlin), 485-614.

SPENCER, B. W. and JONES, B. G. [1971] "Statistical Investigation of Pressure and Velocity Fields in the Turbulent Two Stream Mixing Layer", AIAA Paper No. 71-613.

SREENIVASAN, K. R., TAVOULARIS, S. and CORRSIN, S. [1981] "A Test of Gradient Transport and its Generalizations", 3rd International Symposium on Turbulent Shear Flows, U. C. Davis, 9-11 September 1981 (Published by Springer-Verlag 1982, Eds. Bradbury, L. J. S., Durst, F., Launder, B. E., Schmidt, F. W. and Whitelaw, J. H. Turbulent Shear Flows 3), 96-112.

TENNEKES, H. and LUMLEY, J. L. [1972] A First Course in Turbulence (MIT Press).

TOWNSEND, A. A. [1951] "On the fine structure of turbulence" Proc. Roy. Soc. A 208, 534-542.

VAN ATTA, C. W. and ANTONIA, R. A. [1980] "Reynolds number dependence of skewness and flatness factors of velocity derivatives", Phys. Fluids 23(2), 252-257.

WYGNANSKI, I. and FIEDLER, H. E. [1970] "The Two Dimensional Mixing Region", J. Fluid Mech. 41(2), 327-361.

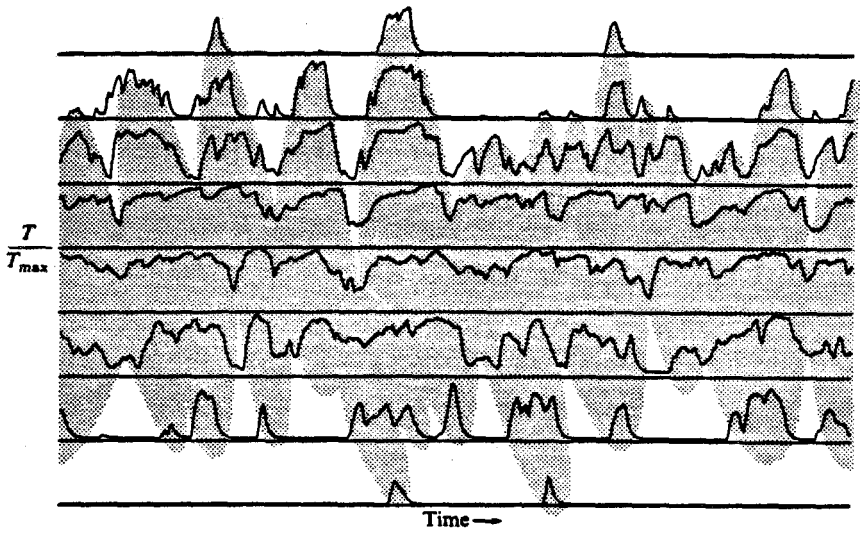

FIGURE 1. Temperature vs. time time traces for $\phi = 1$, $\Delta T_{flm} = 93$ K High speed ($U_1 = 22$ m/s) fluid (1% F_2 + 99% N_2) on top trace. Low speed ($U_2 = 8.8$ m/s) fluid (1% H_2 + 99% N_2) on bottom. Probe positions at y/x = 0.076, 0.057, 0.036, 0.015, -0.008, -0.028, -0.049, -0.070. Partial record of 51.2 ms span ($\Delta T_{max} = 81$ K). From Mungal & Dimotakis (1984, figure 4b).

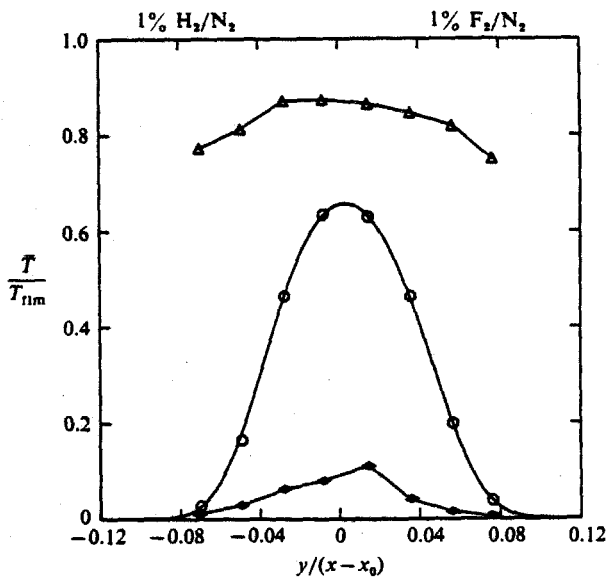

FIGURE 2. Peak, mean and minimum teperatures observed for total record at each station. Experimental parameters as in figure 1. Smooth curve least squares fitted through mean data points. From Mungal & Dimotakis (1984, figure 4c).

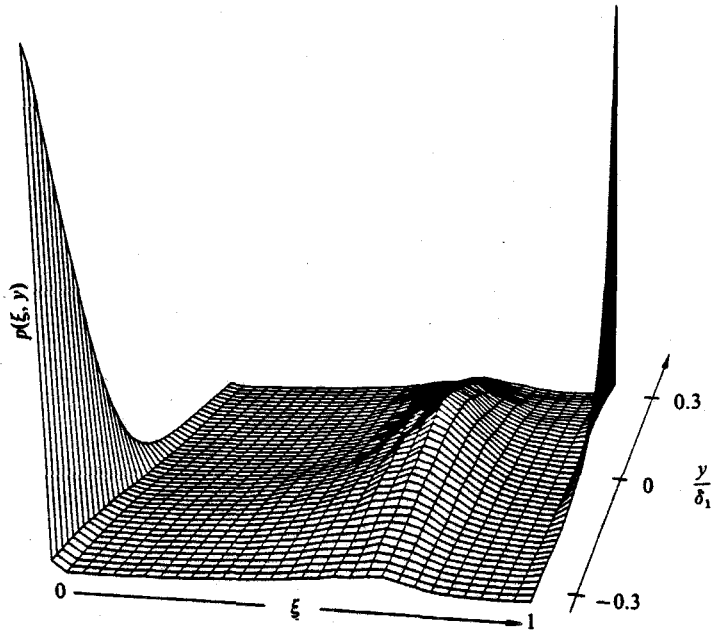

FIGURE 3. Probability density function of the high speed fluid mixture fraction in a liquid layer ($U_2/U_1 \approx 0.38$, $Re \approx 2.3\times10^4$). $\xi \approx 0$ corresponds to low speed fluid, $\xi \approx 1$ corresponds to high speed fluid. From Koochesfahani & Dimotakis (1986, figure 10).

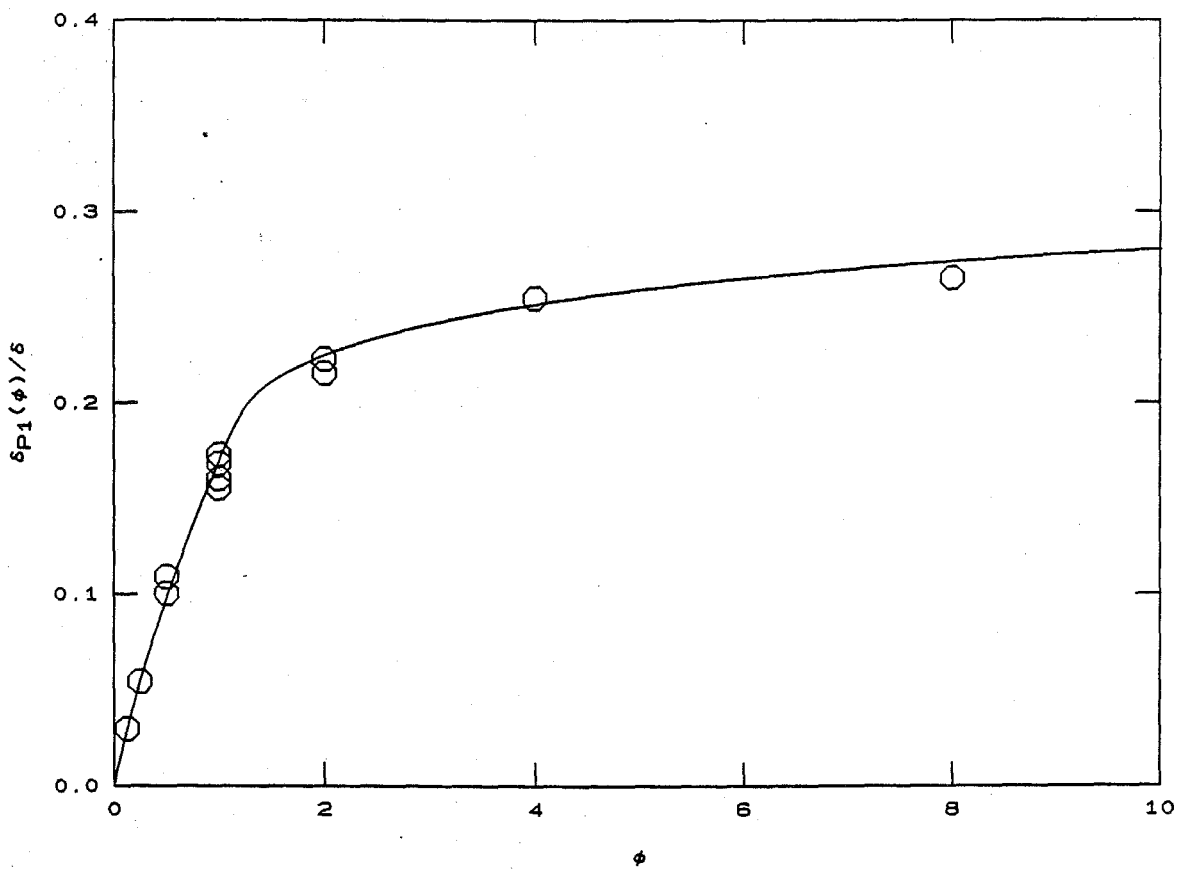

FIGURE 4. Normalized δ_{P1}/δ HF gas phase chemical product thickness (Mungal & Dimotakis 1984) data vs. stoichiometric mixture ratio ϕ. $U_2/U_1 \approx 0.38$, $Re \approx 6.6\times10^4$. Smooth curve drawn to aid the eye.

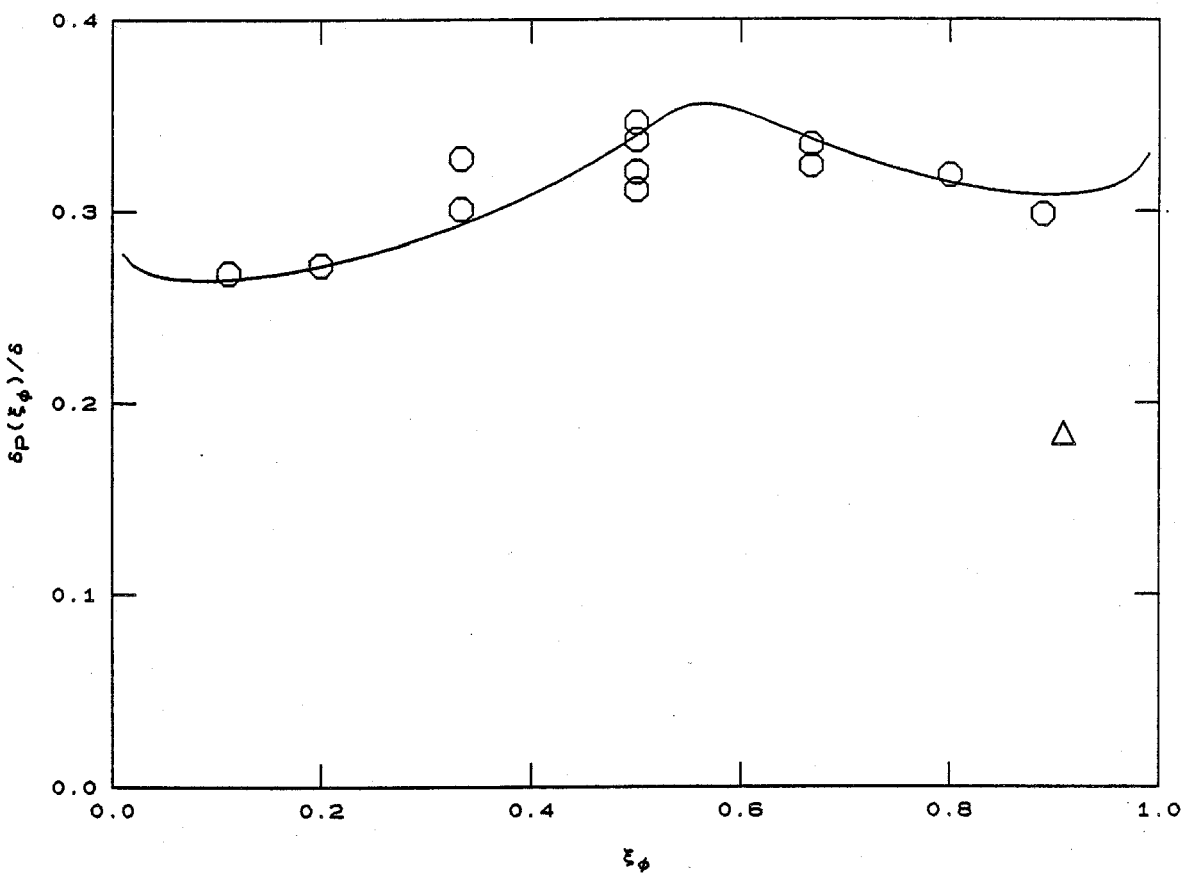

FIGURE 5. Chemical product δ_p/δ volume fraction data vs. stoichiometric mixture fraction ξ_ϕ. Circles from gas phase Mungal & Dimotakis (1984) data (see figure 4). Triangle from liquid phase Koochesfahani & Dimotakis (1986) data ($U_2/U_1 \approx 0.4$, $Re \approx 7.8\times10^4$). Smooth curve transformed from figure 4.

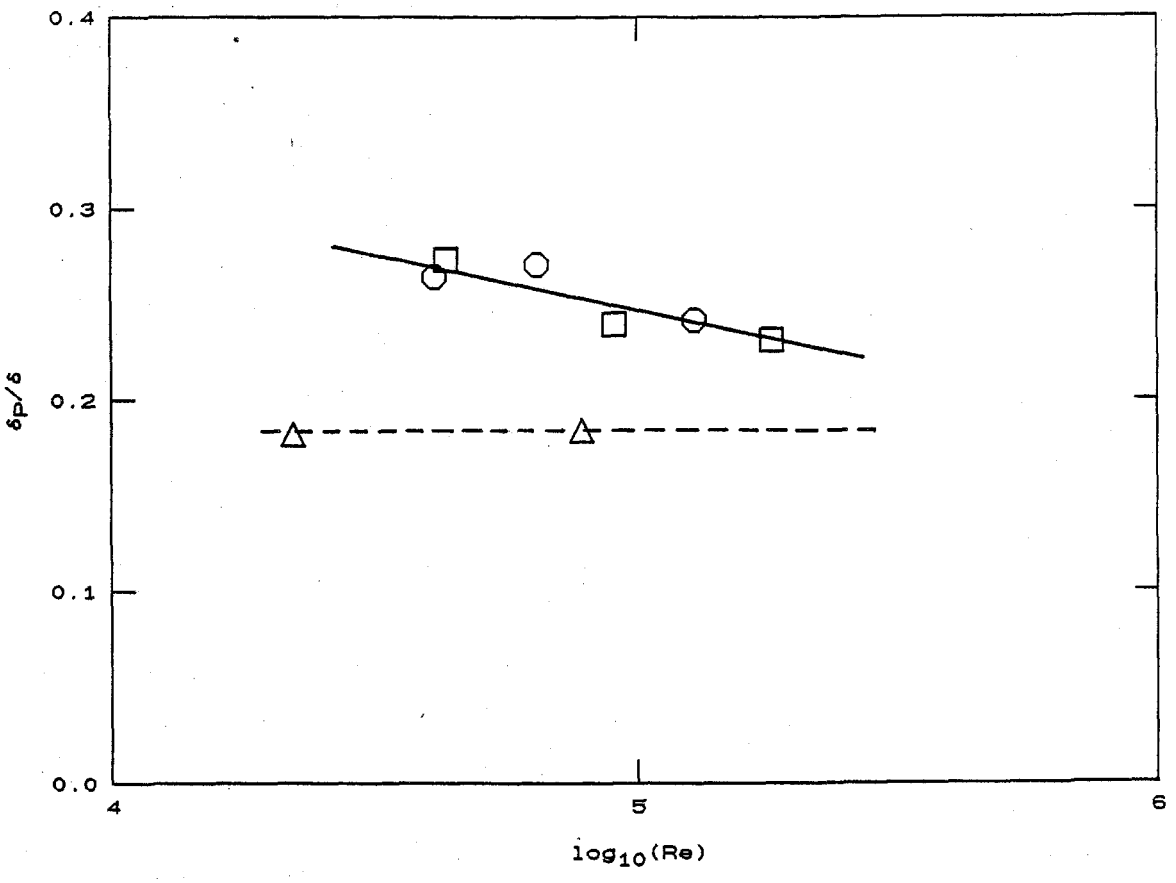

FIGURE 6. Chemical product δ_p/δ volume fraction versus Reynolds number. Circles and squares are for gas phase data (Mungal et al 1985) at ϕ = 1/8. Circles are for initially laminar splitter plate boundary layers, squares for turbulent boundary layers. Triangles for liquid phase data from Koochesfahani & Dimotakis (1986), at ϕ = 10.

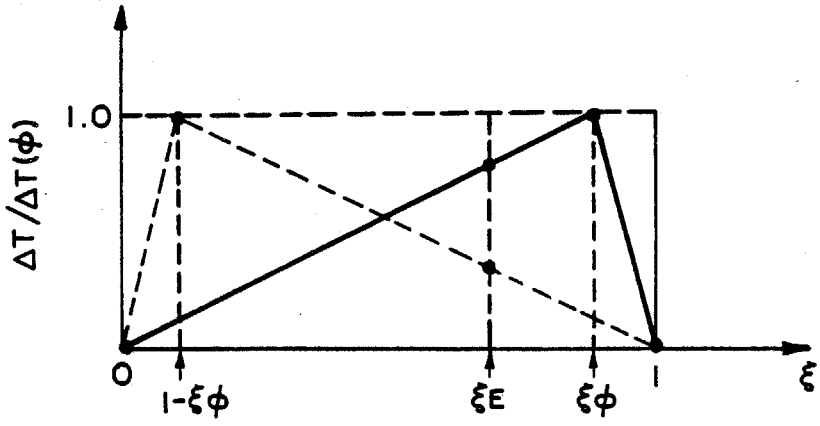

FIGURE 7. Normalized temperature rise for free stream fluids at a stoichiometric mixture fraction $\xi_\phi = \phi/(\phi+1)$, as a function of the high speed mixture fraction ξ. Dashed triangle indicates corresponding function for a "flip" experiment and the resulting temperature rise for a mixture at the entrainment mixture fraction $\xi_E = E/(E+1)$.

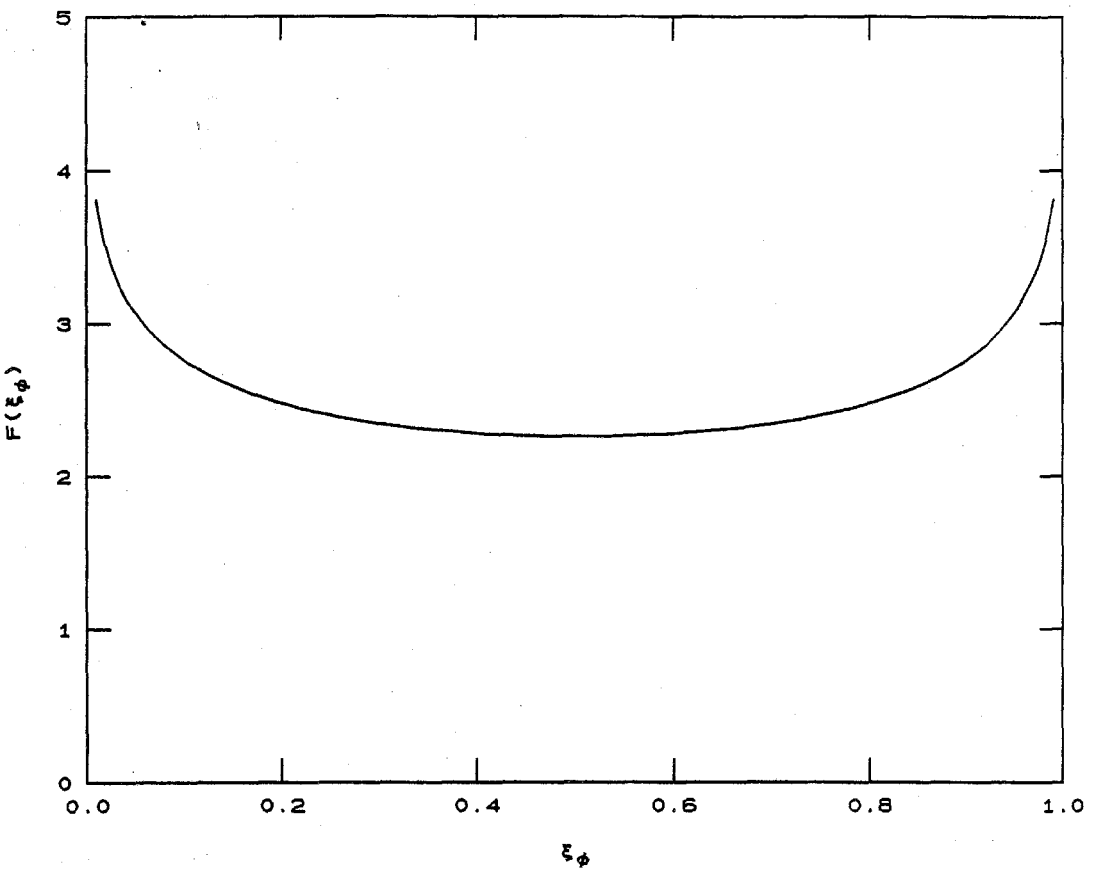

FIGURE 8. Marble & Broadwell (1977) flame sheet function $F(\xi_\phi)$.

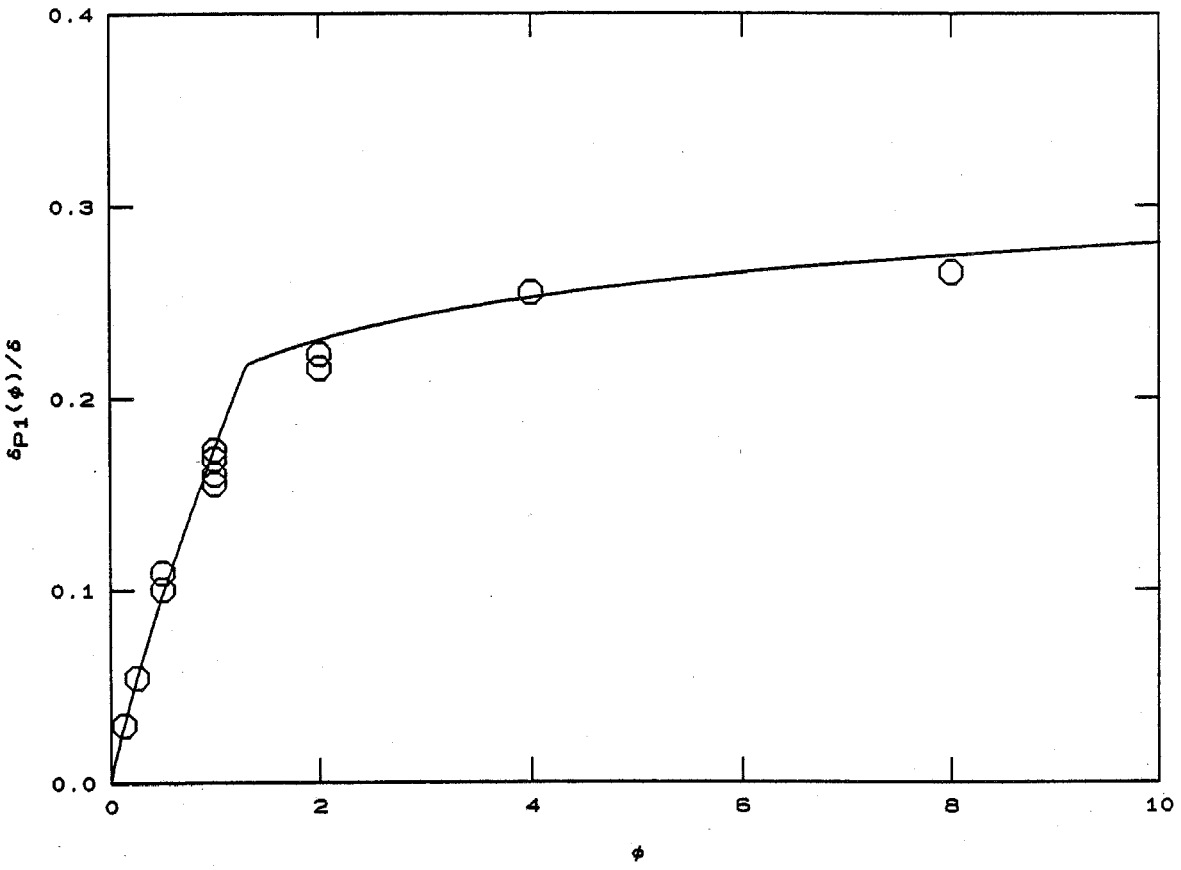

FIGURE 9. Broadwell-Breidenthal model predictions for δ_{P1}/δ gas phase product thickness data of Mungal & Dimotakis (1984) at Sc = 0.8 and Re = 6.6×10^4.

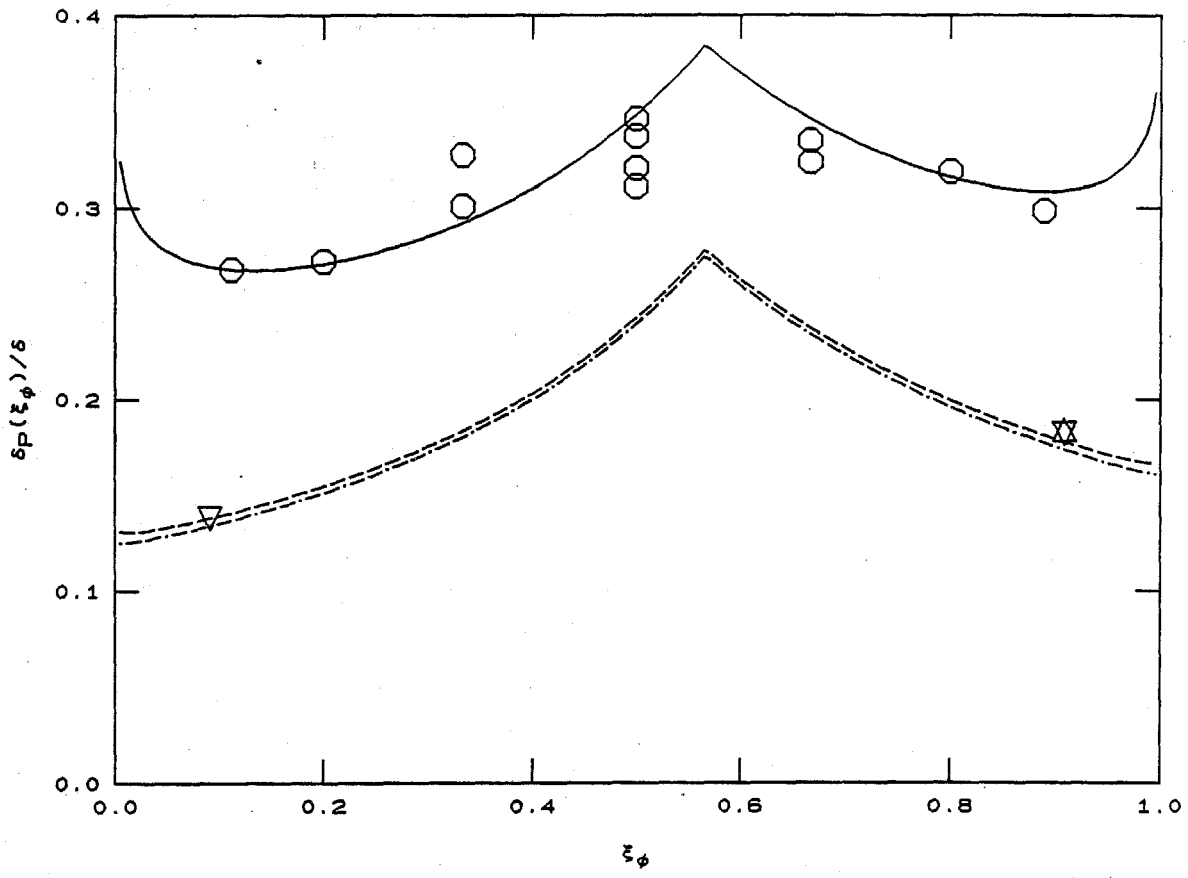

FIGURE 10. Broadwell-Breidenthal model predictions for δ_p/δ vs. ξ_ϕ data. Solid line for gas phase data (circles; Sc ≈ 0.8, Re ≈ 6.6×10^4, Mungal & Dimotakis 1984). Dashed line for liquid phase (Sc ≈ 600, Koochesfahani & Dimotakis 1986) data (inverted triangles; Re ≈ 2.3×10^4). Dot-dashed line for higher Reynolds number point (upright triangle; Re ≈ 7.8×10^4).

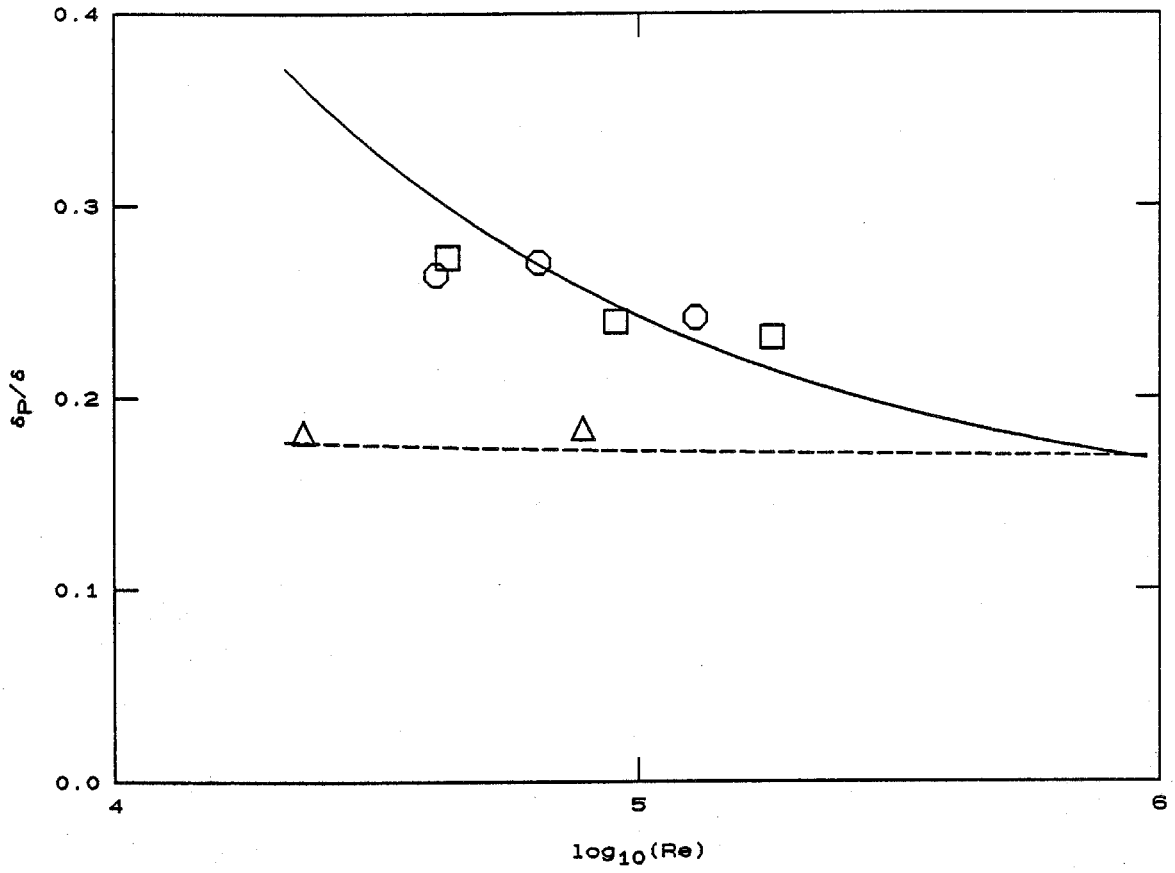

FIGURE 11. Broadwell-Breidenthal model predictions for δ_p/δ dependence on Reynolds number. Solid curve for gas phase data (Mungal et al 1985) at $\phi = 1/8$. Dashed curve for liquid phase data (Koochesfahani & Dimotakis 1986) at $\phi = 10$. Note that curves cross as a result of the larger homogeneously mixed fluid contribution for the liquid phase data at large ϕ.

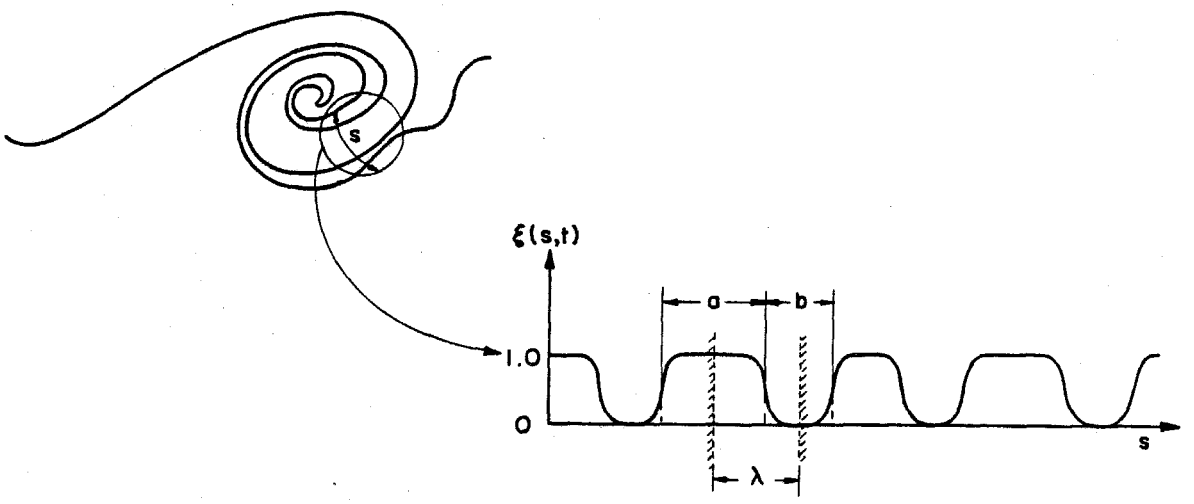

FIGURE 12. Shear layer mixing interface. Inset curve depicts values at fixed time of the conserved scalar $\xi(s,t)$ as a function of the arc length s on a line in the direction of $\nabla\xi$.

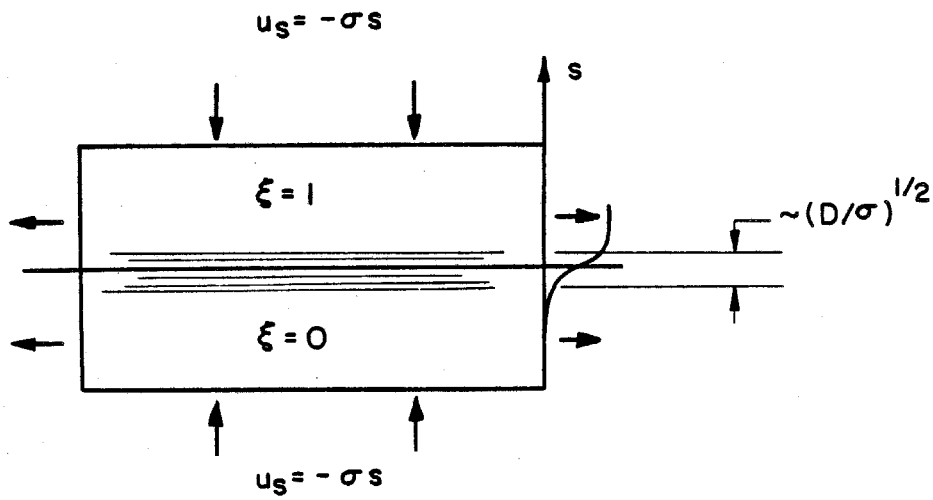

FIGURE 13. Strain-limited diffusion process. Shaded region indicates thickness of equilibrium diffusion layer.

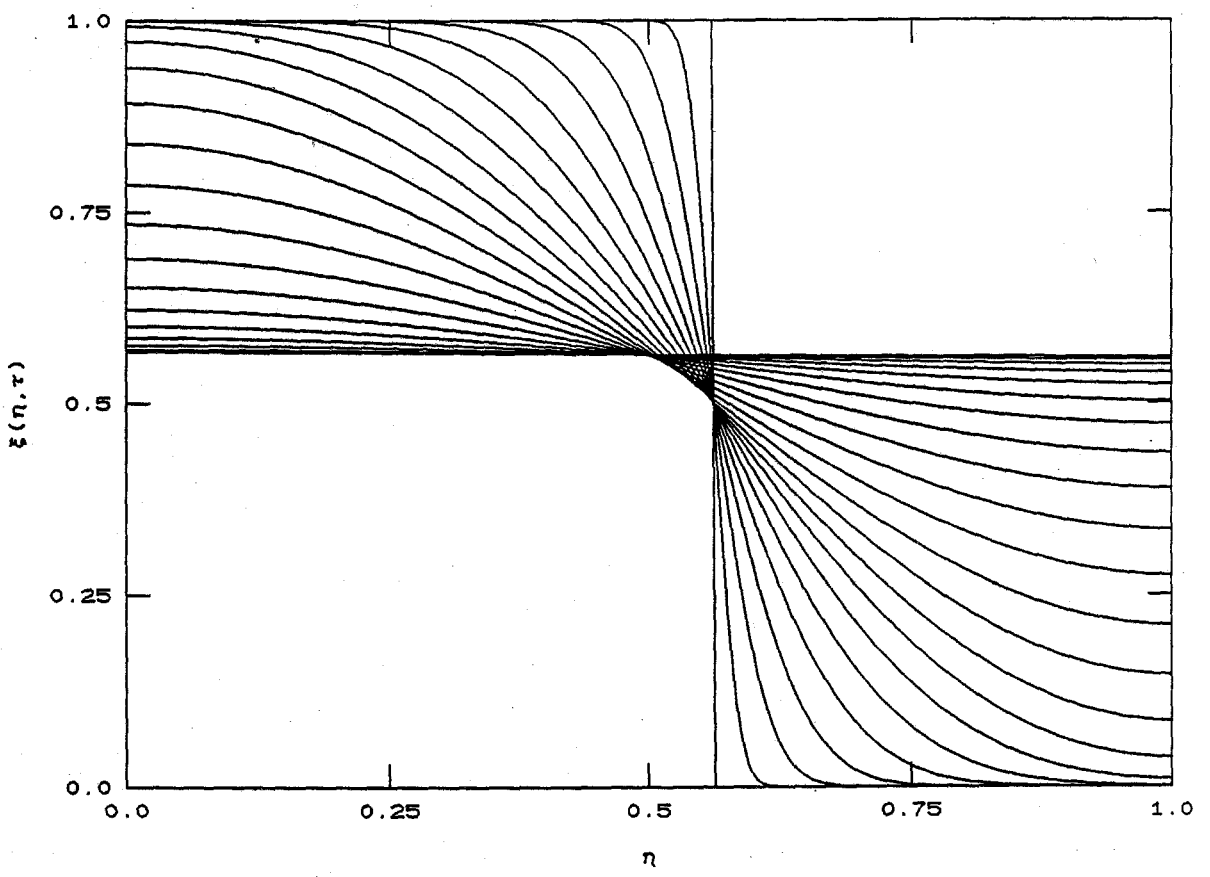

FIGURE 14. Numerical solution sequence $\xi(\eta,\tau)$ for unsteady diffusion of the conserved scalar in an adiabatic cell, corresponding to $\xi_E = E/(E+1)$ for $E = 1.3$. Curves computed for dimensionless times $\tau_{n+1} = \tau_n + n^2 \tau_0$, where $\tau_0 = 1.6\times10^{-4}$.

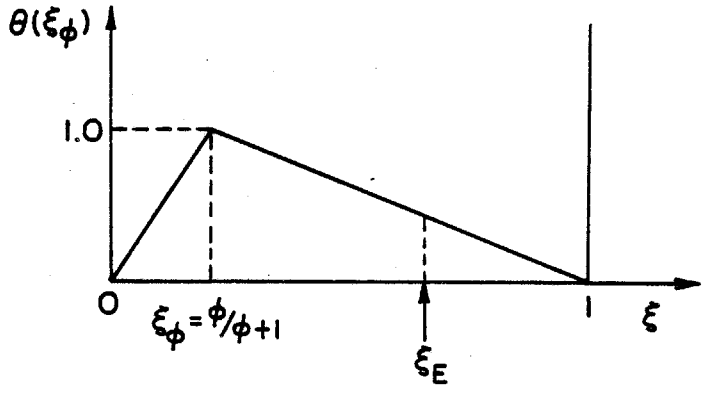

FIGURE 15. Normalized product function (temperature rise) as a function of the stoichiometric mixture fraction ξ, for a given free stream stoichiometric mixture fraction $\xi_\phi = \phi/(\phi+1)$.

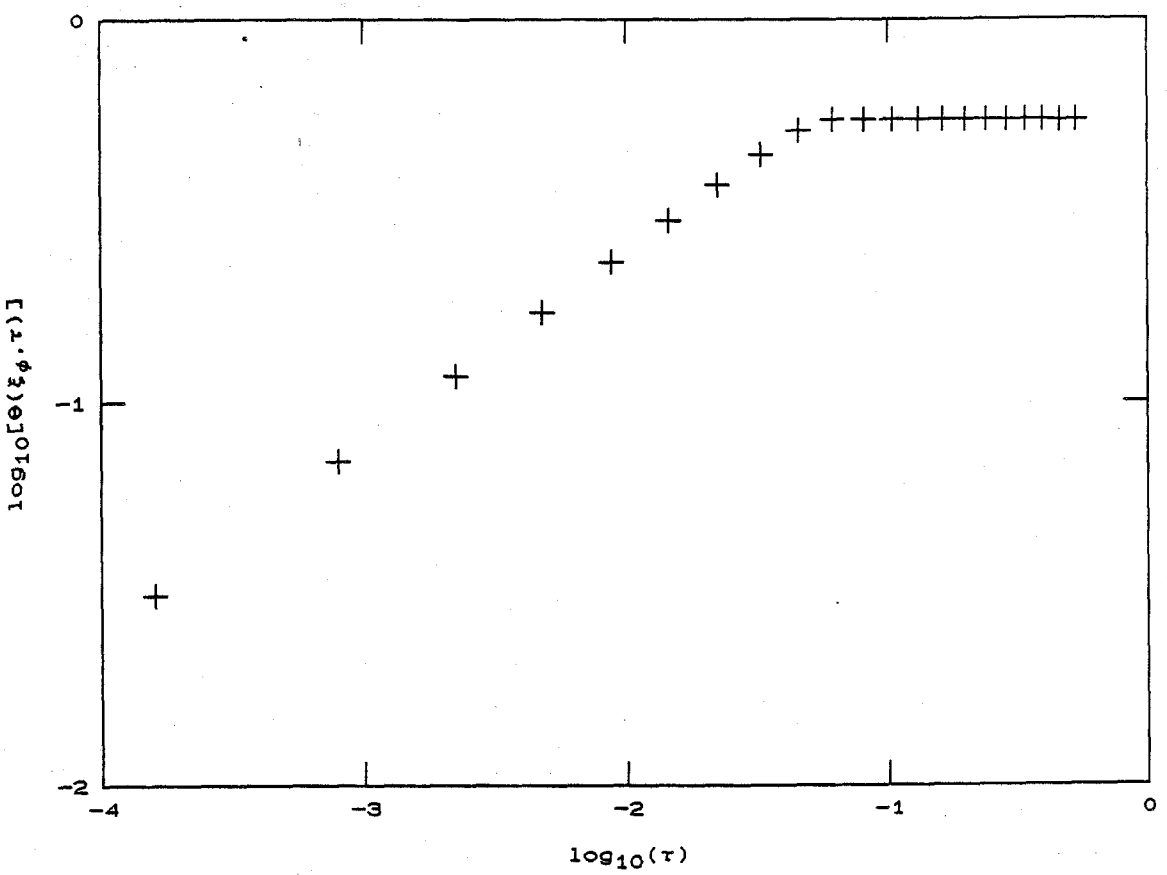

Figure 16(a)

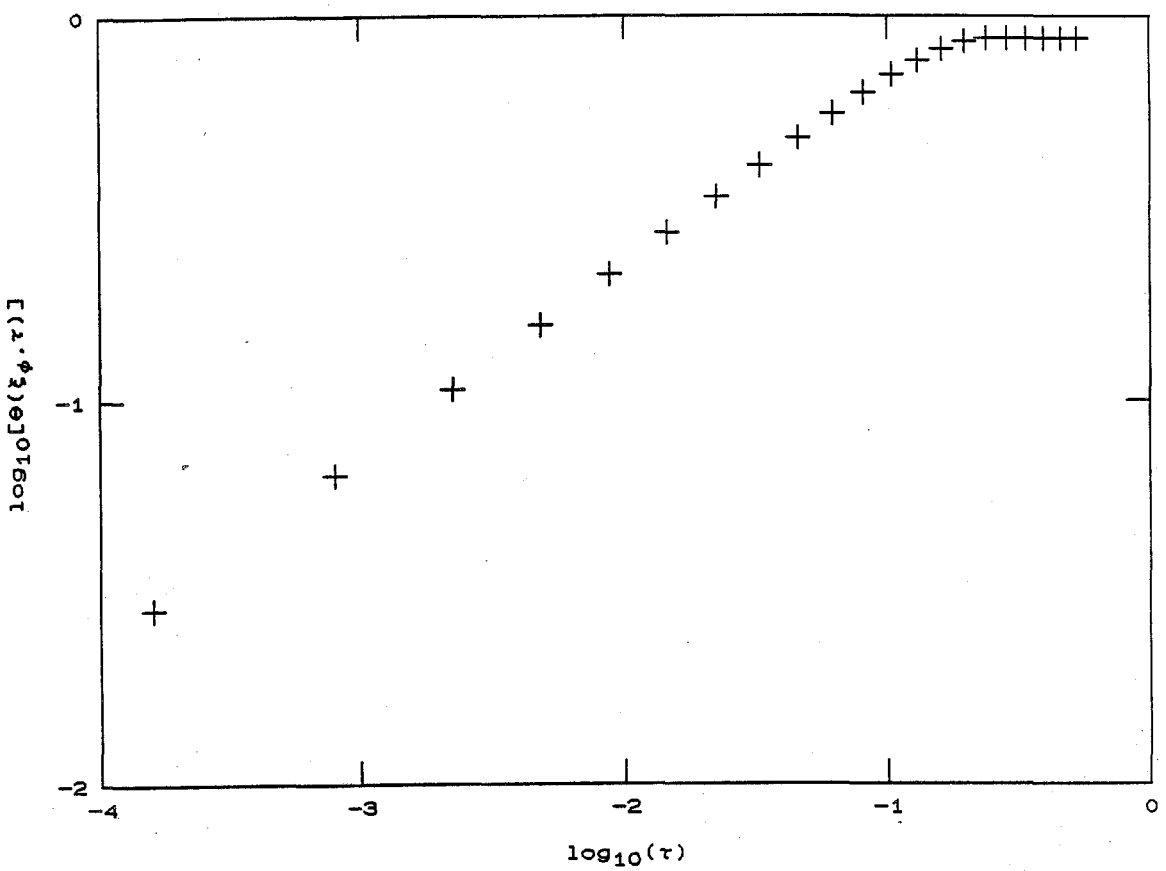

(b)

FIGURE 16. Normalized total chemical product (temperature rise) in λ-cell as a function of the (dimensionless) time τ computed from exact numerical solution sequence in figure 14. (a) $\xi_\phi = 0.2$ ($\phi = 1/4$). (b) $\xi_\phi = 0.5$ ($\phi = 1$).

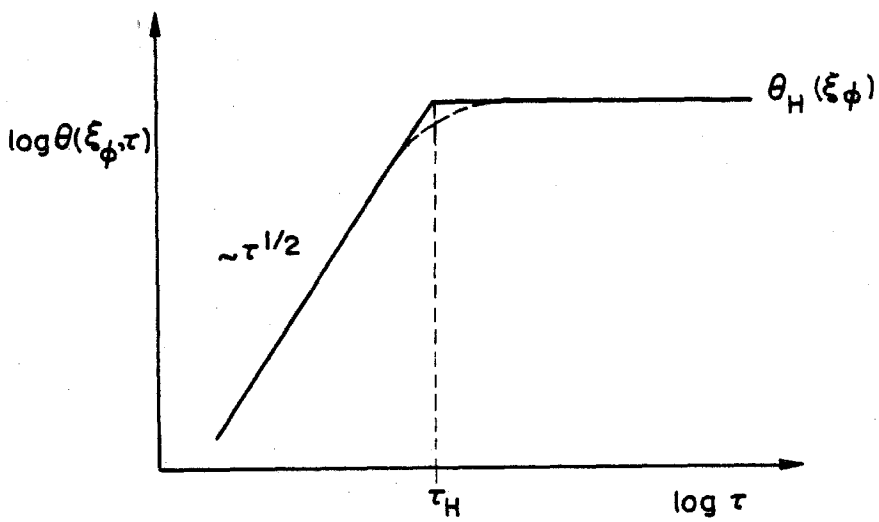

FIGURE 17. Proposed model scaled chemical product (temperature rise) function dependence on dimensionless time τ.

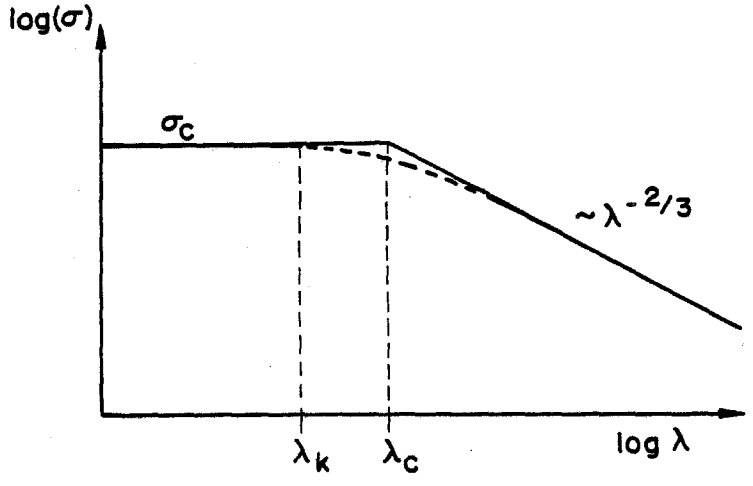

FIGURE 18. Proposed model contraction strain rate dependence on scale λ.

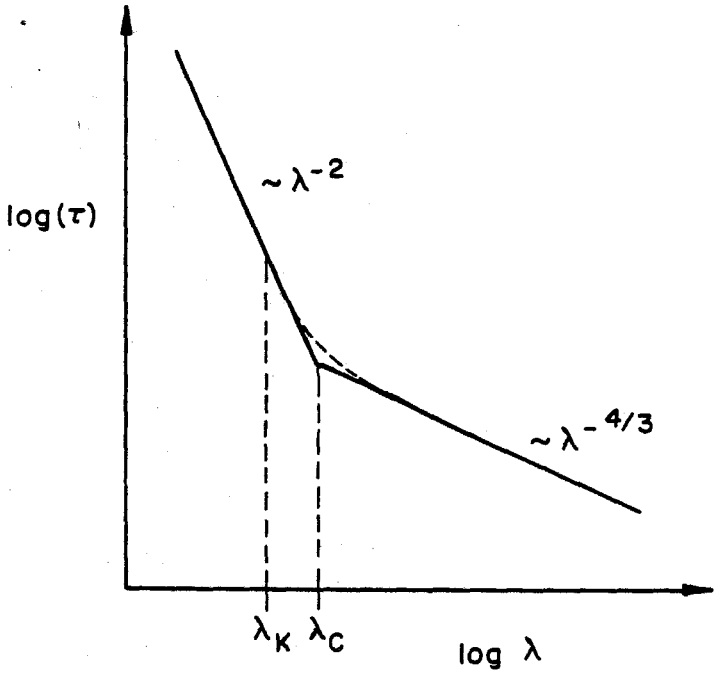

FIGURE 19. Proposed dimensionless "time" τ dependence on scale λ.

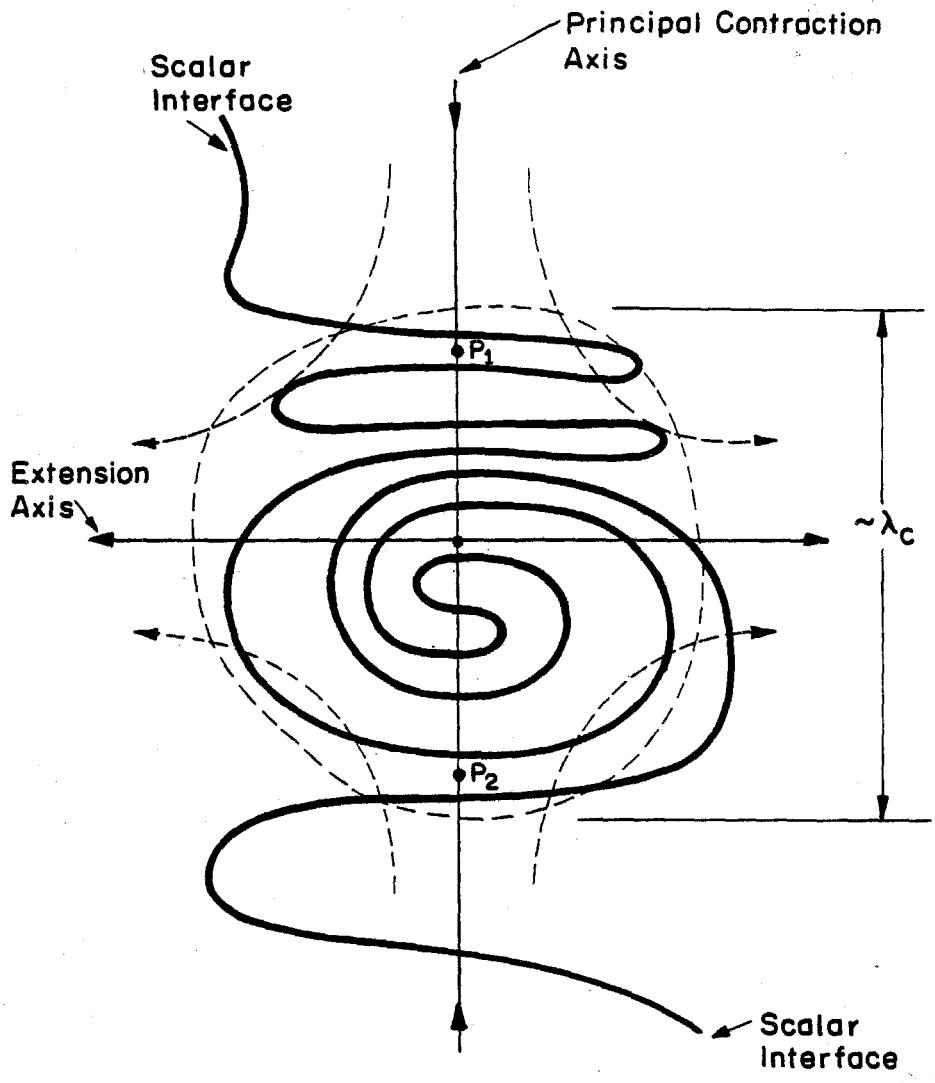

FIGURE 20. Schematic of scalar interface in the interior of a fluid element of extent λ_c.

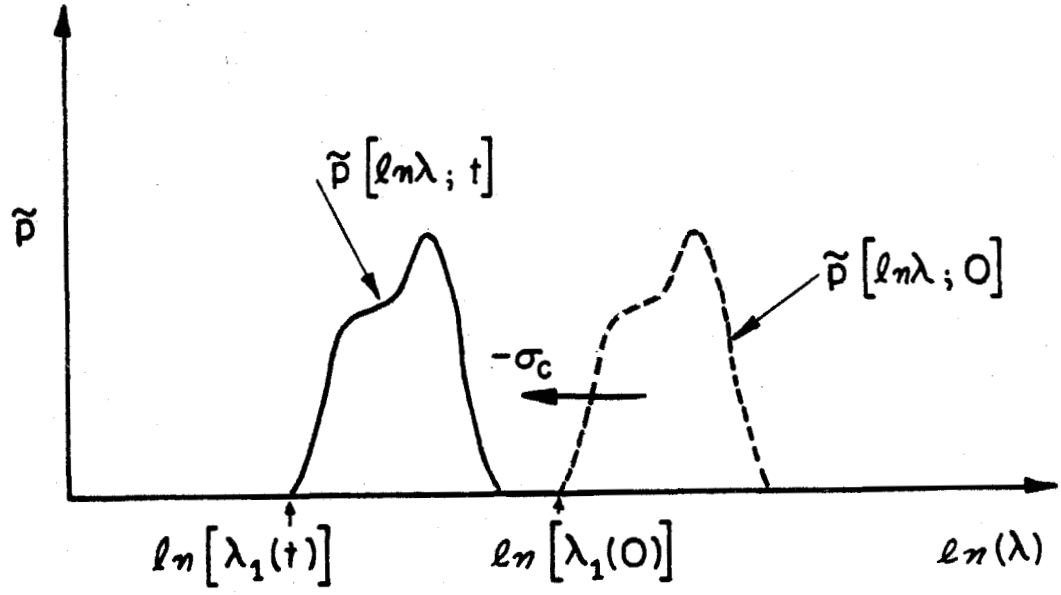

FIGURE 21. Scale packet evolution in the direction of the $-\ln(\lambda)$ axis under the action of a uniform and constant contraction strain rate σ_c.

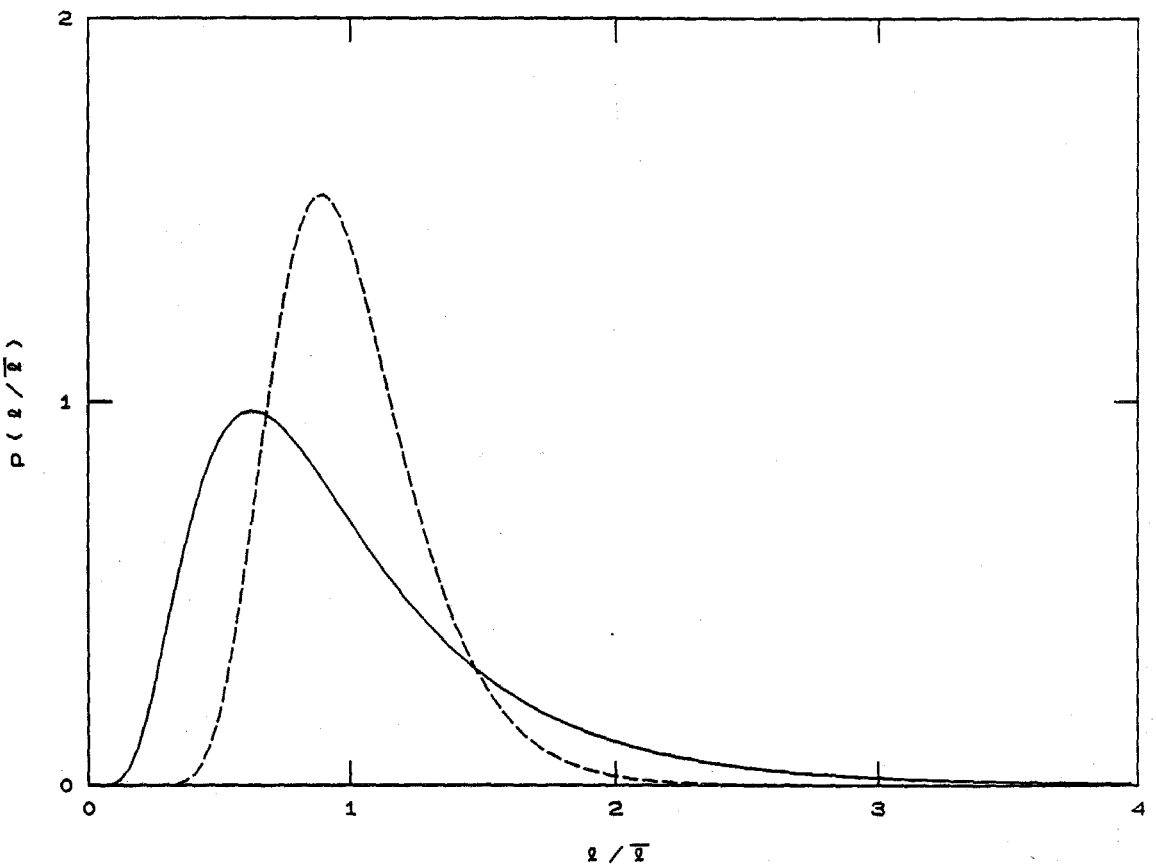

FIGURE 22. Probability density function $p(\ell / \bar{\ell})$ for normalized large scale structure spacings. Dashed curve for $\Sigma_\ell = 0.28$. Solid curve for $\Sigma_\ell = 0.56$.

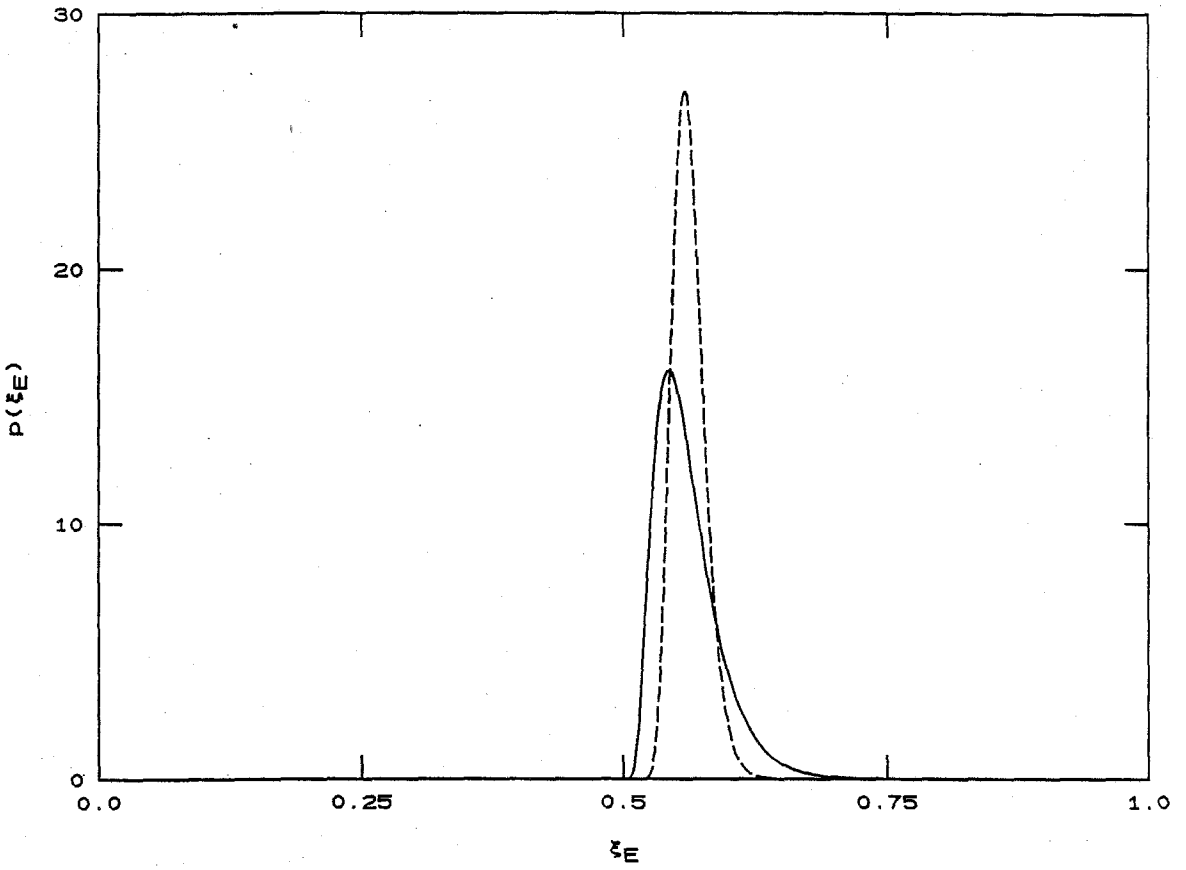

FIGURE 23. Probability density function for entrainment ratio mixture fraction $\xi_E = E/(E+1)$. Dashed curve for $\Sigma_\ell = 0.28$. Solid curve for $\Sigma_\ell = 0.56$.

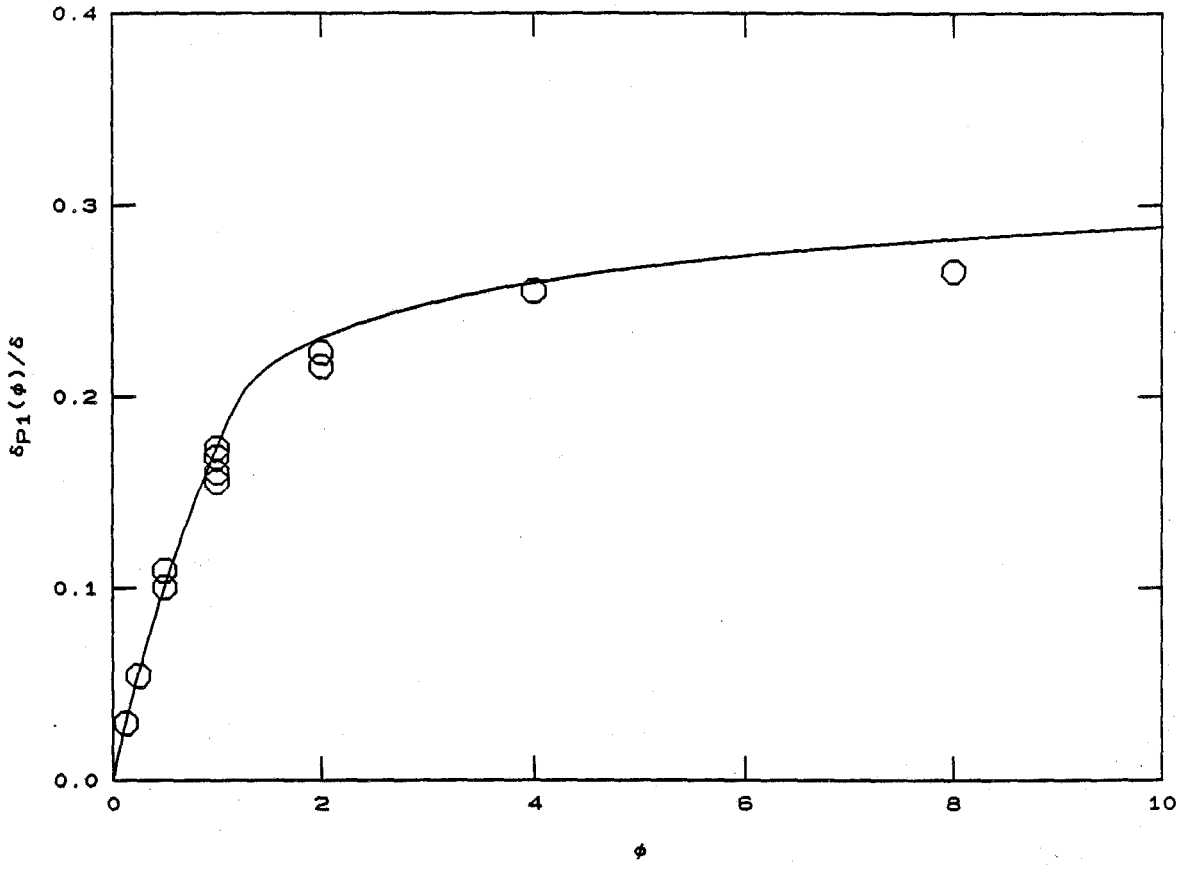

FIGURE 24. Model predictions for $\delta_{p1}(\phi)/\delta$ product thickness. Data legend as in figure 4.

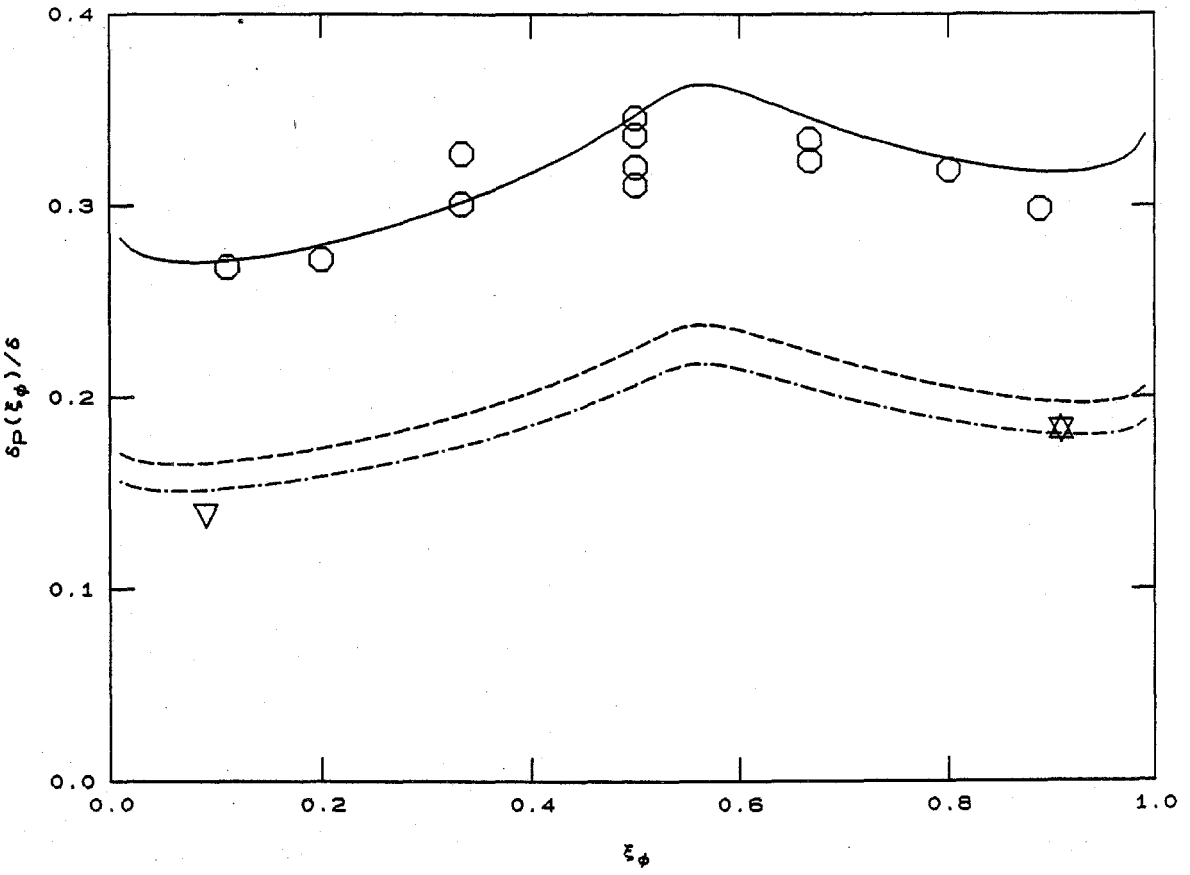

FIGURE 25. Proposed model predictions for δ_p/δ vs. ξ_ϕ data. Solid line for gas phase data (circles; Sc ≈ 0.8, Re ≈ 6.6×10^4, Mungal & Dimotakis 1984). Dashed line for liquid phase (Sc ≈ 600, Koochesfahani & Dimotakis 1986) data (inverted triangles; Re ≈ 2.3×10^4). Dot-dashed line for higher Reynolds number point (upright triangle; Re ≈ 7.8×10^4).

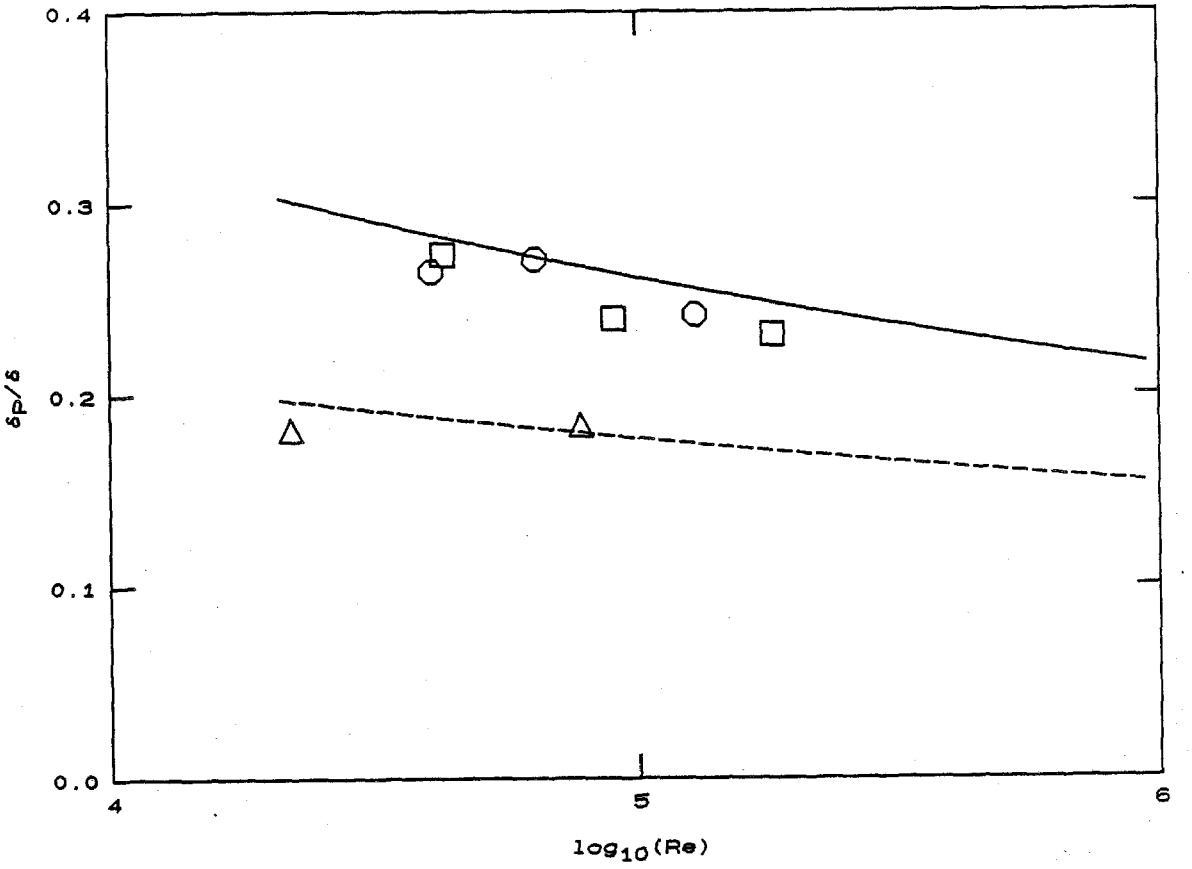

FIGURE 26. Model predictions for δ_p/δ chemical product volume fraction dependence on Reynolds number. Data as in figure 6. Solid line for gas phase data. Dashed line for liquid phase data. Data legend as in figure 6.

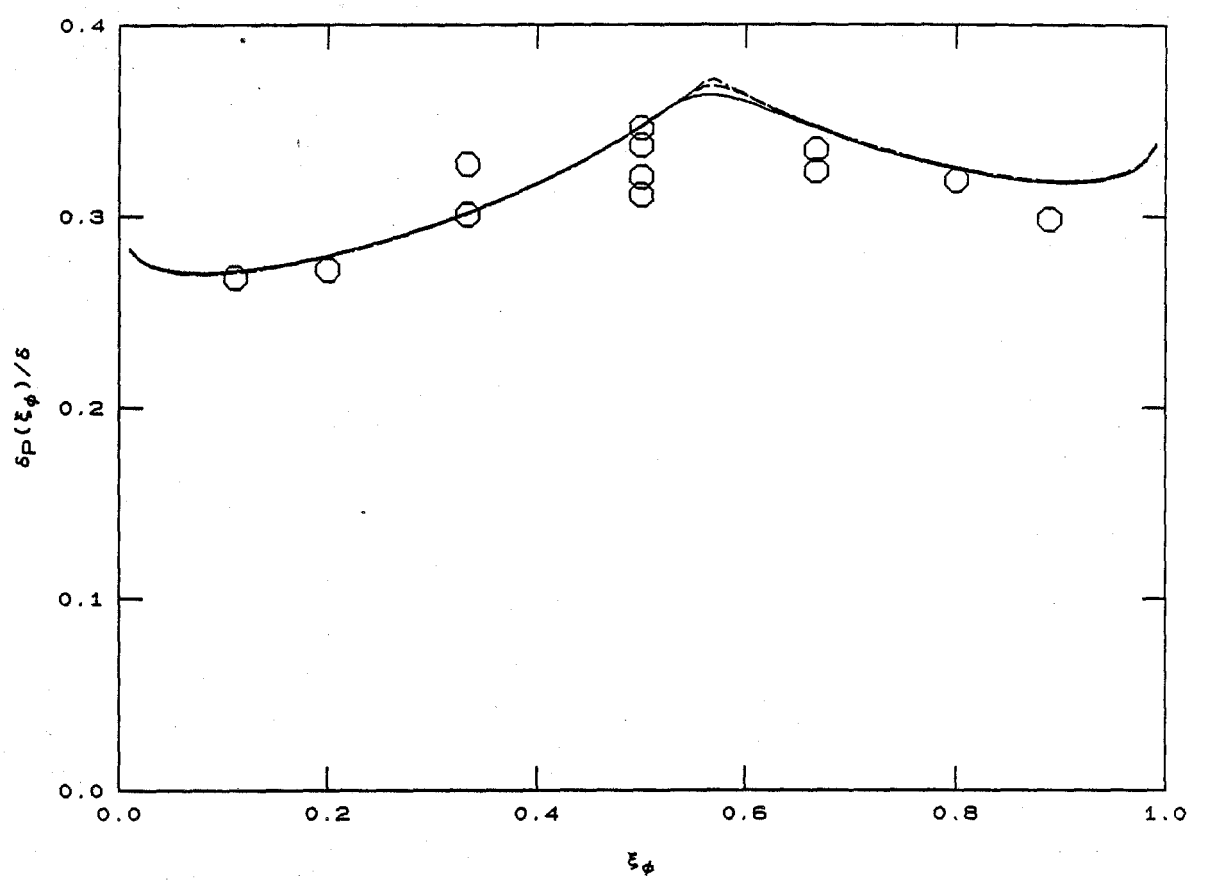

FIGURE 27. Model sensitivity to value of variance Σ_ℓ used in entrainment mixture fraction PDF. Corresponding predictions for $\delta_P(\xi_\phi)/\delta$ chemical product volume fraction. Top (cusped) curve for $\Sigma_\ell = 0$. Middle dashed curve for $\Sigma_\ell = 0.28$. Bottom (solid) curve for $\Sigma_\ell = 0.56$ used in the model.

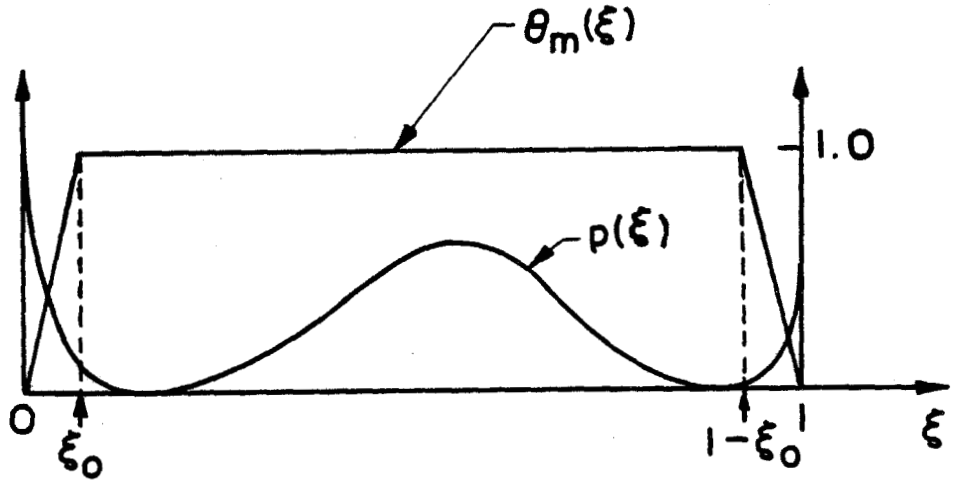

FIGURE 28. "Mixed fluid" normalized function $\theta_m(\xi)$. See text.

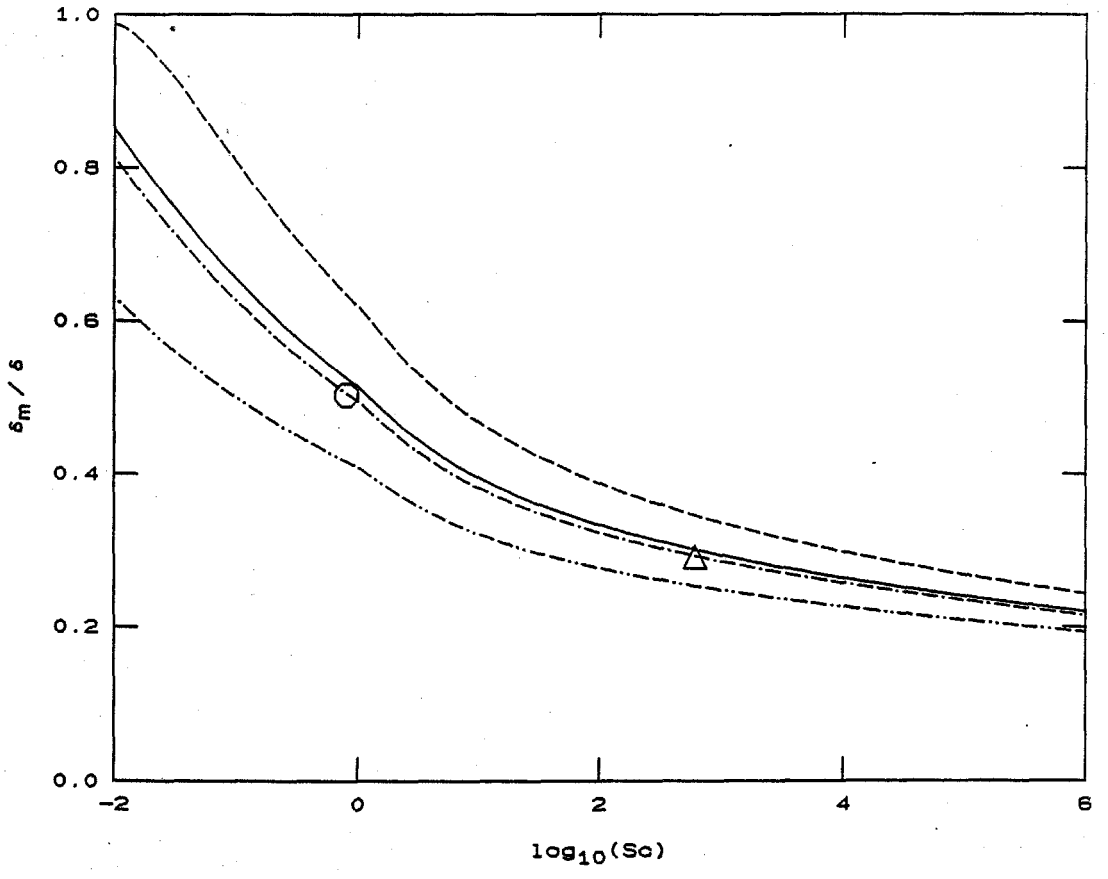

FIGURE 29. Proposed model predictions for mixed fluid volume fraction δ_m/δ as a function of Schmidt number and Reynolds number. Circle derived from Mungal & Dimotakis (1984) data. Triangle from Koochesfahani & Dimotakis (1986) data (see text). Solid curve for Re = 6.6×10^4. Dashed curves, in order of decreasing mixed fluid volume fraction, for Re = 10^4, 10^5 and 10^6.

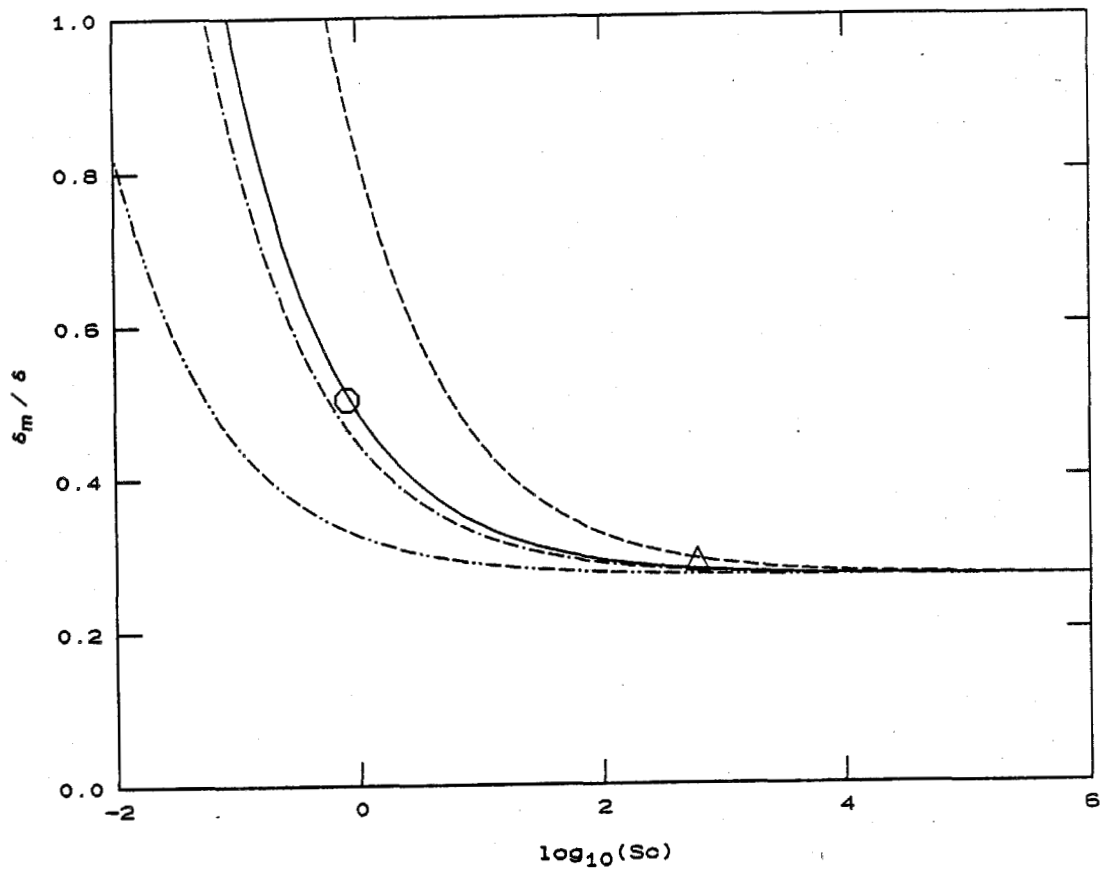

FIGURE 30. Broadwell-Breidenthal model predictions for mixed fluid volume fraction δ_m/δ as a function of Schmidt number and Reynolds number. Note Reynolds number dependence at fixed Schmidt number and asymptotic dependence for large Schmidt numbers. Data legend as in figure 29.